AB INITIO DYNAMICAL STUDY OF CO_2-H_2 VIBRATIONAL ENERGY TRANSFER

By

NARAYANASAMI SATHYAMURTHY

Bachelor of Science
Annamalai University
Annamalainagar, India
1970

Master of Science
Annamalai University
Annamalainagar, India
1972

Submitted to the Faculty of the Graduate College
of the Oklahoma State University
in partial fulfillment of the requirements
for the Degree of
DOCTOR OF PHILOSOPHY
July, 1975

AB INITIO DYNAMICAL STUDY OF CO_2-H_2

VIBRATIONAL ENERGY TRANSFER

Thesis Approved:

Lionel M. Raff
Thesis Adviser

Paul Westhaus

J. Paul Devlin

Dean of the Graduate College

To my Parents

ACKNOWLEDGEMENTS

I wish to express my sincere gratitude to Dr. Lionel M. Raff for his valuable guidance throughout the course of this study.

I take immense pleasure in dedicating this thesis to my parents, Mrs. and Mr. Narayanasami.

I am indebted to Dr. T. Rangarajan for his moral and financial supports since the beginning of my graduate studies. Continued interest of my uncle Mr. G. Janakiraman is gratefully acknowledged.

I am very pleased to acknowledge the following persons: Drs. G. J. Mains, Paul Westhaus and J. Paul Devlin for serving as members of my advisory committee, Mr. Max McKee and Mr. Joe Gray for assistance in computer programming, Dr. D. L. Thompson for providing valuable materials on spline interpolation method, Dr. Henry H. Suzukawa for providing a copy of his thesis, Dr. J. Chandler for his help in multiple regression analysis and Drs. Glen E. Kellerhals and J. J. Hinkel for teaching me various theoretical and computational techniques.

It has always been fun discussing chemistry as well as life with my colleagues and friends and I thank them all. My special thanks are due to Mr. Philip S. Bush and Mr. David Martin for numerous valuable discussions and Mr. G. Prakash and Miss Radha Rangarajan for their patience in proof reading my thesis and giving me nice company through the tiresome hours of thesis-writing.

Financial supports by the Department of Chemistry through a teaching assistantship, NSF grant GP-35869X through a research

assistantship, CONOCO fellowship, Summer Research Award from the OSU College of Arts and Sciences are gratefully acknowledged.

Finally, it is a pleasure to thank Peggy Peaden for her excellent typing job in the preparation of the final copy of this thesis.

TABLE OF CONTENTS

LIST OF TABLES

LIST OF TABLES (Continued)

LIST OF FIGURES

LIST OF FIGURES (Continued)

LIST OF FIGURES (Continued)

CHAPTER I

INTRODUCTION

Understanding of energy transfer processes has gained increased importance in recent years because of the need to develop lasers with better performance. Ultrasonic measurements (1-5) and shock tube studies (6-12) have long been able to provide valuable information on various energy transfer processes. Recently, laser methods (13-29) and molecular beam studies (30) have begun to provide a deeper insight into the problem especially at a molecular level, and this has served as a stimulus to the development of better and more realistic theoretical approaches to the problem.

The basic problem is twofold: one is to compute the potential-energy of the system and the other is to solve the scattering problem for atoms moving under the influence of this potential. Ever since the formulation of the LEPS (London-Eyring-Polanyi-Sato) surface (35) for $H + H_2$ system, semiempirical surfaces (36) have dominated the field. Only recently have <u>ab initio</u> calculations of chemical accuracy become available for simple systems like $H + H_2$ (37), $F + H_2$ (38) and $Li^+ + H_2$ (39) in restricted conformations. Less accurate potential-energy surfaces (40-44) are becoming increasingly available for several systems and well-written computer programs (45) are now able to perform routine calculations of potential-energy for systems of reasonable size. However, these computations can only provide numerical values of the

potential-energy of the system for each specified conformation. In order to be of use in scattering studies, the calculations have to be repeated for several conformations. The resulting tables of numbers then need to be fitted to an analytic function or interpolated numerically. Fitting the values to an analytic function has remained a formidable task (46) and recently, Mclaughlin and Thompson (47) pointed out the possible use of a spline interpolation method to handle this problem numerically. A computer code for a three dimensional spline interpolation has been written and its accuracy tested for quasi-classical trajectory studies as described in Chapter III.

Undoubtedly, the best solution to the scattering problem would be to solve the quantum mechanical equations considering all the electrons and nuclei in the system. Unfortunately, at the present time the difficulties encountered in such a computation are insurmountable in nature for systems of the type CO_2-H_2. Quantum mechanical methods (49-51) are available for atom-diatomic molecule collinear collisions and recently, a detailed three-dimensional quantum mechanical scattering calculation (52) has been reported for the H + H_2 system. On the other hand, since atoms are heavy particles, they might be treated as classical particles. Several semiclassical methods (49) (53) could then be used to study the molecular dynamics. The most popular of them, quasiclassical trajectory analysis was first used by Eyring and Polanyi (54a) and later developed in detail by Wall, Hiller and Mazur (54b) and Karplus, Porter and Sharma (55). The literature on this method has been recently reviewed. Several attempts (51) (52) (56) have been made to check the validity of the quasiclassical method. We have carried out one such study on He + H_2^+ system that is described in Appendix A. Generally,

it has been found that the average of quasiclassical trajectory results agree with that of quantal results and equally important, results from quasiclassical trajectory studies, in several instances, have been found to be in excellent accord with experimental findings in spite of the semiempirical nature of the potential-energy surfaces employed and the approximations made. Thompson (57) showed that the quasiclassical trajectory method could be used to study the vibrational energy transfer in systems of the A + BC type. Suzukawa (58) has recently reported a successful application of the method to a study of the vibrational energy transfer from a polyatomic molecule, carbon dioxide, during its collision with an inert gas atom.

The present study attempts to investigate and solve some of the problems involved in energy transfer processes between a typical polyatomic molecule and a diatomic molecule - carbon dioxide and hydrogen. This particular system was chosen because a great wealth of information is available. Also, it is a versatile system in that several processes, viz., intermolecular vibrational-vibrational (V$\leftrightarrow$V), vibrational-rotational (V$\leftrightarrow$R), vibrational-translational (V$\leftrightarrow$T) and intramolecular vibrational-vibrational (V$\curvearrowright$V) energy transfer can occur. ($\leftrightarrow$ is used to represent the intermolecular processes while $\curvearrowright$ is used for intramolecular processes). At the same time, it is sufficiently simple to be handled theoretically. The existing data exhibit several interesting features. For instance, the mass dependence of energy transfer from different vibrational modes of carbon dioxide is quite different and the temperature dependence is not as predicted by Landau-Teller theory (31). This system has been the focus of several theoretical calculations (32) (33) (34). But the problem of energy transfer between

molecules in general, and carbon dioxide and hydrogen in particular, demands a better treatment than these theories have been able to offer. These theories were unsuccessful because they, necessarily, restricted the geometry of molecular collisions mostly to collinear conformations. They also failed to consider detailed intermolecular potentials. In the present study, the computer program, Gaussian-70 (48), has been employed to compute the (CO_2-H_2) intermolecular potential. The resulting potential-energy values have then been spline-fitted using the routine mentioned before. The details of this procedure are discussed in Chapter II. We have extended Suzukawa's (58) procedure to a study of the energy transfer between CO_2 and H_2. The details of the method are described in detail in Chapter IV, and some preliminary results are reported in Chapter V.

CHAPTER II

POTENTIAL-ENERGY SURFACE

The calculation of a completely ab initio potential-energy hypersurface for the CO_2-H_2 system by varying each of the ten internuclear distances (Figure 1) is beyond the scope of the present study and that of today's computer technology. Even if the potential energy is computed only at 10 points along the direction of each basis vector in the 10 dimensional space of the hypersurface, 10^{10} computations will be needed. However, we may reduce the magnitude of the computational problem while still remaining in the realm of ab initio calculations if the potential energy of the system is defined as the sum of the potential energy of the individual molecules plus the intermolecular potential:

$$V = V_{CO_2} + V_{H_2} + V_{inter} \quad . \tag{II-1}$$

Since only inelastic processes will be considered in this study, such an approximation is not unreasonable. Both carbon dioxide and hydrogen are two spectroscopically well-studied molecules, and accurate spectroscopic information is available for both.

For carbon dioxide (59),

$$V_{CO_2} = V_M(\Delta R_1) + V_M(\Delta R_2) + F_R \Delta R_1 \Delta R_2 + (1/2) F_\alpha R_e^2 \Delta\alpha^2 \tag{II-2}$$

where ΔR_i is the displacement of R_i from the equilibrium internuclear

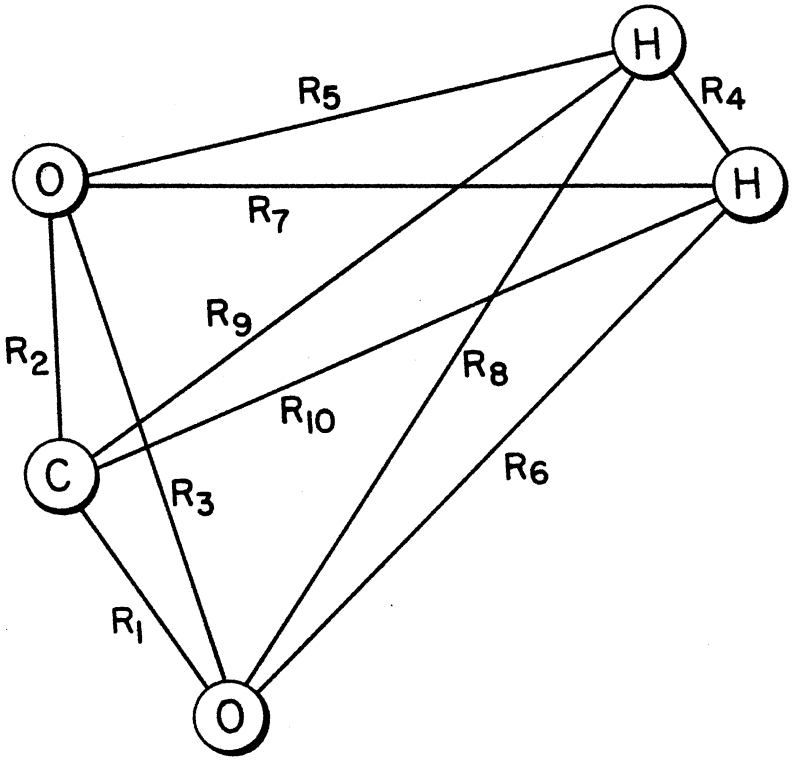

Figure 1. Internuclear Distances in CO_2-H_2 System

distance R_e, $\Delta\alpha$ is the deviation of the O-C-O bond angle from π radians, and F_R and F_α are the stretching and bending force constants of CO_2, respectively. The stretching potential $V_M(\Delta R)$ is fitted accurately by a Morse function,

$$V_M(\Delta R) = D_e(1 - \exp(-\alpha_M \Delta R))^2 \quad . \tag{II-3}$$

The potential is transformed from a function of the valence coordinates $(R_1, R_2, \Delta\alpha)$ to a function of the internuclear distances (R_1, R_2, R_3) by noting that

$$\Delta\alpha = \pi - \arccos(U), \tag{II-4}$$

where

$$U = (R_1^2 + R_2^2 - R_3^2)/2\,R_1R_2 \tag{II-5}$$

The potential paremeters of the CO_2 molecule are given in Table I. Morse parameters (60) for H_2 are also given in Table I.

Vibrational energy transfer is believed to depend mainly on the short-range potential (33). Earlier studies on closed shell systems like $(HF)_2$ (65a), H_2O-H_2 (65b), HCN-HF (65c) and inert gas dimers (65d) have shown that single configuration calculations might give good results in such non-van der Wals regions. This is because, in these regions, correlation energy (66) is not significant and it becomes important only at large distances where dispersion forces are dominant. Hence, the intermolecular potential for CO_2-H_2 was computed by an LCAO-MO-SCF procedure using an extended (split valence) gaussian basis (4-31G) set (61) described in Appendix B. Both molecules are placed in their respective equilibrium positions as determined by geometry optimization using the same LCAO-MO-SCF procedure, with their centers of mass separated by a distance R and their relative orientation specified by angles θ, ϕ

TABLE I

THE POTENTIAL-ENERGY PARAMETERS FOR CO_2 AND H_2

Parameters for CO_2[a]	
D_e	5.453 eV
α_M	3.028 A^{-1}
R_e	1.1615 A
F_R	1.268 mdyne A^{-1} = 7.91481 eV A^{-2}
F_α	0.582 mdyne A^{-1} = 3.63282 eV A^{-2}
Parameters for H_2[b]	
$D_{e_{H_2}}$	4.7466 eV
$R_{e_{H_2}}$	0.7419 A
α_{H_2}	1.9736 A^{-1}

[a] Reference 59

[b] Reference 60

and τ (see Figure 2). The results of the geometry optimization computations are presented in Table II. For $\tau = 0$, intermolecular potential values are reported in Table III for $\{R,\theta,\phi\}$, $1.5 \leq R \leq 5.0$ Å, $0 \leq \theta \leq \pi/2$, $0 \leq \phi \leq \pi$. Some of the distinct orientations investigated are plotted in Figure 3. Values are reported for $\theta = 0$ to $\pi/2$ only since the system is symmetric and the potential for the conformation with $\theta = \theta$ is the same as that for $\theta = \pi - \theta$. Inclusion of conformations with nonzero τ values would undoubtedly produce a better potential-energy surface. If a minimum of 5 points are included in the τ axis for each $\{R,\theta,\phi\}$, computational requirements increase five-fold and the available spline interpolation procedure, to be described in detail in a later part of the thesis can handle only three independent variables. Hence the potential-energy values are reported only for $\tau = 0$. The values in parentheses were obtained by extrapolating lnV vs R plots for small R values ($1.5 \leq R \leq 3.2$) at each angular orientation. Figure 4 shows representative plots for $\phi = 0$ and $\tau = 0$ orientations. In this region, the potential is mainly exponential in nature and the accuracy of the results obtained from these plots is sufficient for the present study since regions with intermolecular potential greater than 1-2 eV is not sampled during thermal and hyperthermal molecular collisions as has been pointed out by Gordon (62). Preliminary studies with trajectories having relative translational energies of 0.1 eV and 1.0 eV support this view. These values are needed only to "fill" the "holes" in the rectangular grid required for numerical interpolation. The values with asterisk on them were obtained by using the symmetry of the system. The zero values in parentheses were taken thus because they were smaller than the inherent error in the calculation. The variation

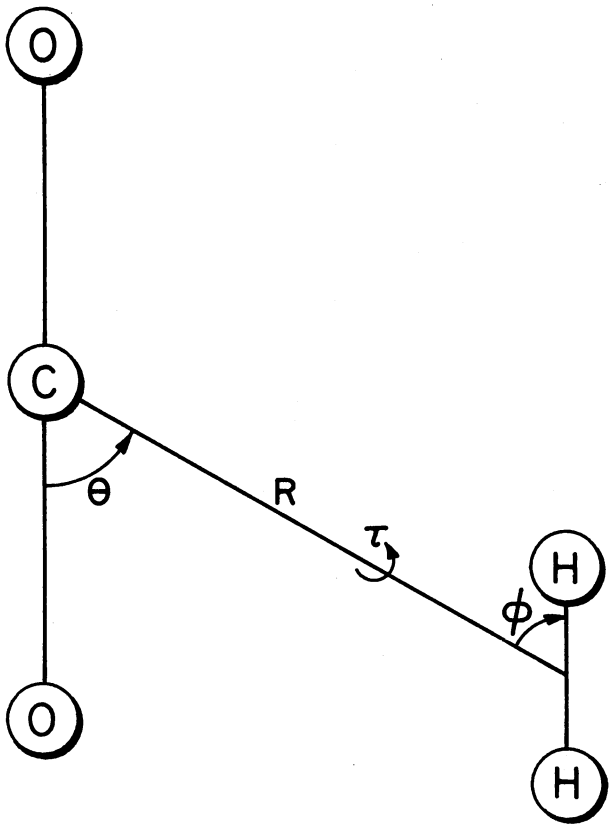

Figure 2. Orientation of CO_2-H_2

TABLE II

RESULTS OF GEOMETRY OPTIMIZATION USING GAUSSIAN 70

	Energy Values in au for Different Basis Sets[a]				
	STO-3G	STO-4G	STO-5G	STO-6G	4-31G
CO_2					
r = 1.10 A					-187.31137
r = 1.15 A	-185.06143	-186.39185	-186.74178	-186.84888	-187.32774
r = 1.20 A	-185.06777	-186.39787	-186.74750	-186.85457	-187.32092
r = 1.25 A	-185.05340	-186.38330	-186.73271	-186.83975	
r_{op} = 1.1903 A	-185.06838				
r_{op} = 1.1896 A		-186.39854			
r_{op} = 1.1889 A			-186.74824	-186.85532	
r_{op} = 1.1603 A					-187.32797
H_2					
r = 0.71	-1.11750	-1.12397	-1.12566		-1.12652
r = 0.73	-1.11719	-1.12361	-1.12529		-1.12683
r = 0.75	-1.11615	-1.12252	-1.12419		-1.12654
r_{op} = 0.7117	-1.11751				
r_{op} = 0.7103		-1.12397			
r_{op} = 0.7100			-1.12566		
r_{op} = 0.7304					-1.12683

[a]Reference 61

TABLE III

THE 4-31G INTERMOLECULAR POTENTIAL FOR CO_2-H_2. ENERGIES ARE MEASURED IN eV FROM THE ENERGY OF CO_2 AND H_2 AT INFINITE SEPARATION. ALL VALUES ARE FOR $\tau = 0$.

R	$\theta = 0$	$\theta = \pi/8$	$\theta = \pi/4$	$\theta = 3\pi/8$	$\theta = \pi/2$
			A. $\phi = 0$		
1.5	(330.)	(86.5)	(24.5)	(7.10)	4.4587
1.8	(56.8)	(31.8)	(9.4)	2.9388	1.8789
2.1	(20.5)	(11.5)	(3.6)	1.2473	0.7591
2.3	(10.2)	(5.82)	1.9205	0.6780	0.4059
2.5	5.1718	3.0139	1.0350	0.3596	0.2144
2.8	1.8817	1.1276	0.3848	0.1331	0.0812
3.0	0.9229	0.5571	0.1903	0.0660	0.0427
3.2	0.4349	0.2636	0.0891	0.0307	0.0229
3.5	0.1266	0.0752	0.0220	0.0071	0.0097
3.8	0.0262	0.0127	-0.0012	-0.0002	0.0049
4.0	0.0024	-0.0024	-0.0062	-0.0011	0.0036
4.5	-0.0102	-0.0094	-0.0055	(0.0)	0.0022
5.0	-0.0065	-0.0053	-0.0020	(0.0)	0.0016
6.0	-0.0017	-0.0013	-0.0004	(0.0)	0.0007
			B. $\phi = \pi/8$		
1.5	(188.7)	(81.5)	(20.9)	(6.3)	(4.31)
1.8	(66.7)	(30.6)	(8.5)	2.7284	1.7699
2.1	(18.5)	(11.0)	(3.39)	1.1672	0.7054
2.3	(11.0)	(5.81)	1.8604	0.6416	0.3720
2.5	(5.37)	2.8956	1.0212	0.3460	0.1928
2.8	1.8372	1.1089	0.3954	0.1336	0.0701
3.0	0.9080	0.5603	0.2038	0.0697	0.0353
3.2	0.4327	0.2738	0.1019	0.0355	0.0179
3.5	0.1299	0.0859	0.0322	0.0118	0.0068
3.8	0.0300	0.0211	0.0065	0.0036	0.0032
4.0	0.0059	0.0044	0.0001	0.0019	0.0023
4.5	-0.0079	-0.0054	-0.0019	0.0014	0.0015
5.0	-0.0053	-0.0031	(0.0)	(0.0)	(0.0)

TABLE III (Continued)

R	$\theta = 0$	$\theta = \pi/8$	$\theta = \pi/4$	$\theta = 3\pi/8$	$\theta = \pi/2$
			C. $\phi = \pi/4$		
1.5	(131.6)	(56.8)	(14.6)	(5.81)	3.6584
1.8	(49.4)	(23.1)	6.6027	2.4085	1.5171
2.1	(17.8)	(9.03)	3.0418	1.0197	0.5806
2.3	(9.03)	4.9554	1.7335	0.5568	0.2935
2.5	4.6088	2.7610	0.9600	0.2984	0.1432
2.8	1.7408	1.0736	0.3799	0.1139	0.0445
3.0	0.8740	0.5531	0.2003	0.0590	0.0186
3.2	0.4265	0.2786	0.1037	0.0300	0.0066
3.5	0.1368	0.0953	0.0366	0.0104	0.0004
3.8	0.0385	0.0298	0.011	0.003	-0.0007
4.0	0.0138	0.0122	0.0049	0.0021	-0.0007
4.5	-0.0026	-0.0003	0.0010	(0.0)	-0.0001
5.0	-0.0023	(0.0)	(0.0)	(0.0)	(0.0)
			D. $\phi = 3\pi/8$		
1.5	(181.3)	(59.1)	(17.8)	(5.26)	3.1839
1.8	(64.1)	(23.6)	(7.10)	2.1608	1.2829
2.1	(21.8)	(9.03)	(2.945)	0.8921	0.4643
2.3	(10.6)	(4.85)	1.6219	0.4762	0.2208
2.5	(5.16)	2.6773	0.8955	0.2474	0.0974
2.8	1.6578	1.0431	0.3520	0.0877	0.0209
3.0	0.8424	0.5405	0.1845	0.0417	0.0029
3.2	0.4194	0.2754	0.0949	0.0185	-0.0038
3.5	0.1424	0.0979	0.0334	0.0042	-0.0056
3.8	0.0462	0.0338	0.0111	0.0003	-0.0044
4.0	0.0210	0.0163	0.0053	-0.0003	-0.0034
4.5	0.0024	0.0029	0.0015	-0.0002	-0.0017
5.0	0.0005	0.0013	0.0010	0.0000	-0.0009
			E. $\phi = \pi/2$		
1.5	(103.5)	(69.4)	(16.8)	(5.26)	3.0047

TABLE III (Continued)

R	$\theta = 0$	$\theta = \pi/8$	$\theta = \pi/4$	$\theta = 3\pi/8$	$\theta = \pi/2$
1.8	(39.6)	(26.6)	(6.82)	2.0980	1.1916
2.1	(15.2)	(10.0)	2.7973	0.8445	0.4192
2.3	(8.0)	(5.2)	1.5785	0.4393	0.1924
2.5	4.2737	2.6787	0.8613	0.2197	0.0795
2.8	1.6264	1.0353	0.3283	0.0694	0.0116
3.0	0.8300	0.5323	0.1666	0.0276	-0.0031
3.2	0.4163	0.2686	0.0817	0.0076	-0.0080
3.5	0.1444	0.0936	0.0253	-0.0031	-0.0079
3.8	0.0491	0.0315	0.0059	-0.0045	-0.0058
4.0	0.0239	0.0150	0.0015	-0.0039	-0.0045
4.5	0.0045	0.0026	-0.0005	(0.0)	-0.0023
5.0	0.0017	(0.0)	-0.0001	(0.0)	(0.0)
			F. $\phi = 5\pi/8$		
1.5	(181.3)*	(75.2)	(20.9)	(5.81)	3.1839*
1.8	(64.1)*	(28.2)	(8.00)	2.2596	1.2829*
2.1	(21.8)*	(10.6)	(3.06)	0.9019	0.4643
2.3	(10.6)*	(5.37)	1.6195	0.4640	0.2208*
2.5	(5.16)*	2.7686	0.8688	0.2278	0.0974*
2.8	1.6578*	1.0549	0.3185	0.0676	0.0209*
3.0	0.8424*	0.5330	0.1545	0.0236	0.0029*
3.2	0.4194*	0.2619	0.0703	0.0027	-0.0038*
3.5	0.1424*	0.0850	0.0161	-0.0078	-0.0056*
3.8	0.0462*	0.0243	-0.0013	-0.0082	-0.0044*
4.0	0.0210*	0.0089	-0.0046	-0.0068	-0.0034*
4.5	0.0024*	-0.0012	-0.0039	-0.0033	-0.0017*
5.0	0.0005*	-0.0010	-0.0019	-0.0016	-0.0009
			G. $\phi = 3\pi/4$		
1.5	(131.6)*	(84.8)	(24.5)	(6.55)	3.6584*
1.8	(49.4)*	(31.2)	(9.21)	2.5885	1.5171*
2.1	(17.8)*	(11.5)	(3.39)	1.0474	0.5806*

TABLE III (Continued)

R	$\theta = 0$	$\theta = \pi/8$	$\theta = \pi/4$	$\theta = 3\pi/8$	$\theta = \pi/2$
2.3	(9.03)*	(5.81)	1.7341	0.5440	0.2935*
2.5	4.6088*	2.9135	0.9176	0.2707	0.1432*
2.8	1.7408*	1.0902	0.3274	0.0841	0.0445*
3.0	0.8740*	0.5398	0.1543	0.0321	0.0186*
3.2	0.4265*	0.2570	0.0663	0.0068	0.0066*
3.5	0.1368*	0.0756	0.0106	-0.0072	0.0004*
3.8	0.0385*	0.0156	-0.0067	-0.0088	-0.0007*
4.0	0.0138*	0.0012	-0.0096	-0.0074	-0.0007*
4.5	-0.0026*	-0.0063	-0.0069	-0.0033	-0.0001*
5.0	-0.0023*	-0.0037	-0.0031	-0.0014	(0.0)
		H.	$\phi = 7\pi/8$		
1.5	(188.7)*	(91.)	(22.2)	(6.96)	(4.31)*
1.8	(66.7)*	(33.1)	(8.85)	2.8862	1.7699*
2.1	(18.5)*	(11.94)	(3.46)	1.1982	0.7054*
2.3	(11.0)*	(6.05)	1.8647	0.6366	0.3720*
2.5	(5.37)*	3.0263	0.9881	0.3271	0.1928*
2.8	1.8372*	1.1198	0.3545	0.1117	0.0701*
3.0	0.9080*	0.5485	0.1685	0.0499	0.0353*
3.2	0.4327*	0.2565	0.0736	0.0184	0.0179*
3.5	0.1299*	0.0710	0.0128	-0.0010	0.0068*
3.8	0.0300*	0.0104	-0.0068	-0.0054	0.0032*
4.0	0.0059*	-0.0038	-0.0104	-0.0051	0.0023*
4.5	-0.0079*	-0.0097	-0.0076	-0.0019	0.0015*
5.0	-0.0053*	-0.0055	-0.0033	-0.0004	(0.0)*
		I.	$\phi = \pi$		
1.5	(330.)*	(86.5)*	(24.5)*	(7.10)*	4.4587*
1.8	(56.8)*	(31.8)*	(9.4)*	2.9388*	1.8789*
2.1	(20.5)*	(11.5)*	(3.6)*	1.2473*	0.7591*
2.3	(10.2)*	(5.82)*	1.9205*	0.6780*	0.4059*
2.5	5.1718*	3.0139*	1.0350*	0.3596*	0.2144*

TABLE III (Continued)

R	$\theta = 0$	$\theta = \pi/8$	$\theta = \pi/4$	$\theta = 3\pi/8$	$\theta = \pi/2$
2.8	1.8817*	1.1276*	0.3848*	0.1331*	0.0812*
3.0	0.9229*	0.5571*	0.1903*	0.0660*	0.0427*
3.2	0.4349*	0.2636*	0.0891*	0.0307*	0.0229*
3.5	0.1266*	0.0752*	0.0220*	0.0071*	0.0097*
3.8	0.0262*	0.0127*	-0.0012*	-0.0002*	0.0049*
4.0	0.0024*	-0.0024*	-0.0062*	-0.0011*	0.0036*
4.5	-0.0102*	-0.0094*	-0.0055*	(0.0)*	0.0022*
5.0	-0.0065*	-0.0053*	-0.0020*	(0.0)*	0.0016*
6.0	-0.0017*	-0.0013*	-0.0004*	(0.0)*	0.0007*

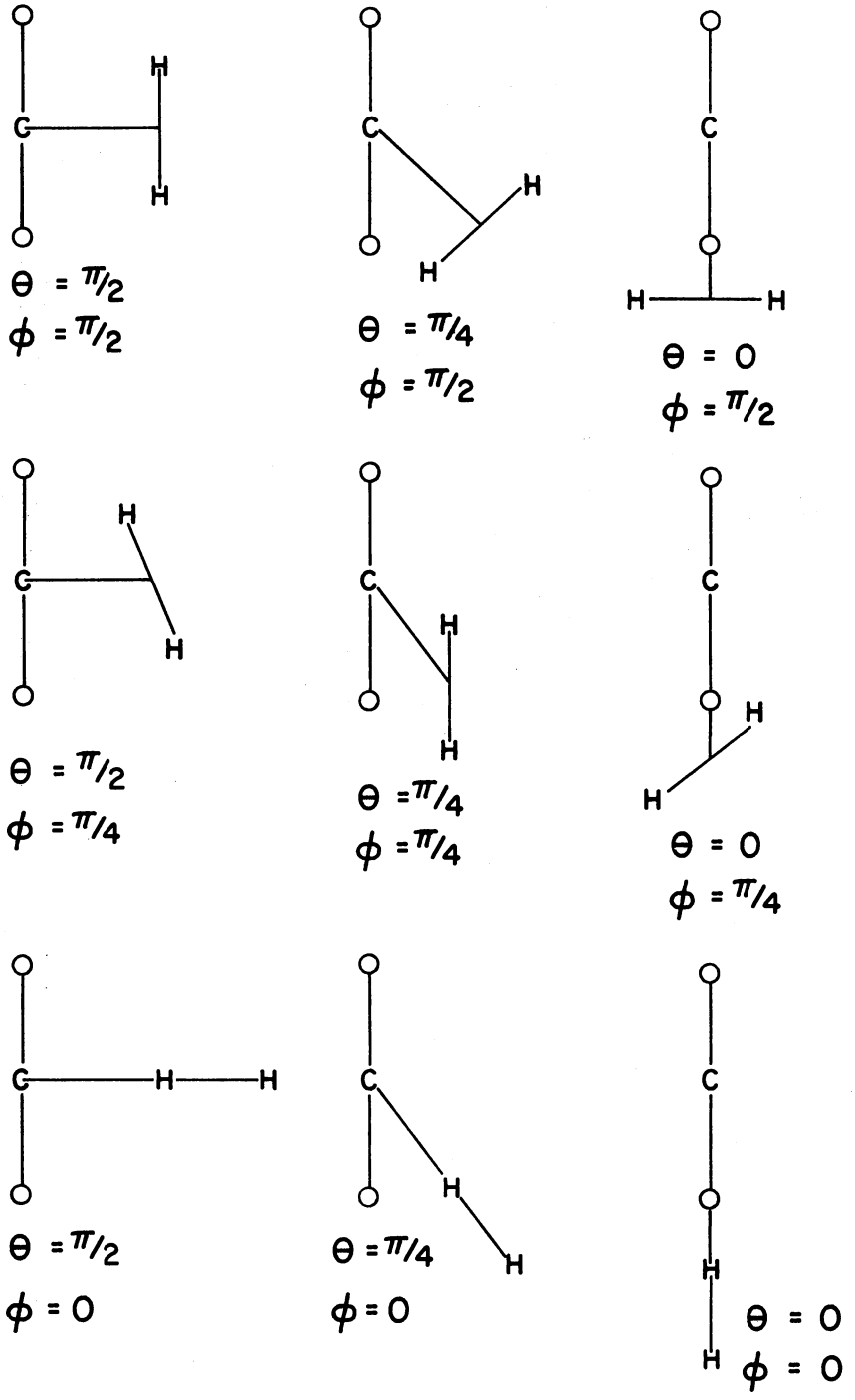

Figure 3. Some Distinct Orientations of H_2 with Respect to CO_2

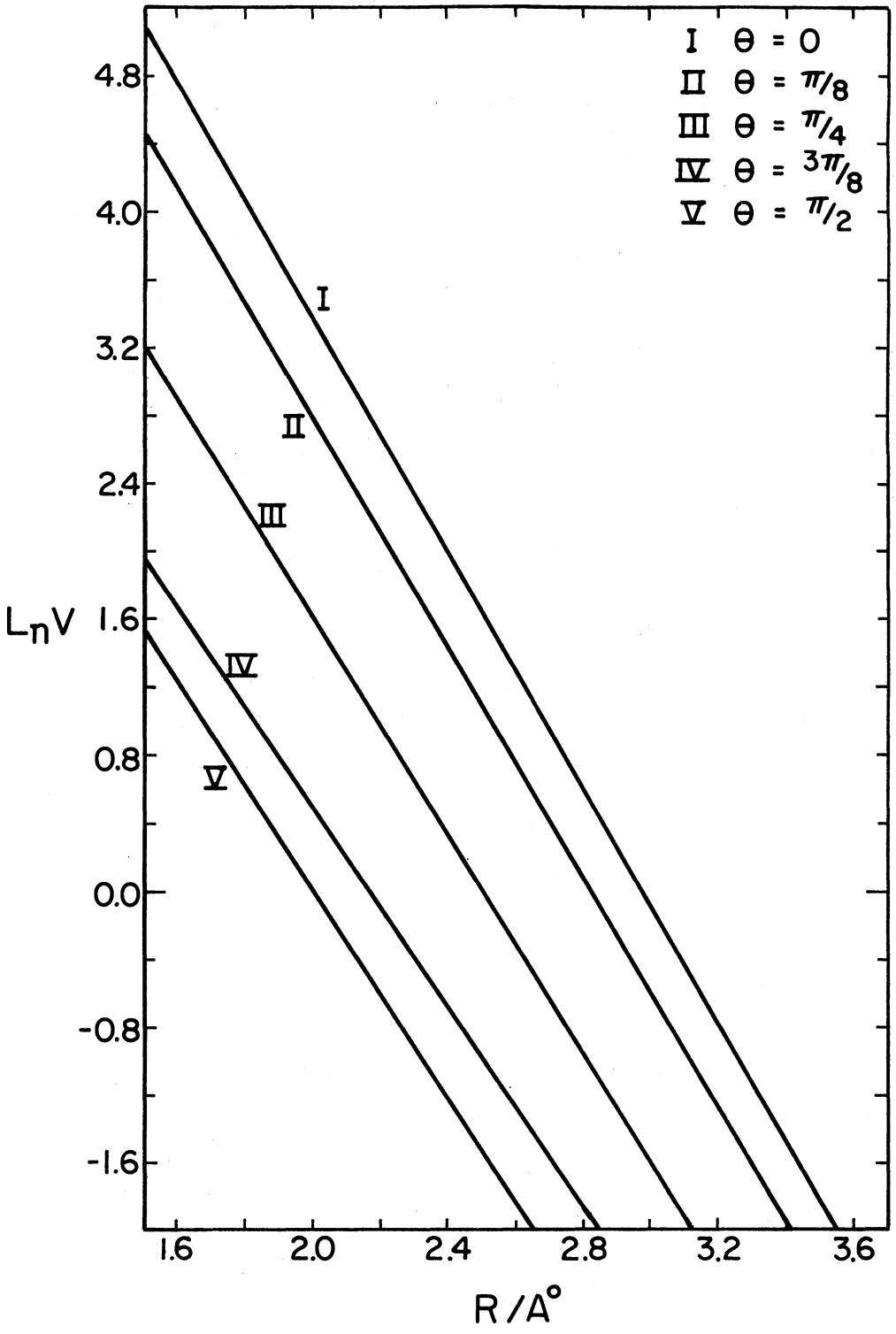

Figure 4. Plot of LnV Against R for $\phi = 0$

of the intermolecular forces between the carbon dioxide and hydrogen molecules is shown in Figures 5-9 where the potential is plotted against the center of mass separation for various orientation angles or against the angles for fixed R values. Figure 5 illustrates the R - dependence of the potential for $\phi = \pi/2$ and $0 \leq \theta \leq \pi/2$. At short distances, the intermolecular potential is rising exponentially and at larger distances, it shows an attractive potential with a minimum at $R = 3.3$ Å, $\theta = \pi/2$, $\phi = \pi/2$ and this is clearly seen by a magnified view in Figure 6. Figure 7 is similar to Figure 5 except that $\phi = \pi/4$. Figure 8 is a cumulative plot with $1.5 \leq R \leq 5.0$, $0 \leq \theta \leq \pi/2$ and $0 \leq \phi \leq \pi/2$. The shapes of these curves are similar to that of the Lennard-Jones potential and Buckingham (6-exp) potential (64) and modified forms of the latter. The data were fitted to these functions:

$$V = C_1/R^6 - C_2/R^{12} \quad \text{(Lennard-Jones)}$$

$$V = A\exp(-BR) - C/R^6 \quad \text{(Buckingham-6-exp)}$$

$$V = A\exp(-BR) - C/R^6 - D/R^8 \quad \text{(Buckingham-6,8-exp)}$$

$$V = A\exp(-BR) - C/R^6 - D/R^8 - E/R^{10} \quad \text{(Buckingham-6,8,10-exp).} \qquad \text{(II-6)}$$

Table IV lists some of these parameters for specified angular orientations. The reproducibility of the original data by these functions is excellent in most of the cases, standard error estimate being as low as 0.02 kcal/mole. A closer look at Figures 5, 7 and 8 reveals that the potential is strongly dependent upon θ and less dependent on ϕ as one would expect from chemical intuition. The explicit dependence of the potential upon θ and ϕ is plotted in Figure 9 for R = 2.8 A. The top curve is for $\theta = 0$ and the bottom curve is for $\phi = 0$.

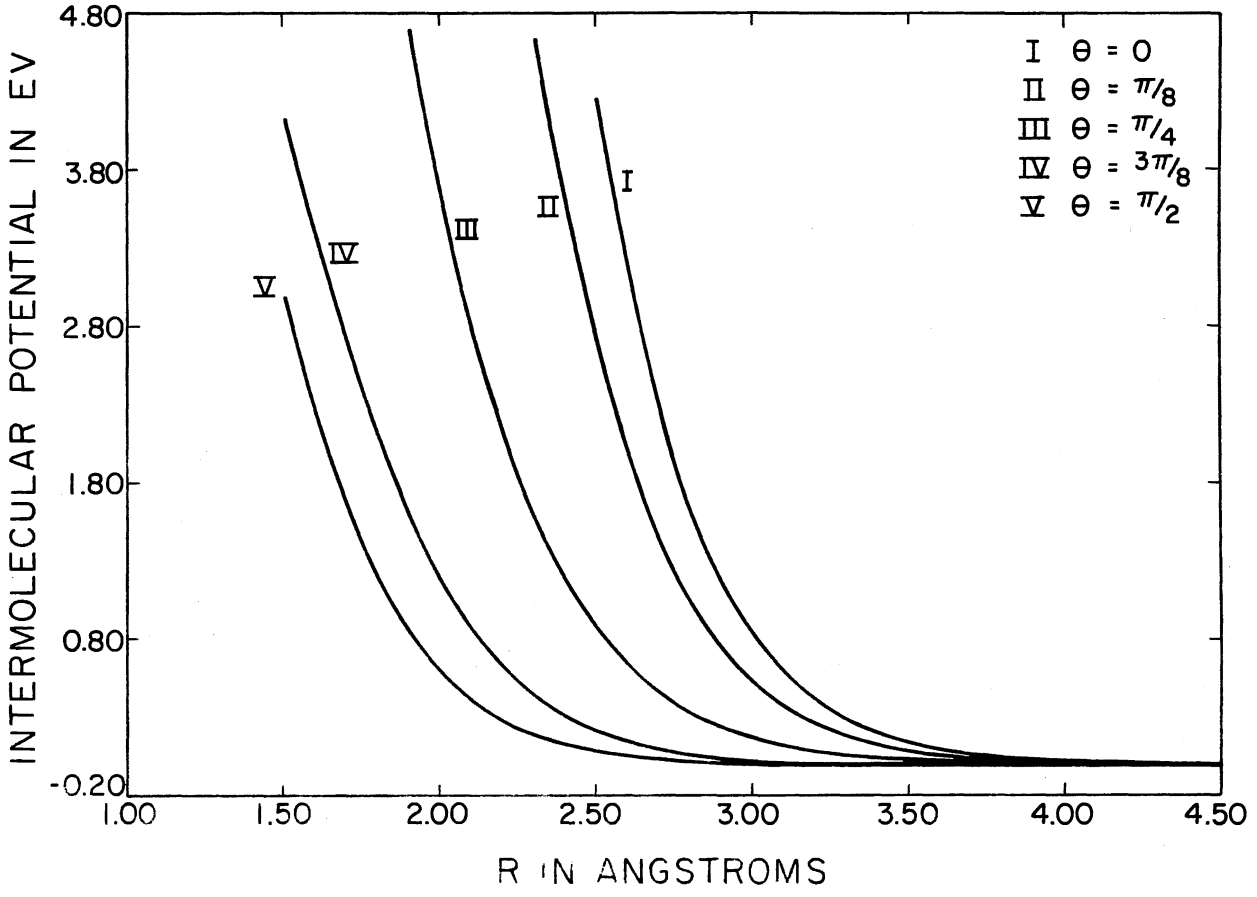

Figure 5. Plot of Intermolecular Potential Against Center of Mass Separation R for $\phi = \pi/2$

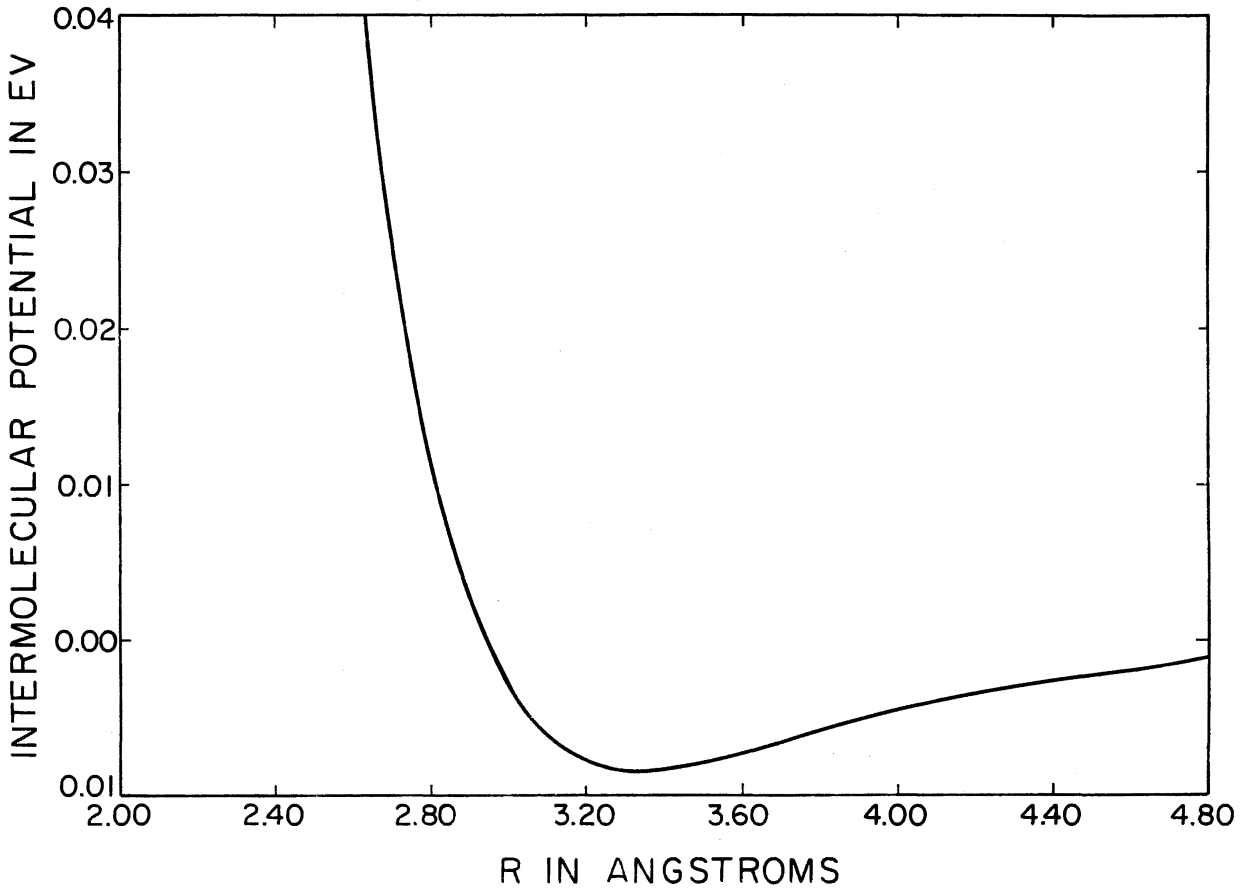

Figure 6. Plot of Intermolecular Potential Against R for $\theta = \pi/2$ and $\phi = \pi/2$

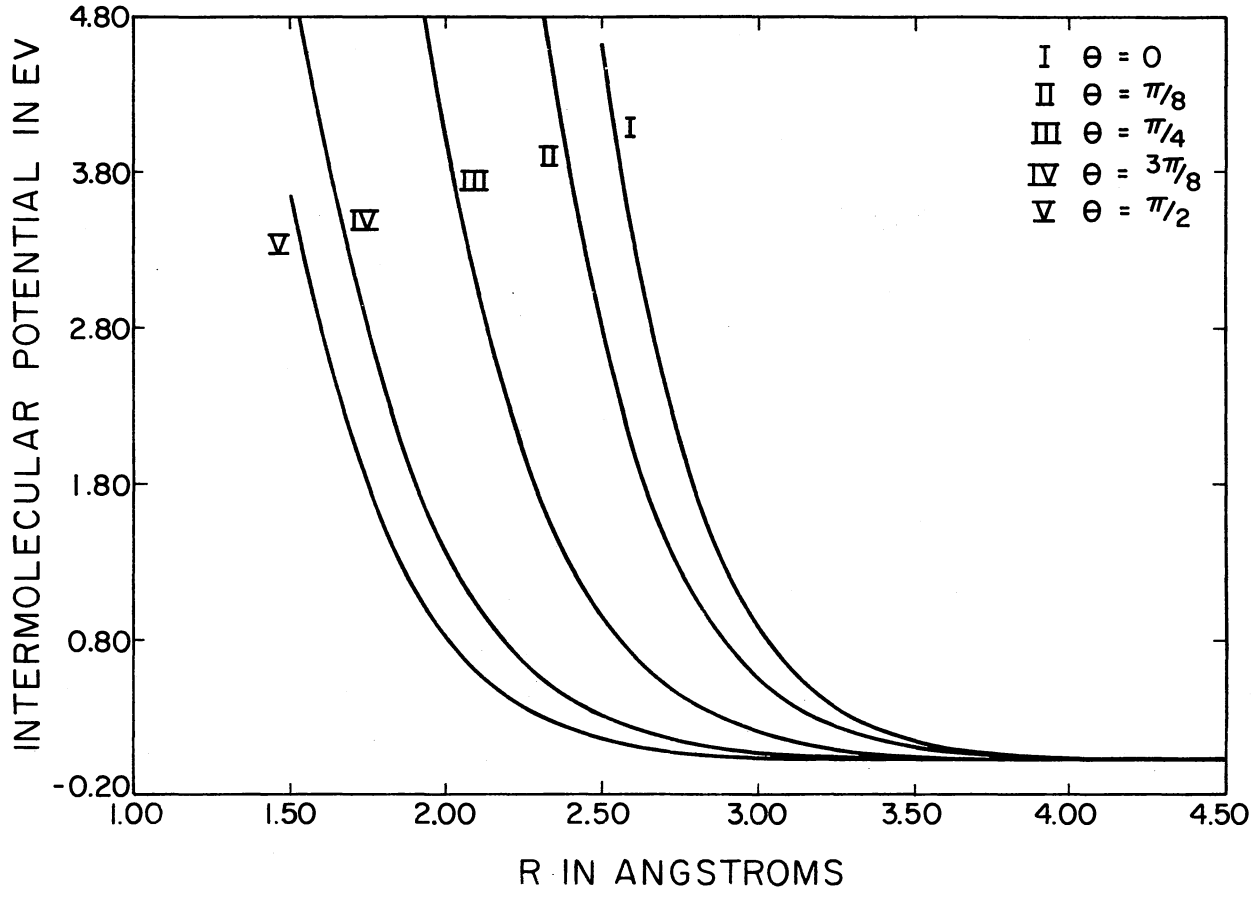

Figure 7. Plot of V vs R for $\phi = \pi/4$ and $0 \leq \theta \leq \pi/2$

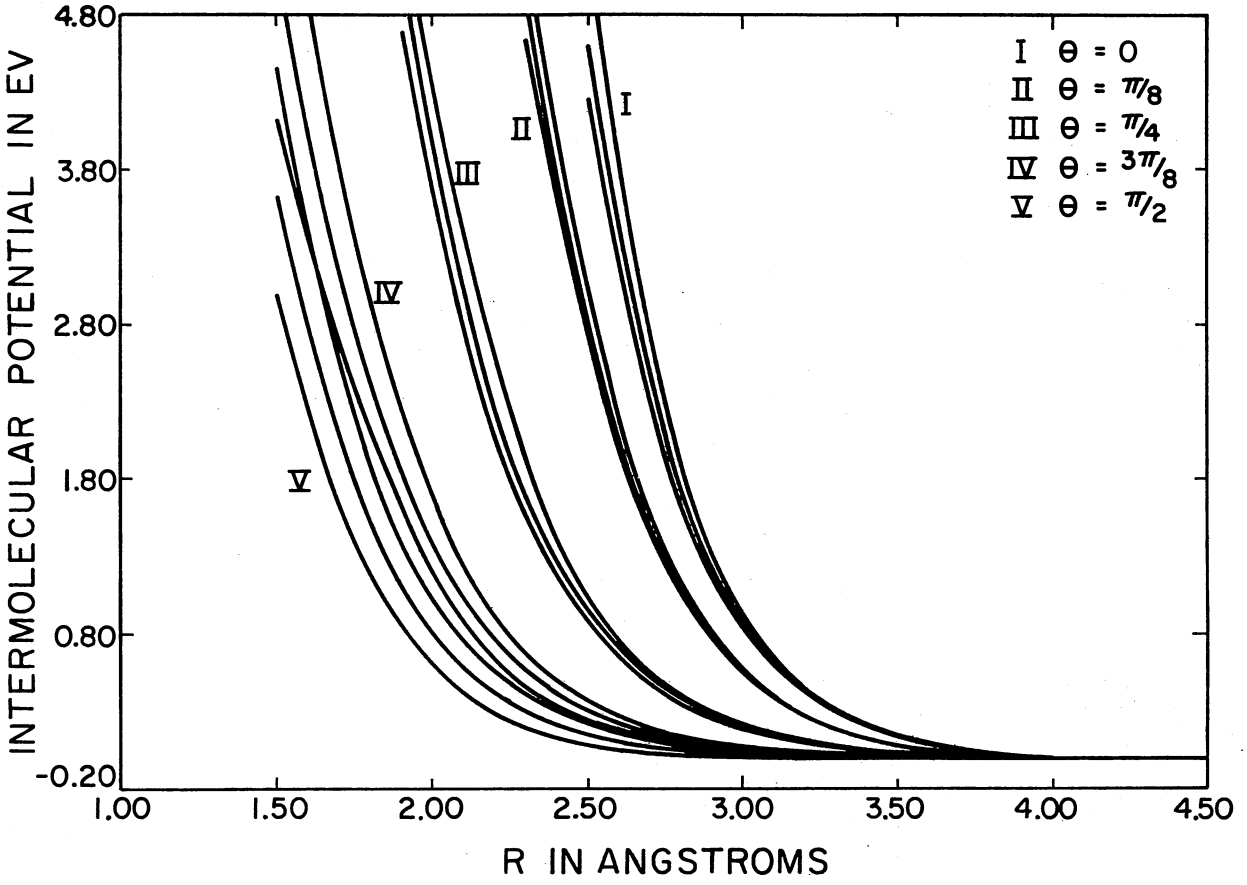

Figure 8. Plot of V vs R for $0 \leq \theta \leq \pi/2$ and $0 \leq \phi \leq \pi/2$

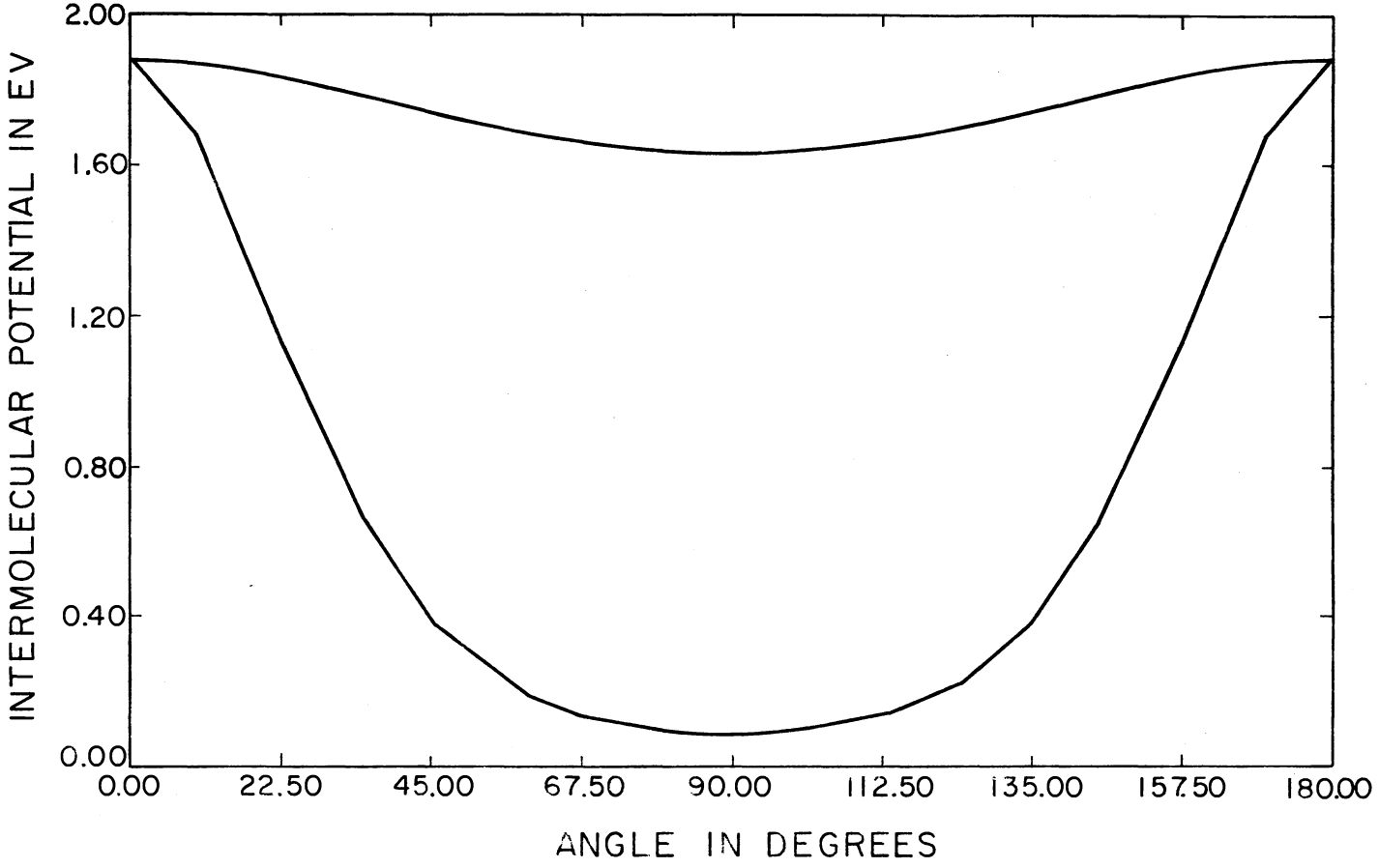

Figure 9. The Potential Against ϕ and θ for R = 2.8 Å. Along the Top Curve θ = 0 and Along the Bottom Curve ϕ = 0

TABLE IV

PARAMETERS FOR BUCKINGHAM-6-EXP AND -6,8-EXP FUNCTION-FIT TO INTERMOLECULAR POTENTIAL AS A FUNCTION OF R.

FUNCTION: $Aexp(-BR) - C/R^6$

Orientation	A	B	C	Std. Deviation/ kcal/mole
$\theta = \pi/2, \phi = \pi/2$	18197.363	3.332088	633.740739	0.02
$\theta = \pi/2, \phi = \pi/4$	14941.187	3.166095	512.63576	0.05
$\theta = \pi/2, \phi = 0$	12332.596	3.031009	318.39683	0.06
$\theta = \pi/4, \phi = \pi/2$	35332.310	2.863556	1877.2844	0.10
$\theta = \pi/4, \phi = \pi/4$	35502.304	2.766954	3116.2839	0.20
$\theta = \pi/4, \phi = 0$	60448.212	3.022612	1885.9131	0.03
$\theta = 0, \quad \phi = 0$	434081.49	3.2207934	4631.3604	0.02

Function: $Aexp(-BR) - C/R^6 - D/R^8$

Orientation	A	B	C	D	Std. Deviation/ kcal/mole
$\theta = \pi/2, \phi = \pi/2$	17544.272	3.2947341	681.06552	-97.973643	0.02
$\theta = \pi/2, \phi = \pi/4$	15735.892	3.2119111	397.97521	202.51047	0.04
$\theta = \pi/2, \phi = 0$	12992.140	3.0915746	118.76246	321.92372	0.05
$\theta = \pi/4 \quad \phi = \pi/2$	75761.984	3.1312229	116.79657	15031.561	0.02

The variation of potential with respect to two variables is represented by a series of intermolecular potential contour plots in Figures 10-18. It is difficult to write functions with more than one independent variable to describe the variation of these potential values correctly. In the early stages of the study using Marquardt's method (63), about 100 potential values (some of them were for nonzero τ also) were fitted to a 50 parameter function described in Appendix C with a standard deviation of 0.165 kcal/mole only to find out that it could not predict the potential correctly at 'arbitrary' conformations especially when R is large. Since attempts to fit the data to an analytic function proved futile, attention was diverted to numerical interpolation. The best choice proved to be a three dimensional cubic spline interpolation method. Details of the method, with a critical study of its accuracy and usefulness in a molecular dynamics study are presented in Chapter III. The same method is used in interpolating the intermolecular potential for the CO_2-H_2 system.

Derivatives of the Potential Energy of the System

Quasiclassical trajectory studies use the derivatives of the potential energy with respect to the coordinates of the system. Once the derivatives with respect to the distances and angles have been evaluated, they can easily be transformed to derivatives with respect to the cartesian coordinates of the system. For details of the coordinates and distances used the reader is referred to Figure 19. The potential energy of the system has already been described:

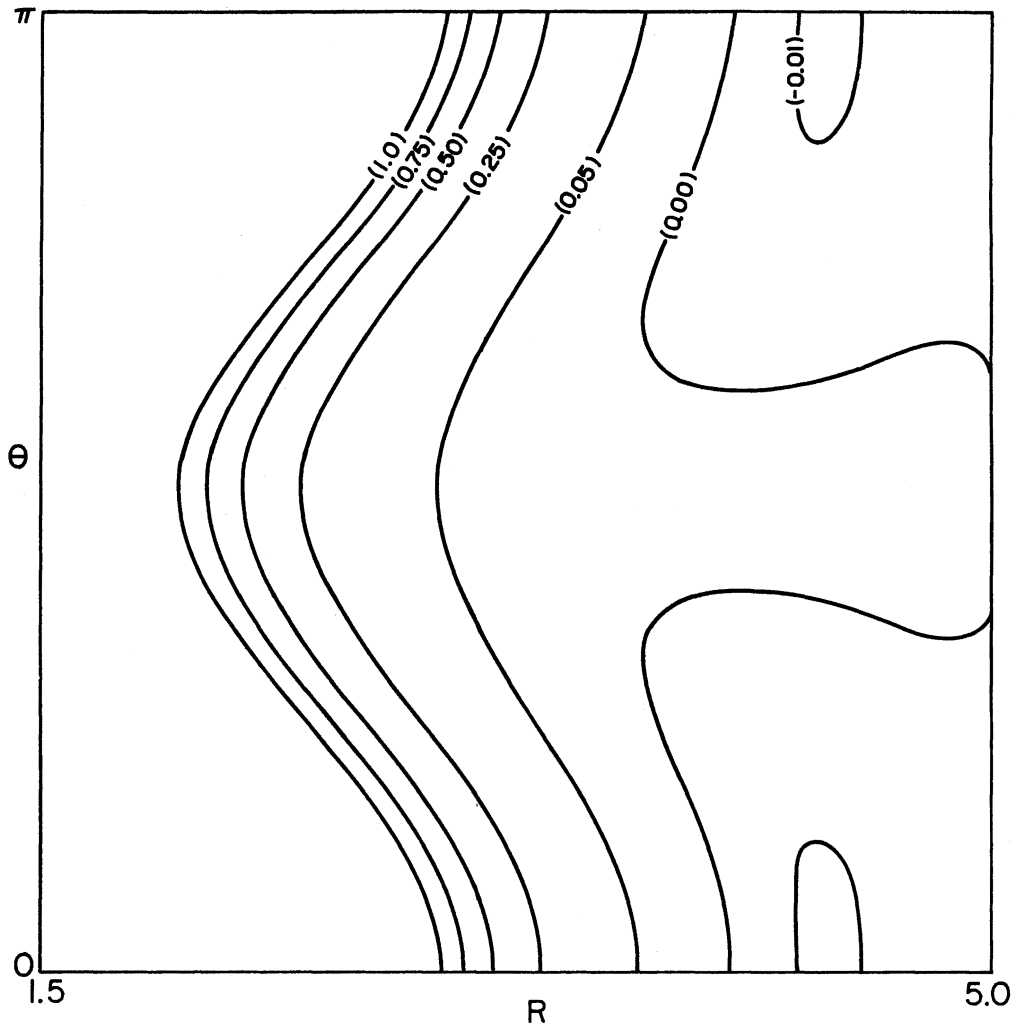

Figure 10. Intermolecular Potential Contours for $\phi = 0$

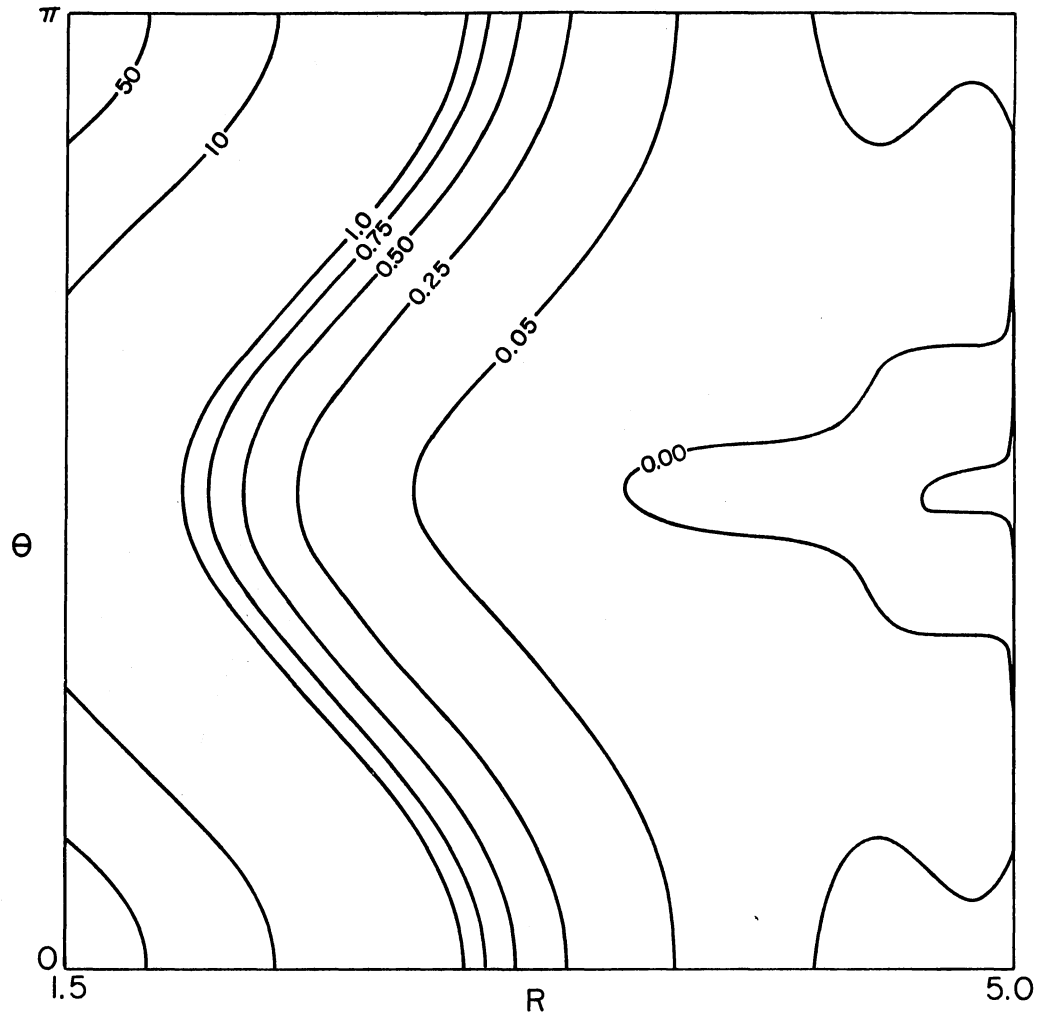

Figure 11. Intermolecular Potential Contours for $\phi = \pi/4$

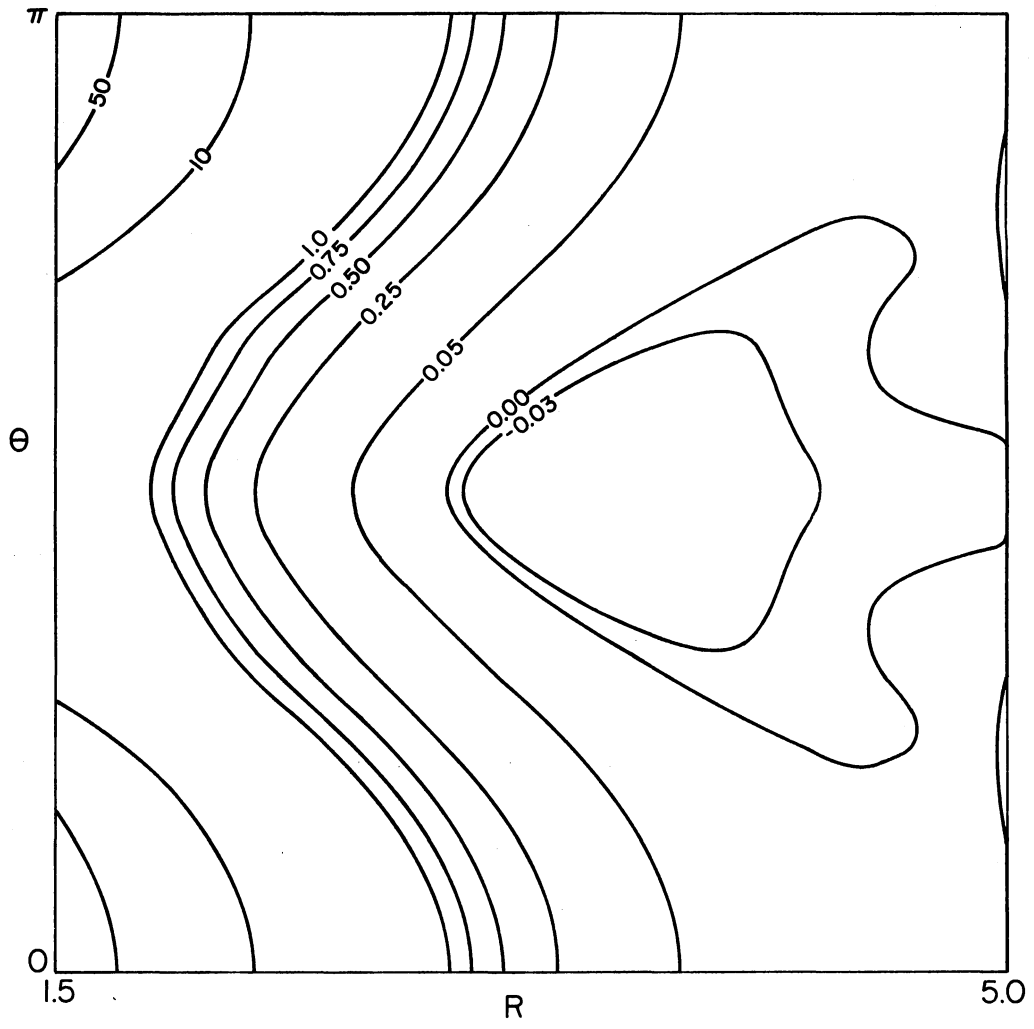

Figure 12. Intermolecular Potential Contours for $\phi = \pi/2$

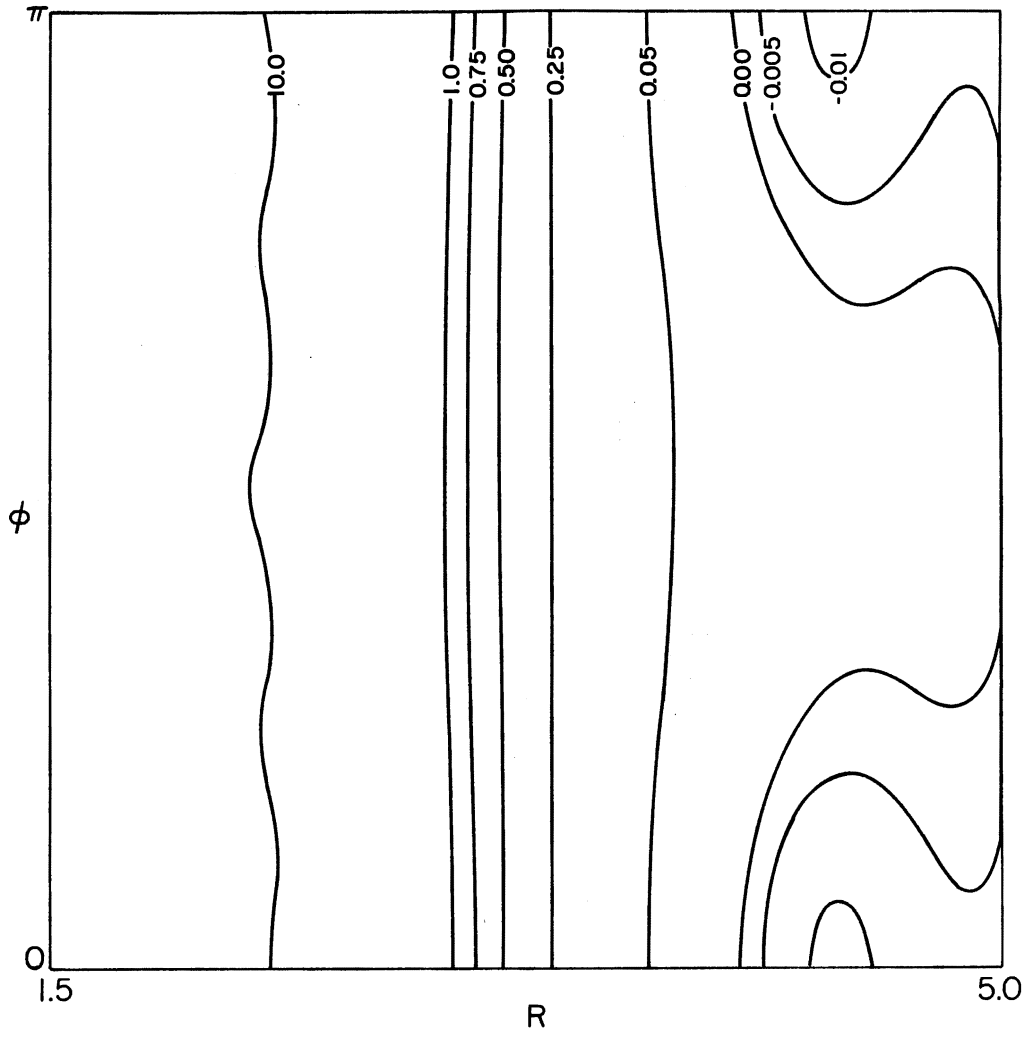

Figure 13. Intermolecular Potential Contours for $\theta = 0$

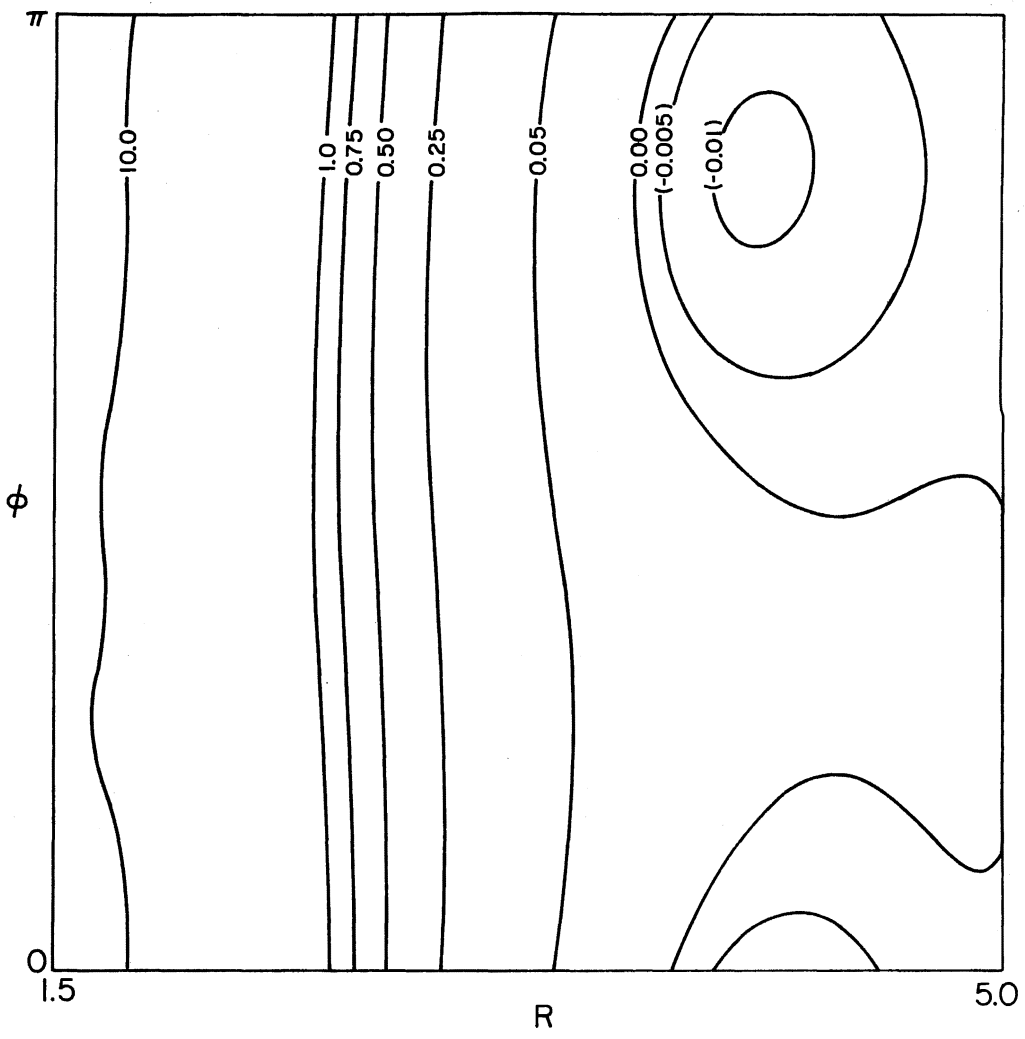

Figure 14. Intermolecular Potential Contours for $\theta = \pi/4$

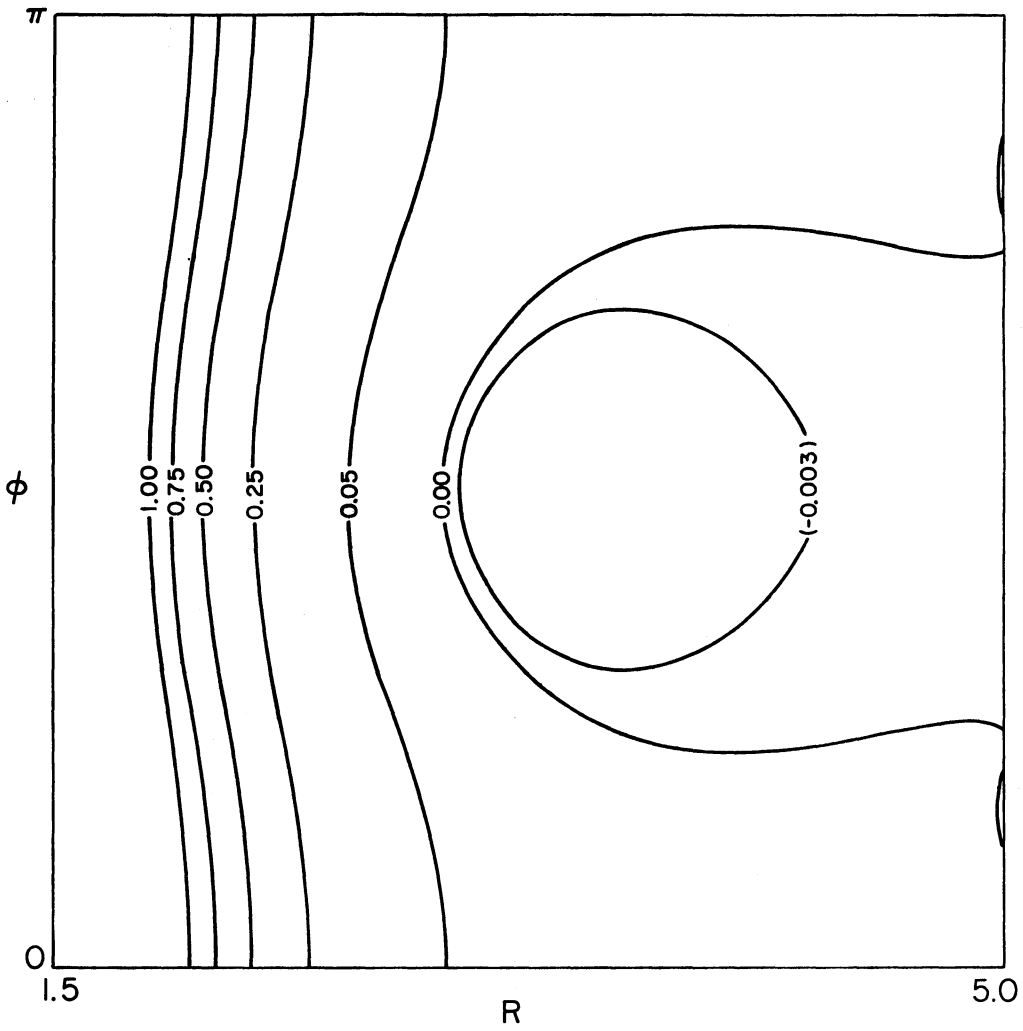

Figure 15. Intermolecular Potential Contours for $\theta = \pi/2$

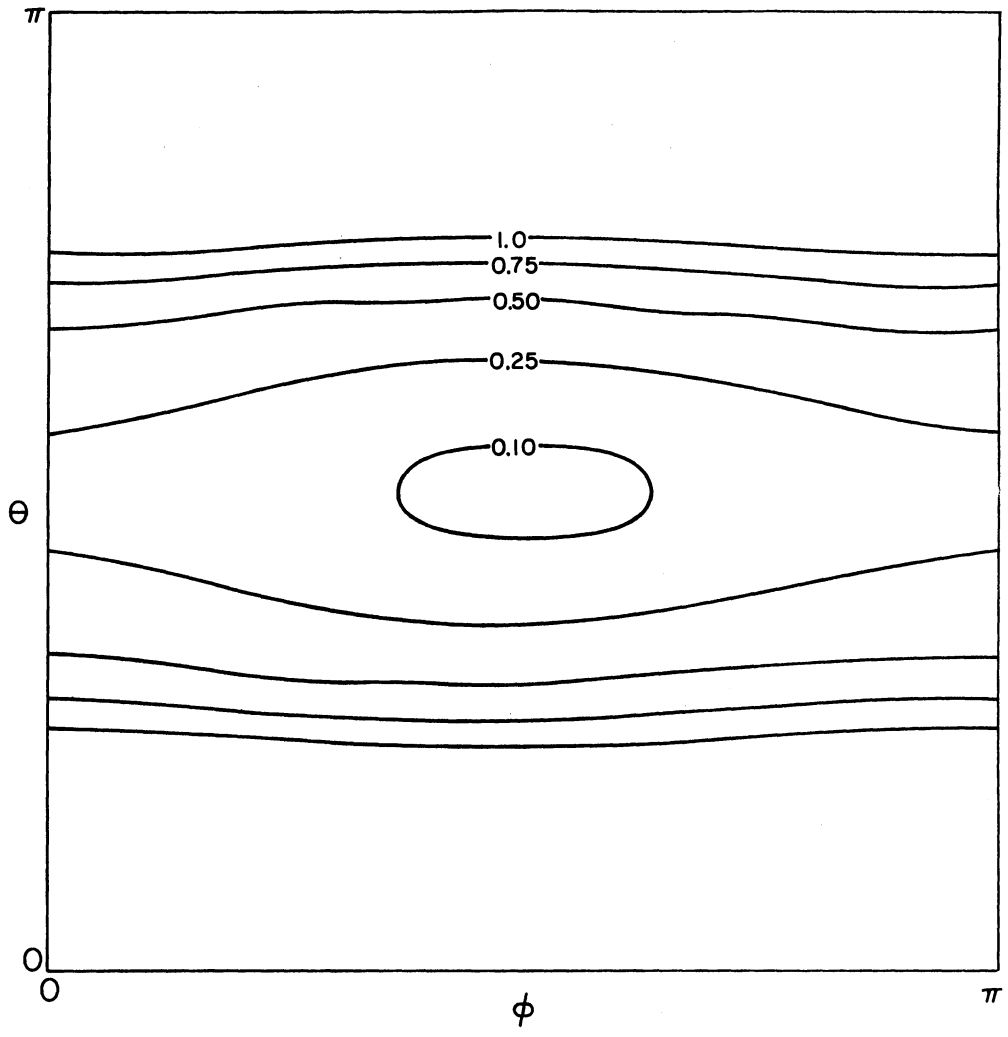

Figure 16. Intermolecular Potential Contours When R = 2.5 Å

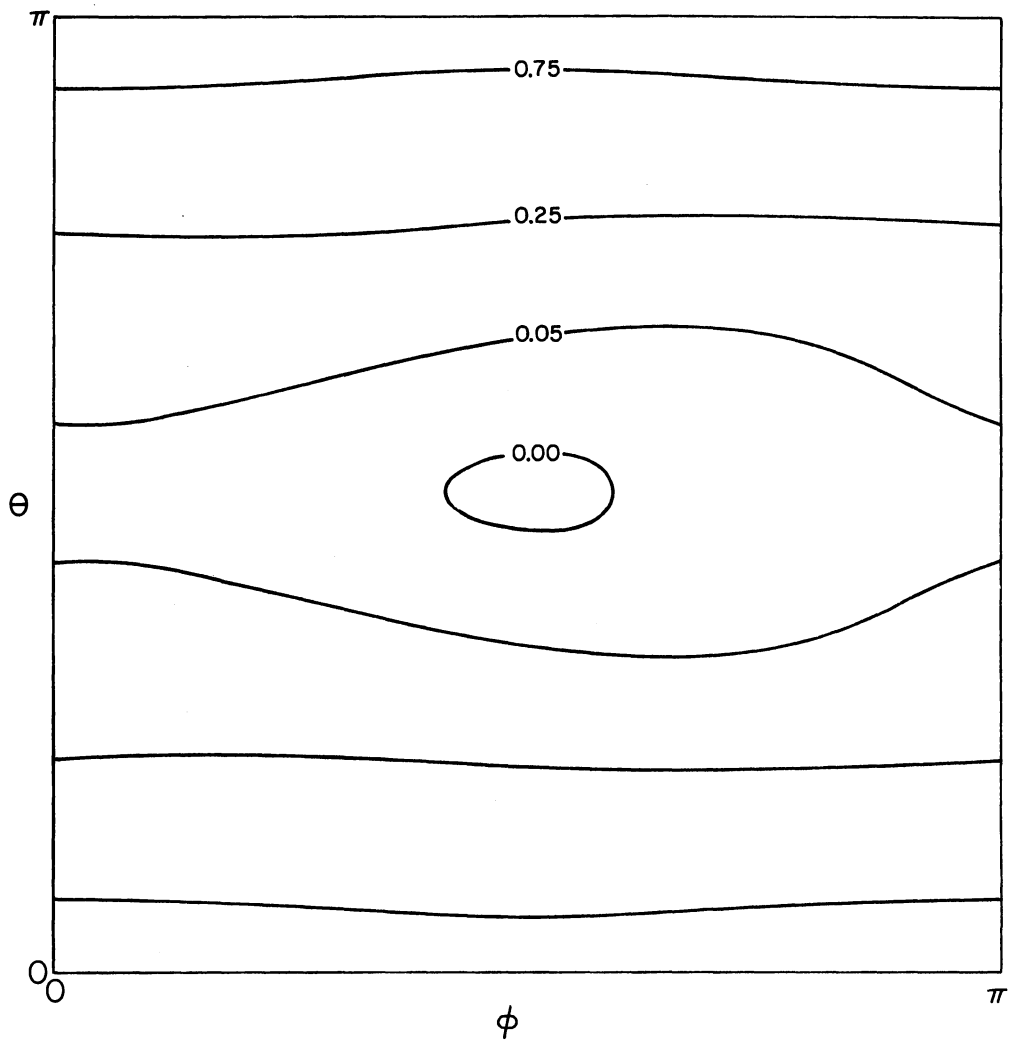

Figure 17. Intermolecular Potential Contours When R = 3.0 Å

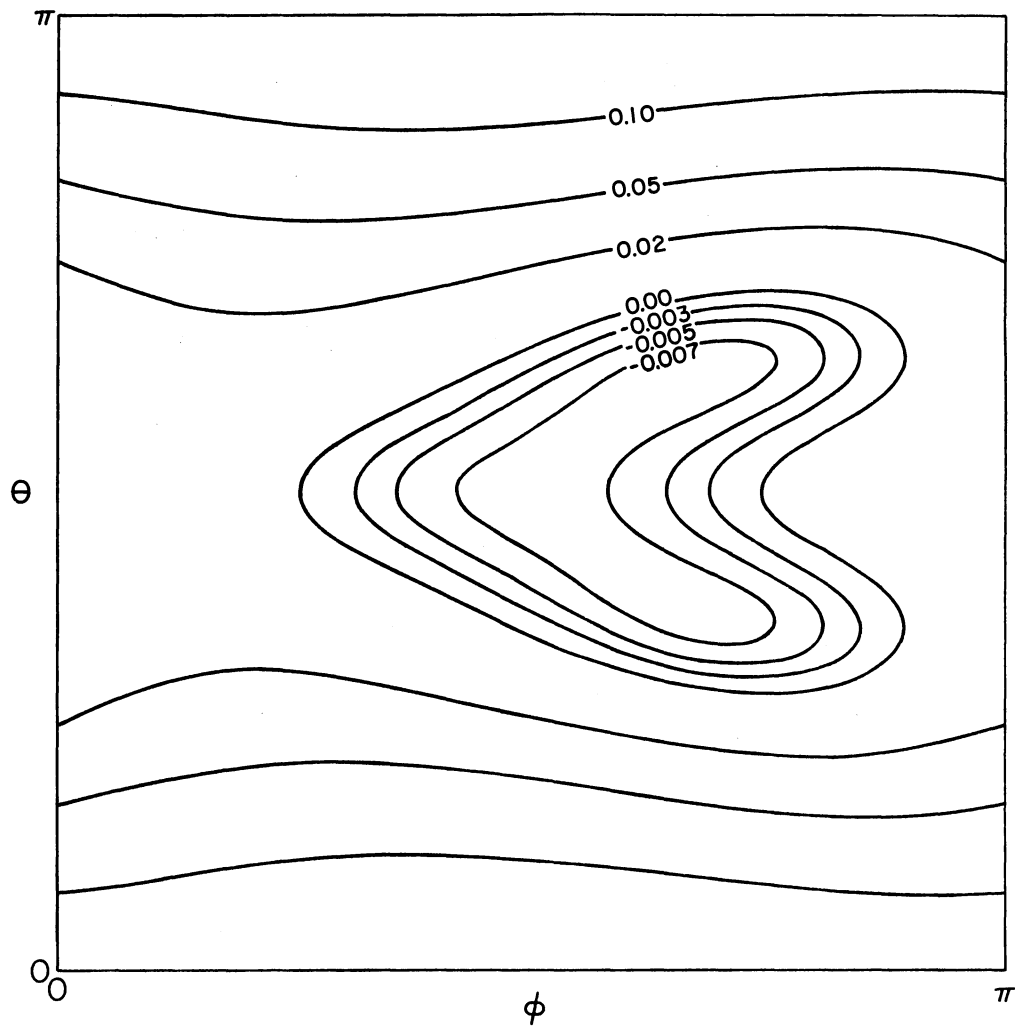

Figure 18. Intermolecular Potential Contours for R = 3.5 Å

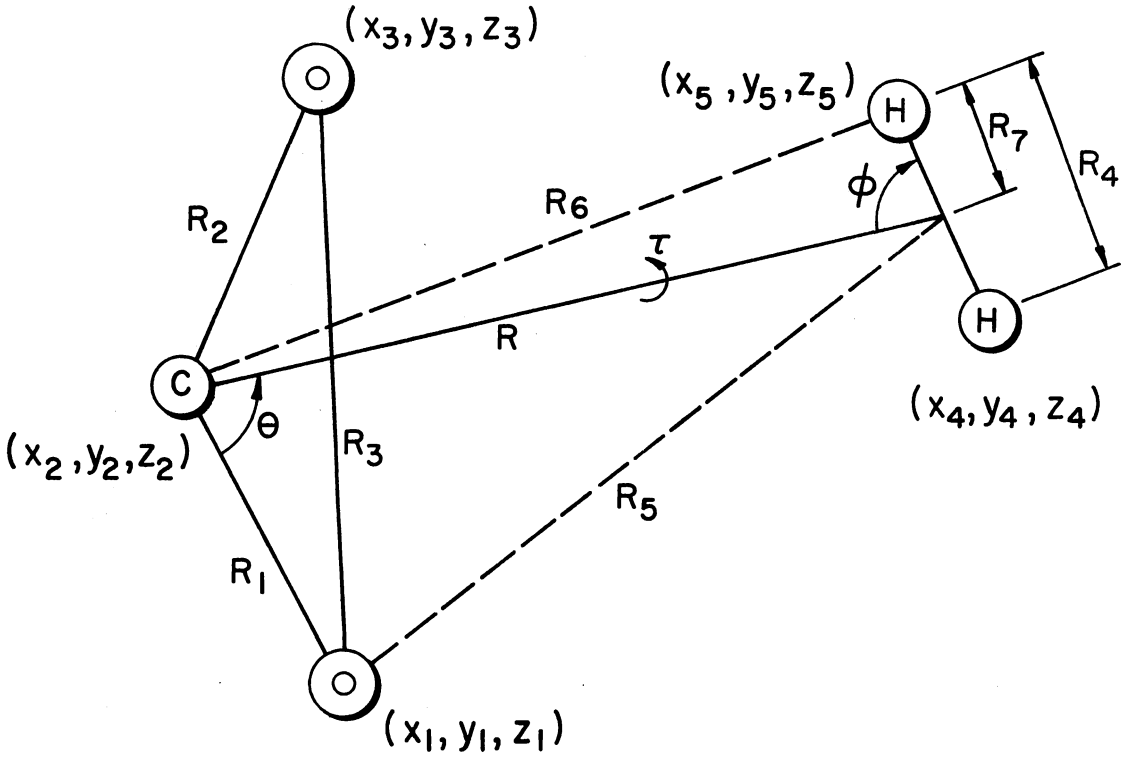

Figure 19. Coordinates, Distances and Angles Used in Calculation of Derivatives of Potential-Energy of the CO_2-H_2 System

$$V = V_{CO_2} + V_{H_2} + V_{inter}$$

$$= V_{CO_2}(R_1,R_2,R_3) + V_{H_2}(R_4) + V_{inter}(R,\theta,\phi). \qquad \text{(II-7)}$$

Since we assumed the potential to be independent of angle τ, the derivative of the potential with respect to an ith coordinate, q_i, is

$$\frac{\partial V}{\partial q_i} = \frac{\partial V_{CO_2}}{\partial q_i} + \frac{\partial V_{H_2}}{\partial q_i} + \frac{\partial V_{inter}}{\partial q_i}$$

$$= \sum_{j=1}^{3} \frac{\partial V_{CO_2}}{\partial R_j} \frac{\partial R_j}{\partial q_i} + \frac{\partial V_{H_2}}{\partial R_4} \frac{\partial R_4}{\partial q_i} + \frac{\partial V_{inter}}{\partial R} \frac{\partial R}{\partial q_i}$$

$$+ \frac{\partial V_{inter}}{\partial \theta} \frac{\partial \theta}{\partial q_i} + \frac{\partial V_{inter}}{\partial \phi} \frac{\partial \phi}{\partial q_i} . \qquad \text{(II-8)}$$

Relations between angles and distances and distances and coordinates are as follows:

$$\theta = \arccos\left[\frac{R_1^2 + R^2 - R_5^2}{2R_1R}\right]$$

$$\phi = \arccos\left[\frac{R_7^2 + R^2 - R_6^2}{2R_7R}\right] = \arccos\left[\frac{R_7^2 + R^2 - R_6^2}{R_4R}\right] \qquad \text{(II-9)}$$

$$R_1^2 = (x_2 - x_1)^2 + (y_2 - y_1)^2 + (z_2 - z_1)^2$$

$$R_2^2 = (x_2 - x_3)^2 + (y_2 - y_3)^2 + (z_2 - z_3)^2$$

$$R_3^2 = (x_3 - x_1)^2 + (y_3 - y_1)^2 + (z_3 - z_1)^2$$

$$R^2 = \left(\frac{x_4 + x_5}{2} - x_2\right)^2 + \left(\frac{y_4 + y_5}{2} - y_2\right)^2 + \left(\frac{z_4 + z_5}{2} - z_2\right)^2$$

$$R_4^2 = (x_4 - x_5)^2 + (y_4 - y_5)^2 + (z_4 - z_5)^2$$

$$R_5^2 = \left(\frac{x_4 + x_5}{2} - x_1\right)^2 + \left(\frac{y_4 + y_5}{2} - y_1\right)^2 + \left(\frac{z_4 + z_5}{2} - z_1\right)^2$$

$$R_6^2 = (x_5 - x_2)^2 + (y_5 - y_2)^2 + (z_5 - z_2)^2$$

$$R_7^2 = R_4^2/4 \quad . \tag{II-10}$$

The calculation of the derivatives of distances with respect to the coordinates is trivial and only the nonzero derivatives of angles with respect to distances are reported here:

$$\begin{aligned}
\partial\theta/\partial R_1 &= (R\cos\theta - R_1)/R_1 R \sin\theta \\
\partial\theta/\partial R &= (R_1\cos\theta - R)/R_1 R \sin\theta \\
\partial\theta/\partial R_5 &= R_5/R_1 R \sin\theta \\
\partial\phi/\partial R &= (R_7\cos\phi - R)/RR_7 \sin\phi \\
\partial\phi/\partial R_7 &= (R\cos\phi - R_7)/RR_7 \sin\phi \\
\partial\phi/\partial R_6 &= R_6/R_7 R \sin\phi
\end{aligned} \tag{II-11}$$

Values of $(\frac{\partial V_{inter}}{\partial R})$, $(\frac{\partial V_{inter}}{\partial \theta})$, and $(\frac{\partial V_{inter}}{\partial \phi})$ are obtained from the 3D spline interpolation. The derivatives with respect to R_1, R_2, R_3 and R_4 are:

$$\begin{aligned}
\partial V/\partial R_1 &= 2\alpha_M D_e[\exp(-\alpha_M \Delta R_1) - \exp(-2\alpha_M \Delta R_1)] \\
&\quad + F_R \Delta R_2 + F_\alpha R_e^2 \Delta\alpha(\frac{1}{R_2} - \frac{U}{R_1})(1 - U^2)^{-\frac{1}{2}}
\end{aligned}$$

$$\begin{aligned}
\partial V/\partial R_2 &= 2\alpha_M D_e[\exp(-\alpha_M \Delta R_2) - \exp(-2\alpha_M \Delta R_2)] \\
&\quad + F_R \Delta R_1 + F_\alpha R_e^2 \Delta\alpha(\frac{1}{R_1} - \frac{U}{R_2})(1-U^2)^{-\frac{1}{2}}
\end{aligned}$$

$$\partial V/\partial R_3 = -F_\alpha R_e^2 \Delta\alpha(1 - U^2)^{-\frac{1}{2}} R_3/(R_1 R_2)$$

$$\partial V/\partial R_4 = 2\alpha_{H_2} D_{e_{H_2}} [\exp(-\alpha_{H_2} \Delta R_4) - \exp(-2\alpha_{H_2} \Delta R_4)] \tag{II-12}$$

Appendix D lists expressions for derivatives of the total potential with respect to each of the cartesian coordinates after omission of the zero-valued quantities.

Validity of the Potential Energy of the System

The lack of detailed experimental knowledge of the potential energy of the CO_2-H_2 system makes it difficult to assess its accuracy. Only the qualitative features of the hypersurface have been checked as has been described in the earlier part of the chapter. Recent ab initio calculations reportedly have yielded satisfactory results for the intermolecular potentials of different systems (65) like $(HF)_2$, H_2O-H_2 and HCN-HF. Short range interactions are known to be well-predicted by single determinant LCAO-MO-SCF calculations for closed shell systems (65), while accurate predictions of long range forces requires the use of configuration interaction studies (66). It is generally believed that short range forces play a dominant role in vibrational energy transfer processes (33) and hence, it is likely that this potential-energy hypersurface for CO_2-H_2 is sufficiently accurate to yield meaningful results in a molecular dynamics study. Plans are being made to carry out configuration interaction calculations on this system to further assess its accuracy.

In order to choose the appropriate basis set for our calculation, potential energies of CO_2 and H_2 were calculated using different basis sets, and the results are reported in Table V. The energy is lower when extended basis sets rather than minimal basis sets are used. Results are improved when the number of gaussian functions is increased. However, the improvement is less for the case of the interaction

TABLE V

ENERGY VALUES FROM CALCULATIONS USING DIFFERENT BASIS SETS

	minimal basis sets				extended basis sets		
Molecule	STO-3G	STO-4G	STO-5G	STO-6G	4-31G	5-31G	6-31G
CO_2	-185.06838	-186.39854	-186.74824	-186.85532	-187.32797	-187.47666	-187.51497
H_2	-1.11751	-1.12397	-1.12566	-	-1.12683	-1.12683	-1.12683

potential (V) and is still less in the case of the difference in interaction potentials (ΔV). This is illustrated in Table VI. Since only the derivatives of the potential and not the absolute values are of interest to us, extended basis (4-31G) set should suffice our purposes.

Preliminary studies were made to test the validity of the assumption that the intermolecular potential is independent of the geometry of the individual molecules and is also independent of the angle τ. Intermolecular potentials were computed for the CO_2-H_2 system at three different $\{R,\theta,\phi\}$ for $\tau = 0$ with both molecules in their equilibrium geometries or either of them in a distorted configuration. A comparison of the results given in Table VII shows that the error involved is not serious. Results for different τ but same $\{R,\theta,\phi\}$ are reported in Table VIII. Obviously, the change in potential with change in τ of as much as $\pi/2$ is not significantly large (maximum being 0.035 eV) when compared to the result of corresponding change in θ or ϕ. The increased effort involved in computing more ab initio points and the fact that 'good' four-dimensional interpolation procedures are not available makes this change less important.

The present study uses only a 13x9x9 grid in the $\{R,\theta,\phi\}$ space of the intermolecular potential hypersurface. The interpolation reproduces the input data but this is not necessarily a reliable check on the accuracy of the numerical interpolation. At typical conformations encountered during the course of a nonreactive trajectory, the interpolated values are compared with the ab initio results in Table IX, and the agreement is good, the standard deviation being 0.014 eV. It may be possible to improve the agreement by imposing the boundary condition $F_1 = F_N$, $F''_1 = F''_N$ in the θ and ϕ axes instead of using

TABLE VI

RESULTS OF INTERMOLECULAR POTENTIALS USING DIFFERENT BASIS SETS

Configuration	4-31G		5-31G		6-31G	
	E	$\Delta E = V_{inter}$	E	$\Delta E = V_{inter}$	E	$\Delta E = V_{inter}$
CO_2	-187.327970		-187.476661		-187.514968	
H_2	-1.126828		-1.126828		-1.126828	
CO_2H_2, $R = \infty$	-188.454798	0.0	-188.603489	0.0	-188.641796	0.0
CO_2H_2, $R = 1.8$, $\theta = \phi = \tau = \pi/2$	-188.408541	0.04626	-188.557129	0.04636	-188.595416	0.04638
CO_2H_2, $R = 4.0$, $\theta = \phi = \tau = 0$	-188.454729	0.00007	-188.603356	0.00013	-188.641660	0.00014
Change in intermolecular potential		0.04619		0.04623		0.04624

TABLE VII

INTERACTION POTENTIAL FOR EQUILIBRIUM AND NON-EQUILIBRIUM GEOMETRIES

Configuration	Energy	Interaction Potential		V_{inter} for Equil. geometries
CO_2^{eq}	-187.32797			
H_2^{eq}	-1.12683			
CO_2^{*}	-187.32092			
H_2^{*}	-1.11774			
$CO_2^{*}H_2^{eq}$, $R = 2.5$, $\theta = \phi = \pi/2$	-188.44476	0.00299	Average = 0.00310	0.00308
$CO_2^{eq}H_2^{*}$, $R = 2.5$, $\theta = \phi = \pi/2$	-188.44249	0.00322		
$CO_2^{*}H_2^{eq}$, $R = 1.8$, $\theta = \phi = \pi/2$	-188.40454	0.04321	Average = 0.04462	0.04379
$CO_2^{eq}H_2^{*}$, $R = 1.8$, $\theta = \phi = \pi/2$	-188.39967	0.04604		
$CO_2^{*}H_2^{eq}$, $R = 3.0$, $\theta = \phi = 0$	-188.40914	0.03861	Average = 0.03785	0.03782
$CO_2^{eq}H_2^{*}$, $R = 3.0$, $\theta = \phi = 0$	-188.40862	0.03709		

*Refers to distorted geometry: $r_{CO} = 1.20$ and $r_{HH} = 0.8564$ and eq refers to optimized geometry.

TABLE VIII

INTERMOLECULAR POTENTIAL AS A FUNCTION OF τ

			Potential Values in eV for		
R/Å	θ/rad	φ/rad	$\tau = 0$	$\tau = \pi/4$	$\tau = \pi/2$
1.5	$\pi/2$	$\pi/2$	3.0046	2.9977	2.9834
2.1	$\pi/2$	$\pi/2$	0.4193	0.4514	0.4818
3.0	$\pi/2$	$\pi/2$	-0.0030	0.0056	0.0143
2.1	$\pi/2$	$\pi/4$	0.5806	0.6006	0.6197
3.0	$\pi/2$	$\pi/4$	0.0186	0.0234	0.0282
3.0	$\pi/4$	$\pi/2$	0.1665	0.1726	0.1782
2.5	$\pi/4$	$\pi/4$	0.9601	0.9332	0.9562
3.0	$\pi/4$	$\pi/4$	0.2003	0.1652	0.1852

TABLE IX

COMPARISON OF (13x9x9) 3D SPLINE INTERPOLATED RESULTS WITH GAUSSIAN-70 RESULTS AT TYPICAL CONFORMATIONS

			V_{inter} in eV	
R/A°	θ/deg	φ/deg	Spline	Gaussian-70
4.90684	70.10	67.56	-0.0001	-0.0001
3.60775	79.89	58.54	-0.0016	-0.0002
2.64324	84.04	72.67	0.0526	0.0530
2.29157	87.88	99.47	0.2069	0.2062
2.27661	89.07	112.74	0.2429	0.2425
2.55840	93.24	127.11	0.1018	0.1035
2.95712	96.89	124.40	0.0153	0.0207
4.28538	126.79	33.47	0.0003	-0.0008
3.08976	126.94	15.12	0.0956	0.0789
2.63668	129.52	7.64	0.04876	0.4958
2.87553	130.28	17.72	0.2460	0.2202
3.16081	134.28	30.19	0.1143	0.0794
4.09819	142.72	53.09	0.0055	-0.0065
			Standard deviation	0.014 eV

Lagrangian interpolation method as described in Appendix E. Also, a finer grid may be employed for the interpolation. This may not necessarily require additional ab initio computations. Repeated application of 1D spline interpolation procedure along each line of the grid may be sufficient enough to accomplish this as 1D spline interpolation is far more accurate than 2D and 3D spline interpolations. The accuracy of the derivatives of the potential cannot be tested with complete certainty as no known values are available. However, correct behavior of derivatives is ensured in the framework of spline interpolation procedure, i.e., the function and the first and second derivatives are required to be continuous at the knots. Therefore, it is hoped that the 13x9x9 grid interpolation yields reasonably accurate derivatives of the potential with respect to R, θ and ϕ.

CHAPTER III

QUASICLASSICAL TRAJECTORY STUDIES USING 3D SPLINE INTERPOLATION OF AB INITIO SURFACES

Ab initio calculations yielded tables of numbers for the (CO_2-H_2) intermolecular potential. As was indicated in Chapter II, initial attempts to fit those values to an analytic function were unsuccessful. Therefore, three dimensional cubic spline interpolation method was employed to interpolate the potential-energy values numerically. The computer code for this procedure has been written and its accuracy tested by quasiclassical trajectory studies on He + H_2^+ and D + ClH systems. The following is a reproduction of the paper that has been accepted for publication in the Journal of Chemical Physics and it describes the method and the results obtained in our study.

Introduction

The investigation of the dynamics of a chemical reaction under conditions for which the Born-Oppenheimer separation of electronic and nuclear motion is accurate requires that the stationary-state Schrodinger Equation be solved for the system energy as a function of the nuclear coordinates. If this solution is to be effected by an ab initio procedure, a number of difficulties immediately arise. First, a majority of collisional systems of interest may involve large, many-electron atoms so that the mathematical difficulties encountered in the

accurate solution of the Schrodinger Equation become insurmountable. Second, if the system has sufficient simplicity to permit solution of the quantum mechanical problem, the number of statistically important nuclear geometries for which the energy must be computed may be so large so as to preclude the calculation. Finally, if the above two problems can be overcome, there arises the problem of using in a scattering calculation the discrete set of energy values that make up the ab initio potential-energy hypersurface. Such calculations generally require either the energy or the gradients of the energy over a continuum of nuclear geometries so that it becomes necessary to devise some method for interpolation between the discrete set of ab initio points and also for extracting the gradients of the hypersurface.

This latter problem has generally been attacked by fitting the computed ab initio energy values to some analytic function. For example, Krauss and Mies (67) employed a combination of exponential functions and Legendre polynomials to fit their numerical values for the He-H_2 surface. A similar form was also employed by Gordon and Secrest (68) to fit their results for this same system. White and Hayes (69) have carried out quantum mechanical scattering studies on the Li^+-H_2 system using an analytical fit to an ab initio surface obtained by Lester (70). The $D^+ + H_2$ reaction has been investigated by Csizmadia, Polanyi, Roach, and Wong (71) using a Wall-Porter (72) fit to the ab initio surface (73). More recently Polanyi and Schreiber (74) have investigated the $F + H_2$ reaction dynamics by fitting the collinear ab initio surface for FHH obtained by Bender, O'Neil, Pearson, and Schaefer (75) to an LEPS-type function (76).

While the above approach has been moderately successful, it encounters several obvious difficulties. The parametrized analytic function employed to fit the ab initio surface is arbitrary and may fit well in some regions but poorly in others. The difficulties so encountered are illustrated by recent studies of inelastic scattering in the $He-H_2$ system by Alexander and Berard (77) using four different analytic fits to the Gordon-Secrest (68) ab initio potential surface. These difficulties have recently been discussed by Secrest (78) and by Alexander (79). In addition, a considerable amount of effort may be expended in an unsuccessful attempt to fit the ab initio points to a given form. For example, Polanyi and Schreiber (74) were unable to fit the Bender, et al. (75) surface using a hyperbolic map function (80), and Yarkoni, et al. (81) were unable to obtain a suitable analytic fit to their ab initio surface for the $(HF)_2$ system.

An alternate approach has recently been employed by McLaughlin and Thompson (82) in their study of the $HeH^+ + H_2$ reaction dynamics. In this study the SCF-CI ab initio surface obtained by Benson and McLaughlin (83) for the planar H_3He^+ system with C_{2v} symmetry was represented by a combination of a two-dimensional cubic spline fit and a one-dimensional cubic spline fit. These authors have concluded on the basis of their study that multidimensional spline fitting of ab initio points can serve as a useful, objective interpolator.

It is undoubtedly true that a spline fit has a number of attractive features. The procedure is relatively general; thus removing the necessity of making an arbitrary choice of an analytic interpolation function. The procedure ensures the continuity of the energy and the first two derivatives over the entire hypersurface and thus facilitates

the computation of the gradients required for a quasiclassical trajectory calculation. Several problems and unanswered questions remain however! A full, three-dimensional cubic spline fitting routine has yet to be developed and tested. The number of ab initio points needed is not accurately known. The relative increase in computer computation time over that required for analytic semiempirical surfaces is not known, and finally the overall accuracy of the procedure in quasiclassical trajectory studies has been only partially evaluated.

The present paper reports the development of a full three-dimensional cubic spline fitting routine. The accuracy of the spline procedure has been investigated for Morse potentials, Lennard-Jones potentials, and a collinear He-H_2^+ potential-energy hypersurface. In addition, its accuracy when employed in a three-dimensional quasiclassical trajectory study has been examined for the D + HCl exchange reaction and inelastic He-H_2^+ collisions. Section II presents the algorithm for three-dimensional spline interpolation. The results are given and discussed in Section III, and the final section summarizes all conclusions.

Three Dimensional Cubic Splines

The theory of splines has previously been discussed in several standard references (84). The treatment presented here closely follows that of Walsh, Ahlberg, and Nelson (84) and that of Jordan (85). McLaughlin and Thompson (82) have presented a similar discussion restricted to one and two-dimensional cubic splines.

The cubic spline approximation consists of joining the assigned points with cubics, requiring that the slopes and curvatures be

continuous at the junction points which are referred to as nodes or knots. Let x be a point in the ith interval, $x_i \le x \le x_{i+1}$. Further let $x_1 < x_2 < x_3 < \text{---} < x_{N-1} < x_N$. Let F(x) be the value of the function that is to be splinefitted, and let $S_i(x)$ be the approximating cubic spline in the ith interval:

$$S_i(x) = A_i x^3 + B_i x^2 + C_i x + D_i \ . \qquad \text{(III-1)}$$

Differentiation of Eq(III-1) twice followed by equating the result to F''(x) at the nodes yields

$$S_i''(x) = F_{i+1}'' \ \frac{(x - x_i)}{\Delta_i} + F_i'' \ \frac{(x_{i+1} - x)}{\Delta_i} \qquad \text{(III-2)}$$

where

$$\Delta_i = x_{i+1} - x_i \ . \qquad \text{(III-3)}$$

Integration of Eq(III-2) twice followed by equating the result to the function values at the nodes gives, after some algebraic rearrangement,

$$\begin{aligned} S_i(x) = {} & \frac{F_i''}{6\Delta_i} [x_{i+1} - x]^3 + \frac{F_{i+1}''}{6\Delta_i} [x - x_i]^3 \\ & + \left[\frac{F_{i+1}}{\Delta_i} - \frac{F_{i+1}''\Delta_i}{6}\right] [x - x_i] \\ & + \left[\frac{F_i}{\Delta_i} - \frac{F_i''\Delta_i}{6}\right] (x_{i+1} - x) \ . \end{aligned} \qquad \text{(III-4)}$$

The spline function is thus defined for arbitrary x in the ith interval in terms of the second derivatives at the ith and (i + 1) nodes. The first derivatives can be obtained directly from Eq(III-4):

$$S_i'(x) = \frac{-F_i''}{2\Delta_i}(x_{i+1} - x)^2 + \frac{F_{i+1}''}{2\Delta_i}(x - x_i)^2$$

$$+ (F_{i+1} - F_i)/\Delta_i - (F_{i+1}'' - F_i'')\Delta_i/6 \ . \qquad \text{(III-5)}$$

By requiring the derivatives to match at the nodes, i.e.,

$$S_i'(x_{i+1}) = S_{i+1}'(x_{i+1}) \ , \qquad \text{(III-6)}$$

the unknown second derivatives may be obtained in terms of the known function values. The result is

$$\frac{\Delta_i}{6}F_i'' + \frac{(\Delta_i + \Delta_{i+1})}{3}F_{i+1}'' + \frac{\Delta_{i+1}}{6}F_{i+2}''$$

$$= (F_{i+2} - F_{i+1})/\Delta_{i+1} - (F_{i+1} - F_i)/\Delta_i \ , \qquad \text{(III-7)}$$

for $(i = 1,2,3,4\ldots(N-2))$.

Equation (III-7) represents a set of N - 2 linear equations in N unknowns. Two more equations are therefore required to completely specify the spline fit. In the present work a four-point Lagrangian interpolation as described in Appendix E was employed to estimate the values of $S_1'(x_1)$ and $S_{N-1}'(x_N)$. These values, coupled with Eq(III-5), provide the two additional equations required for the one-dimensional spline fit.

The above equations may be recast in matrix form:

$$S_i(x) = \underset{\sim}{P}_i(x)^* \underset{\sim}{C}_i \ , \qquad \text{(III-8)}$$

where

$$\underset{\sim}{P}_i(x)^* = (P_i(x - x_i),\ P_i(x_{i+1} - x),\ P_i''(x - x_i),\ P_i''(x_{i+1} - x)) \qquad \text{(III-9)}$$

and

$$\underset{\sim}{C}_i^* = (F_{i+1}'',\ F_i'',\ F_{i+1},\ F_i) \qquad \text{(III-10)}$$

with

$$P_i(x) = \frac{x^3}{6\Delta_i} - \frac{x\Delta_i}{6} \quad . \tag{III-11}$$

The N linear equations yielding the second derivatives form a tridiagonal matrix equation which is easily solved (84a) (85). It has the form

$$\underset{\sim}{A}\underset{\sim}{F}'' = \underset{\sim}{B}\underset{\sim}{F} + \underset{\sim}{G} \tag{III-12}$$

where

$$\underset{\sim}{F}^* = (F_1, F_2, F_3, \ldots, F_N)$$

$$\underset{\sim}{F}''^* = (F_1'', F_2'', F_3'', \ldots, F_N'')$$

$$\underset{\sim}{G}^* = (-S_1'(x_1), 0, 0, \ldots 0, S_{N-1}'(x_N))$$

$$A_{11} = \Delta_1/3 \qquad A_{12} = \Delta_1/6 \qquad A_{1j} = 0 \quad \text{for } j > 2$$

$$B_{11} = -1/\Delta_1 \qquad B_{12} = 1/\Delta_1 \qquad B_{ij} = 0 \quad \text{for } j > 2$$

$$\left.\begin{aligned} A_{i,i-1} &= \Delta_{i-1}/6 \quad , \quad B_{i,i-1} = 1/\Delta_{i-1} \\ A_{ii} &= (\Delta_{i-1} + \Delta_i)/3 \quad , \quad B_{ii} = -[1/\Delta_i + 1/\Delta_{i-1}] \\ A_{i,i+1} &= \Delta_i/6 \quad , \quad B_{i,i+1} = 1/\Delta_i \end{aligned}\right\} \quad 2 \le i \le N-1$$

$$A_{ij} = 0 = B_{ij} \text{ for } j \neq i-1, i, \text{ or } i+1$$

and

$$A_{N,N-1} = \Delta_{N-1}/6 \quad , \quad A_{NN} = \Delta_{N-1}/3 \quad , \quad A_{Nj} = 0 \quad \text{for } j < N-1$$

$$B_{N,N-1} = 1/\Delta_{N-1} \quad , \quad B_{NN} = -1/\Delta_N \quad , \quad B_{Nj} = 0 \quad \text{for } j < N-1 \quad .$$

The above procedure has been extended to two-dimensions in a convenient manner by Jordan (85) and by DeBoor (86). Let the function to be splinefitted, F_{ij}, be given at grid coordinates (x_i, y_j) on a rectangular grid of points with interval sizes Δ_i and Δ_j in the x and y directions, respectively, where $i = 1,2, \ldots, I$ and $j = 1,2, \ldots, J$. Define $\underset{\sim}{P}_j(y)$ and $P_j(y)$ in a manner analogous to Eqs.(III-9) and

(III-11), respectively, and let F_{ij}^{xx} be F_i'' on the 1D spline curve to F_{ij} for fixed j with F_{ij}^{yy} being the corresponding quantity for the spline fit to F_{ij} at fixed i. The quantities F_{ij}^{yyxx} represent the fourth derivatives required by the 1D spline fit to F_{ij}^{yy} for fixed i with j = 1,2, ... , J. The second and fourth derivatives are obtained by repeated solution of Eq(III-12). The spline interpolation then has the form (85,86)

$$S_{ij}(x,y) = [P_i(x)^* C_{ij}]P_j(y) \qquad \text{(III-13)}$$

where

$$C_{ij} = \begin{bmatrix} F^{yyxx}_{i+1,j+1} & F^{yyxx}_{i+1,j} & F^{xx}_{i+1,j+1} & F^{xx}_{i+1,j} \\ F^{yyxx}_{i,j+1} & F^{yyxx}_{ij} & F^{xx}_{i,j+1} & F^{xx}_{ij} \\ F^{yy}_{i+1,j+1} & F^{yy}_{i+1,j} & F_{i+1,j+1} & F_{i+1,j} \\ F^{yy}_{i,j+1} & F^{yy}_{ij} & F_{i,j+1} & F_{ij} \end{bmatrix} \qquad \text{(III-14)}$$

for i = 1,2, ..., (I - 1) and j = 1,2, ..., (J - 1).

The first derivatives with respect to x and y are

$$S^x_{ij}(x,y) = [\underset{\sim}{P}'_i(x)^* \underset{\sim}{C}_{ij}]\underset{\sim}{P}_j(y)$$

and $$\qquad \text{(III-15)}$$

$$S^y_{ij}(x,y) = [\underset{\sim}{P}'_i(x)^* \underset{\sim}{C}_{ij}]\underset{\sim}{P}'_j(y) \ .$$

The extension of the procedure to three dimensions is straightforward. Following the earlier notation let $F_{i,j,k}$ be given at grid points (x_i,y_j,z_k) for i = 1,2, ..., I; j = 1,2, ..., J, and k = 1,2, ..., K. We now

(1) Splinefit $F_{i,j,k}$ for fixed (j,k) to determine $F^{xx}_{i,j,k}$

$(i = 1,2, \ldots, I)$.

(2) Repeat step (1) for fixed(i,k) to determine $F^{yy}_{i,j,k}$

$(j = 1,2, \ldots, J)$.

(3) Repeat step (1) for fixed (i,j) to determine $F^{zz}_{i,j,k}$

$(k = 1,2, \ldots, K)$.

(4) Splinefit the second partials to obtain $F^{yyxx}_{i,j,k}$, $F^{yyzz}_{i,j,k}$, and $F^{xxzz}_{i,j,k}$.

(5) Splinefit the values of $F^{yyxx}_{i,j,k}$ for each (i,j) pair to obtain $F^{yyxxzz}_{i,j,k}$.

Step (1) requires the solution of I linear equations given by Eq(III-2) for each fixed value of j and k. Thus the complete set of $F^{xx}_{i,j,k}$ values requires (J·K) sets of I linear equations to be solved. Steps (2) and (3) require the solution of (I·K) sets of J linear equations and (I·J) sets of K linear equations, respectively. Step (4) requires the solution of (J·K) sets of I linear equations and 2(J·I) sets of K linear equations. Finally, in the fifth step (I·J) sets of K equations must be solved.

The three-dimensional spline function is given by (19)

$$S_{i,j,k}(x,y,z) = \sum_{\ell=1}^{4} \sum_{m=1}^{4} \sum_{n=1}^{4} P_i^{\ell}(x)\, P_j^{m}(y) P_k^{n}(z)\, C^{\ell mn}_{i,j,k} \qquad \text{(III-16)}$$

where the elements of $P_i(x)$ are given by Eqs.(III-9) and (III-11) with $P_j(y)$ and $P_k(z)$ defined similarly, and

$$C^{\ell ml}_{i,j,k} = \begin{bmatrix} F^{yyxxzz}_{i+1,j+1,k+1} & F^{yyxxzz}_{i+1,j,k+1} & F^{xxzz}_{i+1,j+1,k+1} & F^{xxzz}_{i+1,j,k+1} \\ F^{yyxxzz}_{i,j+1,k+1} & F^{yyxxzz}_{i,j,k+1} & F^{xxzz}_{i,j+1,k+1} & F^{xxzz}_{i,j,k+1} \\ F^{yyzz}_{i+1,j+1,k+1} & F^{yyzz}_{i+1,j,k+1} & F^{zz}_{i+1,j+1,k+1} & F^{zz}_{i+1,j,k+1} \\ F^{yyzz}_{i,j+1,k+1} & F^{yyzz}_{i,j,k+1} & F^{zz}_{i,j+1,k+1} & F^{zz}_{i,k,k+1} \end{bmatrix}$$

and

$$C^{\ell m3}_{i,j,k} = \begin{bmatrix} F^{yyxx}_{i+1,j+1,k+1} & F^{yyxx}_{i+1,j,k+1} & F^{xx}_{i+1,j+1,k+1} & F^{xx}_{i+1,j,k+1} \\ F^{yyxx}_{i,j+1,k+1} & F^{yyxx}_{i,j,k+1} & F^{xx}_{i,j+1,k+1} & F^{xx}_{i,j,k+1} \\ F^{yy}_{i+1,j+1,k+1} & F^{yy}_{i+1,j,k+1} & F_{i+1,j+1,k+1} & F_{i+1,j,k+1} \\ F^{yy}_{i,j+1,k+1} & F^{yy}_{i,j,k+1} & F_{i,j+1,k+1} & F_{i,j,k+1} \end{bmatrix} \qquad \text{(III-17)}$$

In Eq(III-17) ℓ and m refer to row and column indices, respectively, and $C^{\ell m2}_{i,j,k}$ and $C^{\ell m4}_{i,j,k}$, are identical to $C^{\ell m1}_{i,j,k}$ and $C^{\ell m3}_{i,j,k}$, respectively, except that the index $k+1$ is replaced by k.

The first derivatives are computed from eq(III-16). They are

$$S^{x}_{i,j,k}(x,y,z) = \sum_{\ell=1}^{4} \sum_{m=1}^{4} \sum_{n=1}^{4} P_i^{\ell'}(x)\, P_j^{m}(y)\, P_k^{n}(z)\, C^{\ell mn}_{i,j,k} \qquad \text{(III-18)}$$

with similar equations for $S^{y}_{i,j,k}(x,y,z)$ and $S^{z}_{i,j,k}(x,y,z)$. The $P_i^{\ell'}(x)$ values are readily obtained from Eq(III-11).

Results and Discussion

An indication of the accuracy of a one-dimensional spline fit has been investigated for the cases of chemical bond potentials and weak van der Waals type interactions. The Morse function for the H_2 molecule (76) and the Lennard-Jones potential for the Ar_2 molecule (87) were used to generate function values at different nodes. These values were then splinefitted using Eqs(III-8)-(III-12) with a four-point Lagrangian interpolation being used to compute the first derivatives at the end points. Tables X and XI give representative results chosen at random for a 15-point spline fit. It is apparent that the function values are well represented by the spline fit. For example, the

TABLE X

COMPARISON OF A 15-POINT SPLINE FIT WITH EXACT RESULTS FROM MORSE POTENTIAL FOR H_2 (ALL ENERGY VALUES ARE IN eV)

R (au)	Function Value		First Derivative	
	Exact[a]	Spline	Exact[a]	Spline
0.9	-2.49189	-2.49188	-11.5424	-11.5573
1.4	-4.74658	-4.74657	-0.02080	-0.02071
1.9	-3.96600	-3.96664	2.39007	2.38509
2.5	-2.53682	-2.53708	2.14903	2.14609
3.3	-1.2178	-1.2178	1.1777	1.1776
3.9	-0.67321	-0.67314	0.67619	0.67593
4.7	-0.29827	-0.29826	0.30644	0.30660
Std. Deviation:		.00028		0.00237

[a]Reference 76

TABLE XI

COMPARISON OF A 15-POINT SPLINE FIT WITH EXACT RESULTS FROM LENNARD-JONES POTENTIAL FOR Ar_2 MOLECULE (ENERGY VALUES IN JOULES)

R (Å)	Function Value x 10^{20}		First Derivative x 10^{20}	
	Exact[a]	Spline	Exact[a]	Spline
3.332	0	0.56541 x 10^{-3}	-1.1741	-1.1792
3.6	-.15221	-0.15221	-.17578	-.17610
3.74	-.16300	-.16305	-.000036539	+0.002169
4.0	-.14505	-.14525	+.10842	+.11316
4.4	-.099771	-.099774	+.10443	+.10442
5.2	-.042005	-.041995	+.044864	+.044974
6.0	-.018563	-0.18563	+.018002	+.01905
Std. Deviation:		.00025 x 10^{-20}		.00301 x 10^{-20}

[a]Reference 87

standard deviation at 100 randomly selected values of R, ($0.9 \leq R \leq 4.7$) for H_2 is 0.00028. The values of the first derivatives are in reasonable accord with the exact result although the accuracy of the fit is substantially lower than that for the function value itself. This reduced accuracy is reflected by an increased standard deviation of 0.00237.

It is of some importance to examine the variation of the standard deviation with the number of fitting nodes employed. Table XII gives representative results for the H_2 system. As can be seen, there is initially a substantial increase in accuracy as the number of nodes is increased, but the rate of this increase rapidly decreases as the number of nodes rises.

We have also examined the accuracy of one-dimensional spline fits to ab initio results for He - He (88), Xe - Xe, Xe - Ne, and Xe - Ar (89). In general, the accuracy of these fits were found to be comparable to that obtained for H_2 and Ar_2.

The accuracy of a two-dimensional spline fit has been investigated using the semiempirical potential-energy surface for the D-Cl-H system previously employed by Porter, Sims, Thompson, and Raff (90). Both a (10 x 10) and a (15 x 15) spline fit were examined for collinear D-Cl-H conformations with the node positions being chosen so that the node density was approximately proportional to the surface curvature. Figures 20 and 21 show the nodal positions for each fit. Table XIII gives representative results chosen at random for each spline fit. The standard deviations for the function value and both first derivatives are also given. Several points are clear: (1) The (15 x 15) splinefit yields a substantial increase in accuracy. The standard deviations are

TABLE XII

VARIATION OF THE STANDARD DEVIATION OF THE SPLINE INTERPOLATED RESULTS FROM THE EXACT VALUES FOR A MORSE POTENTIAL FOR H_2 AS A FUNCTION OF THE NUMBER OF FITTING NODES

Nodes	Standard Deviation in Potential	Standard Deviation in Derivative
10	3.08×10^{-3}	5.35×10^{-2}
12	8.26×10^{-4}	1.07×10^{-2}
14	4.75×10^{-4}	4.88×10^{-3}
16	1.83×10^{-4}	3.57×10^{-3}
20	1.44×10^{-4}	3.03×10^{-3}

between a factor of 2 to a factor of 3 smaller than the corresponding values for the (10 x 10) fit. This factor roughly corresponds to the ratio of the number of fitting nodes in the two cases, $15^2/10^2 = 2.25$. (2) The function values are again more accurate than the first derivatives, the ratio of standard deviations being between 0.1-0.5 for each spline fit. (3) The overall accuracy of the (15 x 15) two-dimensional fit is less than that of a 15-point one-dimensional fit. Comparison with Table I indicates that the increase in the standard deviations may be as much as a factor of 10.

The full three-dimensional spline fit given by Eq(III-16) has been examined for the ($He + H_2^+$) and the (D + HCl) systems. The $He + H_2^+$ potential-energy surface obtained by Kuntz (91) using a "diatomics-in-molecules" (DIM) approach was used to generate energy values over a

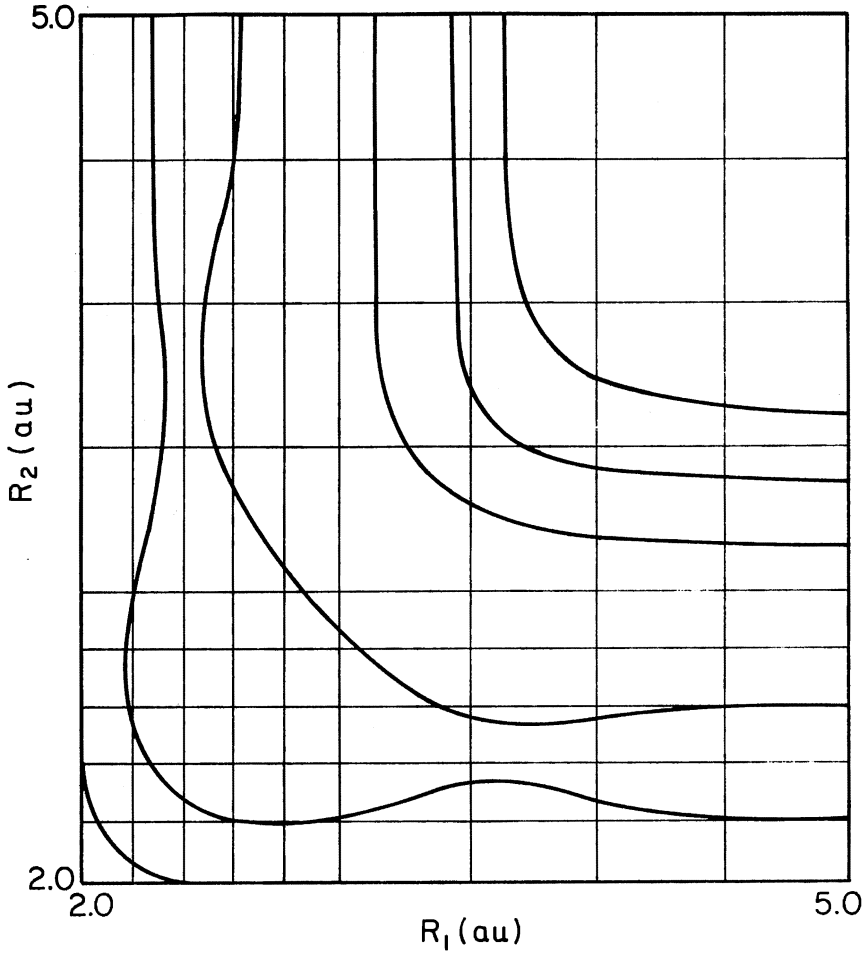

Figure 20. (10 x 10) Grid Designating Node Positions for the D-Cl-H Surface

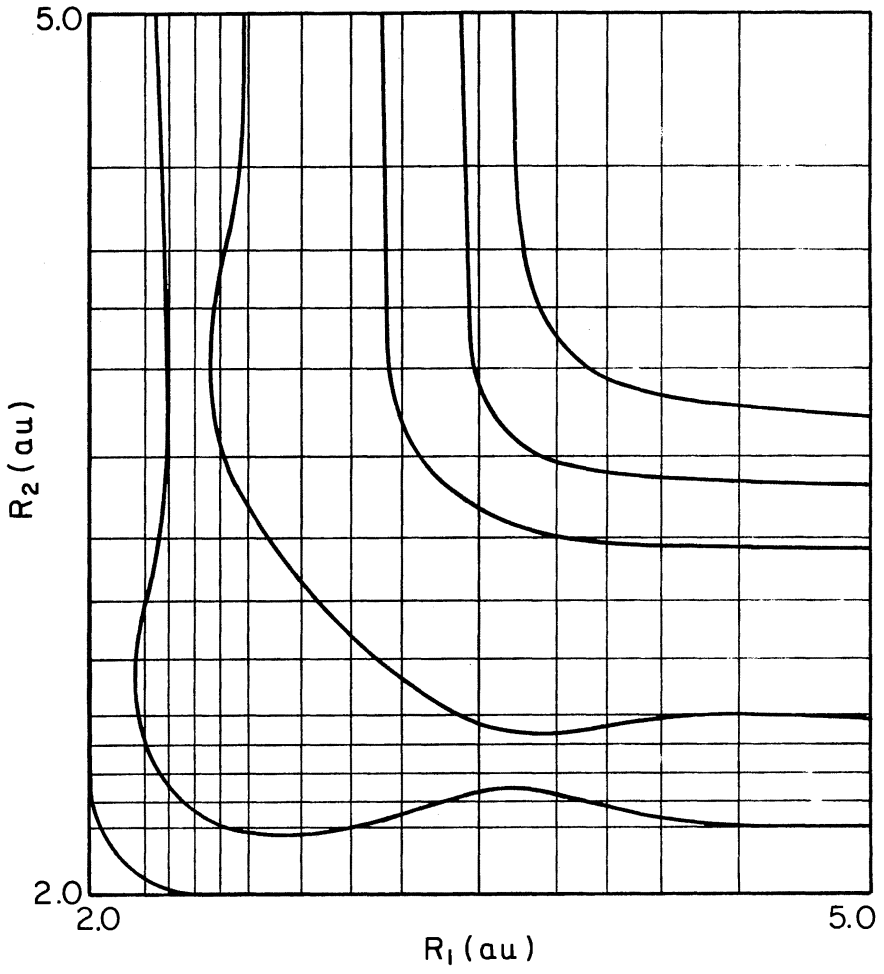

Figure 21. (15 x 15) Grid Designating Node Positions for the D-Cl-H Surface

TABLE XIII

COMPARISON OF SPLINE FIT RESULTS WITH CALCULATED VALUES FOR D + Cl - H SEMIEMPIRICAL POTENTIAL-ENERGY SURFACE (COLLINEAR GEOMETRY) - ALL ENERGY VALUES IN eV

		Exact Values[a]			10 x 10 Spline Fit			15 x 15 Spline Fit		
R (au)	R_2 (au)	E	dE/dR_1	dE/dR_2	E	dE/dR_1	dE/dR_2	E	dE/dR_1	dE/dR_2
4.8000	4.65730	-1.24630	0.43773	0.63240	-1.2415	0.43299	0.63710	-1.24497	0.43620	0.63388
2.6575	3.5797	-4.47986	1.24650	0.25306	-4.48501	1.24176	0.21468	-4.48308	1.24150	0.23807
3.8935	4.7400	-2.06370	1.50838	0.15750	-2.06800	1.52373	0.14577	-2.06690	1.51222	0.14645
2.3300	3.5909	-4.58726	-0.97537	0.07419	-4.59444	-0.95804	0.04122	-4.59057	-0.97816	0.06494
4.0980	4.3716	-1.90120	1.03972	0.45762	-1.90124	1.02506	0.45232	-1.90093	1.03807	0.45797
3.8749	2.0673	-3.87713	-0.20782	-5.18617	-3.87408	-0.18534	-5.17676	-3.87386	-0.20569	-5.18684
4.3420	3.5890	-2.62884	0.16016	1.78210	-2.62485	0.14800	1.77505	-2.62858	0.16347	1.78095
2.9032	3.9408	-3.87888	2.02926	0.04402	-3.88033	2.02711	0.06879	-3.87858	2.02959	0.03923
2.5057	3.4620	-4.65091	0.45127	0.36471	-4.64752	0.44173	0.28953	-4.64871	0.44550	0.31635
2.2610	4.8569	-4.61444	-1.68430	0.01319	-4.62331	-1.69478	0.03600	-4.61605	-1.67526	0.02040
Std. Deviation:					.00514	.01356	.03278	.00240	.00451	.01887

[a]Reference 90

(15 x 15 x 15) grid of internuclear distances. The variables R_1 and R_3 represent the He - H distances while R_2 is the H_2 separation. Figure 22 illustrates the grid spacings for the $R_1 - R_2$ planes. Similar spacing of the nodes was employed for R_3. The accuracy of the three-dimensional spline fit to these points is illustrated by the data given in Table XIV. The twelve results given in this table were randomly selected to avoid prejudicial sampling. Again there are several important features to be noted. (1) The accuracy of the interpolation for large values of R_1, R_2, or R_3 is very poor as can be seen from results (1) and (2) in Table XIV. This is the result of the low density of nodes in this region of configuration space. Since such a region is of minor importance in chemically interesting processes, it is possible that such errors will be relatively unimportant in scattering calculations. (2) The derivatives are again less accurate than the energy values themselves. (3) If one omits the first two results of Table XIV, it is seen that the overall accuracy for the three-dimensional fit is less than that obtained for the two-dimensional case, but the decrease in accuracy with increased dimensionality does not appear to be as great as in going from one to two dimensions.

The variation in accuracy with number of nodes for a three dimensional spline fit is shown in Table XV for the D + HCl surface (90).

We have attempted to assess the utility of the three-dimensional spline interpolation procedure in quasiclassical trajectory studies by comparing the results of such calculations using both the spline fit and the full analytic potential-energy surface. Such a comparison has been made for both the $(He + H_2^+)$ and the (D + HCl) systems. The procedures employed to carry out the three-body quasiclassical

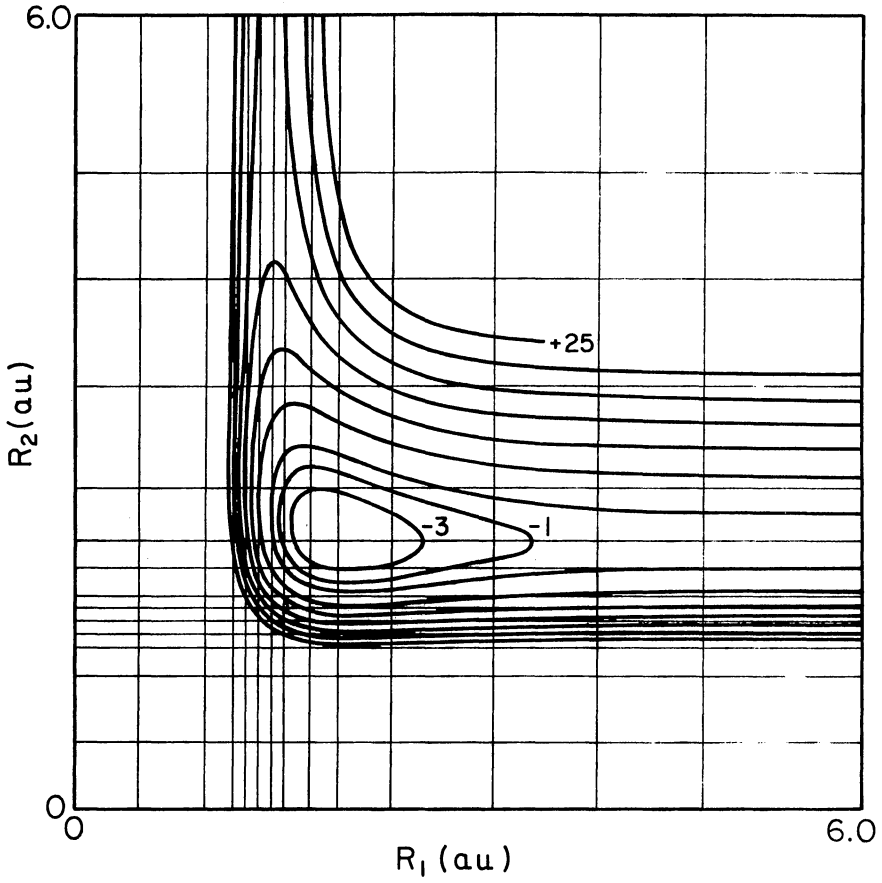

Figure 22. (15 x 15) Grid Designating Node Positions for the He + H_2^+ Surface. R_1 and R_2 are the He-H and H-H Separations, Respectively

TABLE XIV

COMPARISON OF A (15 x 15 x 15) SPLINE FIT WITH CALCULATED RESULTS FOR A DIM He + H_2^+ POTENTIAL-ENERGY SURFACE - ALL ENERGIES ARE IN eV

	R_1 (au)	R_2 (au)	R_3 (au)	E		DE/DR_1		DE/DR_2		DE/DR_3	
				SPLINE	DIM[a]	SPLINE	DIM[a]	SPLINE	DIM[a]	SPLINE	DIM[a]
1)	10.0006	2.1808	8.8675	-0.0448	0.0347	0.0017	0.0000	0.3769	0.3784	-0.0079	0.0000
2)	7.7641	2.3570	6.5602	0.1053	0.1247	-0.0130	0.0001	0.6309	0.6314	-0.0136	0.0006
3)	5.2309	2.1384	4.1491	0.0023	0.0021	0.0052	0.0043	0.3004	0.3005	0.0219	0.0222
4)	3.1847	1.7603	2.2013	-0.1124	-0.1114	0.0299	0.0251	-0.8247	-0.8258	0.0521	0.0513
5)	2.6645	1.8262	1.6071	0.0617	0.0634	-0.1281	-0.1222	-0.7049	-0.7053	-1.2273	-1.2255
6)	2.4314	2.2865	1.5524	0.1381	0.1381	-0.3330	-0.3301	0.3402	0.3378	-1.3569	-1.3578
7)	2.2014	2.8946	2.5327	0.3379	0.3424	0.0747	0.0738	0.9252	0.9166	-0.0628	-0.0628
8)	1.9504	2.6146	2.9224	0.0507	0.0543	0.0705	0.0687	0.7212	0.7341	-0.0731	-0.0748
9)	1.8364	2.1917	3.1360	-0.1785	-0.1782	-0.1924	-0.1929	0.2569	0.2548	-0.0347	-0.0398
10)	2.7851	2.7165	4.6288	0.2839	0.2877	0.1606	0.1614	0.8660	0.8711	0.0050	0.0049
11)	3.9961	2.1859	4.8790	0.0126	0.0127	0.0266	0.0276	0.3885	0.3870	0.0081	0.0072
12)	7.3690	1.8608	6.0324	0.0178	0.0264	-0.0085	0.0002	-0.4193	-0.4190	-0.0086	0.0014
Std. Deviation				0.0249		0.0054		0.0051		.0054	
Std. Deviation (omitting first two results)				0.0037		0.0041		0.0056		.0031	

[a]Reference 91

TABLE XV

DEPENDENCE OF STANDARD DEVIATION UPON NUMBER OF NODES.
3D CASE: D + ClH SURFACE. ENERGIES ARE IN eV

Size of the Grid	Standard Deviations			
	Energy	$\frac{\partial E}{\partial R_1}$	$\frac{\partial E}{\partial R_2}$	$\frac{\partial E}{\partial R_3}$
13 x 13 x 13	.054	.124	.214	.068
15 x 15 x 15	.027	.099	.205	.0425
20 x 20 x 20	.0078	.029	.095	.016

trajectory calculations have been fully described elsewhere (90) (92) (93).

As a first test, individual trajectories with the same set of initial conditions were compared for the spline surface and the analytic surface for both the He + H_2^+ and the D + ClH systems. Table VII gives several such results for the He + H_2^+ system. The coordinates, Q_i (i = 1,2, ... 6) listed in Table XVI have previously been defined (90) (92) (93). It is clear that the trajectories on the analytic and spline surfaces do not match, even in an approximate way! This type of result is typical for both systems. Furthermore, it is a result that could have been anticipated from the data given in Table XIV. The first derivatives of the spline and analytic surfaces are very different in the non-interaction region due to the low density of nodes. Thus, the initial integration steps cause the two trajectories to rapidly diverge. Once the system enters the interaction region, the integrations become more nearly identical, but at that point the spline surface is

TABLE XVI

COMPARISON OF INDIVIDUAL TRAJECTORY RESULTS ON DIM SURFACE[a] AND SPLINE FITTED SURFACE

Q_1	Q_2	Q_3	Q_4	Q_5	Q_6	E_{rot}(eV)	E_{vib}(eV)
			Initial Conditions (au)				
1.9543	0.6079	-1.1985	0.0	0.6975	-9.9756		
			Final Conditions (DIM Surface)[a]				
-.2437	-.9157	1.5228	-8.1951	5.7600	.5056	.6373	.0695
			Final Conditions (Spline Fitted Surface)				
2.0312	.5705	-.2964	-7.6005	6.5563	.3048	.2503	.3729
			Initial Conditions (au)				
-1.4394	1.8827	-.0936	0.0	2.5240	-9.6762		
			Final Conditions (DIM Surface)[a]				
-2.2136	-.7780	-.0016	.7783	4.0063	9.1940	.0157	.1644
			Final Conditions (Spline Fitted Surface)				
-2.2661	.2076	-.5492	.4675	3.3722	9.4669	.0057	.1457
			Initial Conditions (au)				
.2524	2.2237	-.7853	0.0	4.7659	-8.7912		
			Final Conditions (DIM Surface)[a]				
0.0529	2.0912	-.2858	.0258	3.7215	9.3440	.0008	.1365
			Final Conditions (Spline Fitted Surface)				
.0980	2.1329	-.0751	.0203	4.6966	8.8694	.0007	.1383
			Initial Conditions (au)				
1.8437	-.1714	1.4822	0.0	3.4562	-9.3837		
			Final Conditions (DIM Surface)[a]				
1.0133	-.8303	1.6223	-.1026	.5836	10.0219	.0017	.1365
			Final Conditions (Spline Fitted Surface)				
1.4627	-.1781	1.0871	-.0040	1.5110	9.9320	.0000	.1399
			Initial Conditions (au)				
1.1498	2.0279	.4371	0.0	2.1742	-9.7608		
			Final Conditions (DIM Surface)[a]				
-1.9968	-.2398	-1.4268	2.5608	7.2069	6.4859	.1590	.2048
			Final Conditions (Spline Fitted Surface)				
-2.0196	-.7786	-.8971	-2.4553	7.1766	6.5953	.1602	.1358

[a]Reference 91

integrating a trajectory that essentially corresponds to a different set of initial conditions than that being integrated on the analytic surface. Thus the final results exhibit little correspondence.

It would appear that the above situation will always exist unless the density of nodes in the noninteraction regions is significantly increased. Since 3375 nodes are presently being used, such an increase would clearly push the computer time requirement for the ab initio surface computations beyond the limits of present computational facilities. It must therefore be concluded that if a point-by-point match of individual trajectories is to be used as the criterion for acceptability, then spline interpolation must be discarded in quasi-classical trajectory studies.

There is a possibility that the above criterion is too extreme and demanding. If the initial integration errors on the spline surface that result from the low node density in the noninteraction regions merely alter the effective initial conditions in such a manner that the distributions of these effective initial conditions are still in approximate accord with the correct distributions, then the cross sections, energy partitioning and spatial scattering distributions computed on the spline surface will still be in good agreement with those obtained from the full analytic surface even though the individual trajectories do not agree. With this possibility in mind we have computed full spatial scattering and energy partitioning distributions and cross sections on both the spline and analytic surfaces for the $He + H_2^+$ and D + HCl systems.

A total of 92 ($He + H_2^+$) inelastic trajectories were examined on both the spline and DIM surfaces (91). In each trajectory the initial

vibrational and rotational quantum numbers for H_2^+ were set to zero, and all trajectories had an initial relative translational energy of 0.80226 eV. The Monte Carlo averaging over initial orientation, vibrational phase, and impact parameter has been previously described (93). The classical equations of motion were integrated with a Runge-Kutta-Gill procedure using a step size of 2.16×10^{-16} sec.

Figures 23 (a,b,c,d) give computed scattering distributions on both surfaces for θ and ϕ, respectively. As can be seen, the He atom scattering is mainly forward and in-plane ($\phi = 90^{\circ}$ corresponds to in-plane scattering). The final vibrational and rotational energies of H_2^+ are shown in Figures 24 and 25, respectively. It is clear that, within the statistical error of the calculations, distributions predicted by the spline surface are identical to those given by the DIM surface. Table XVII gives the averages of the four distributions for both surfaces.

A more extensive comparison between spline and analytic surfaces has been made for the D + HCl → DCl + H exchange reaction. Raff, Suzukawa, and Thompson (94) have examined a total of 3049 trajectories on the semiempirical potential-energy surface previously formulated by Porter et al. (90). A (15 x 15 x 15) spline fit to this surface was generated using the node spacing illustrated in Figure 21, and 500 classical trajectories were then calculated on this surface. In all calculations the initial relative velocity was 6.050×10^5 cm/sec, and the maximum impact parameter was 4.0 au. The initial HCl vibration-rotation states were averaged over a Boltzmann distribution at 250 K, and integrations over impact parameter, initial relative orientation, and the HCl rotational angular momentum direction and vibrational

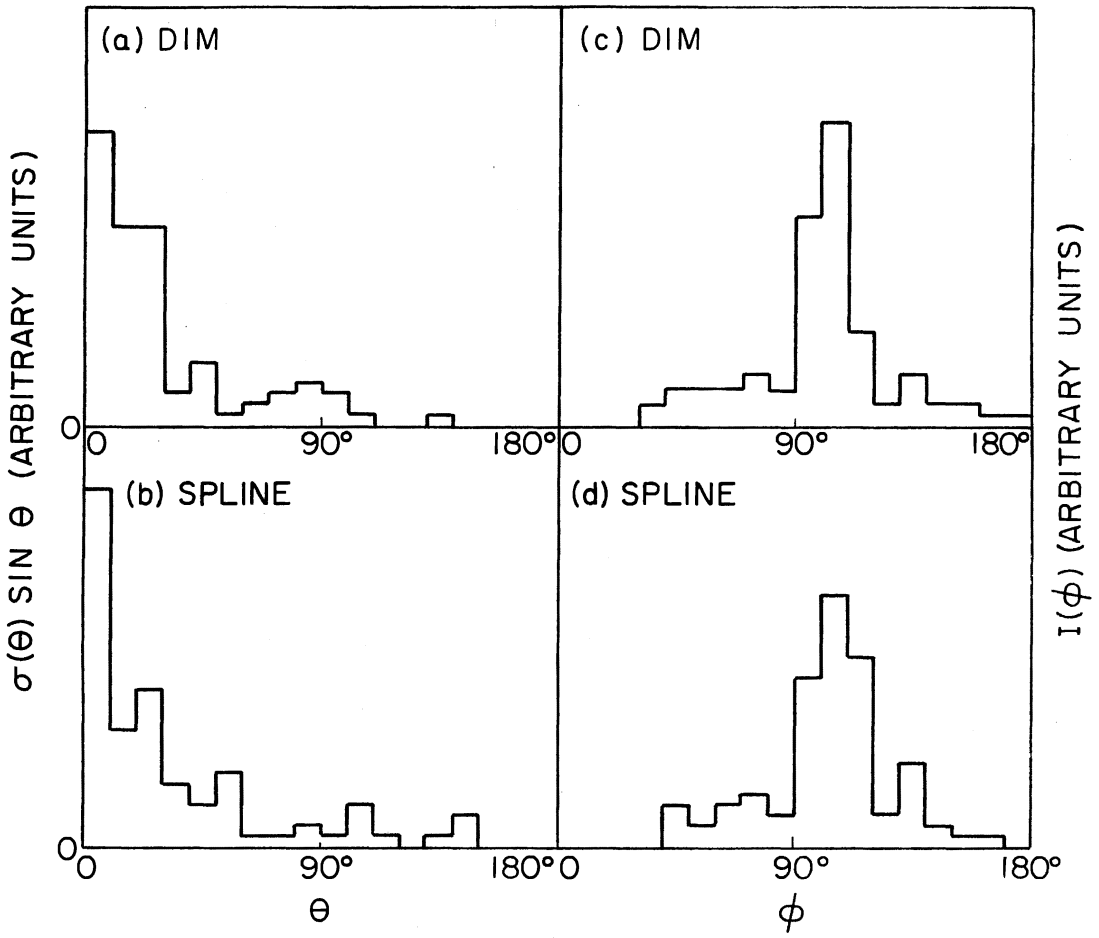

Figure 23. Calculated Spatial Scattering Distribution for the He + H_2^+ Reaction. (a) In-Plane Distribution from DIM Surface. (b) In-Plane Distribution from Spline Fit. (c) Out of Plane Distribution from DIM Surface. (d) Out of Plane Distribution from Spline Fit

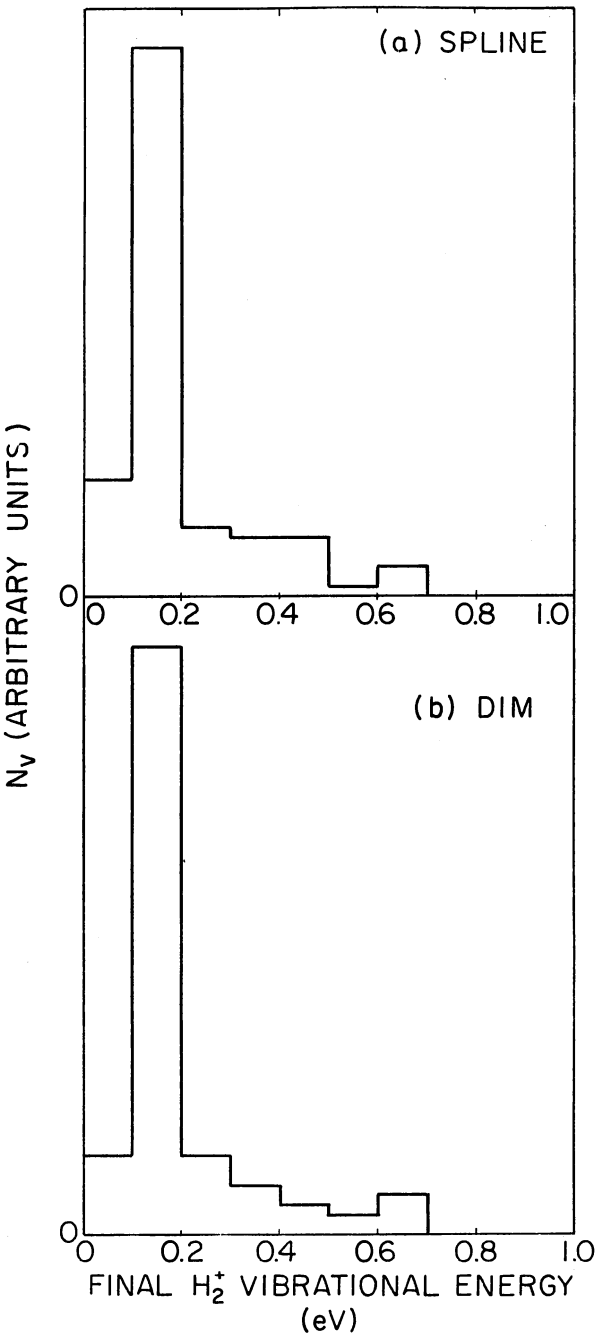

Figure 24. Distribution of Final H_2^+ Vibrational Energy for Inelastic $He + H_2^+$ Encounters.
(a) Spline Fit.
(b) DIM Surface

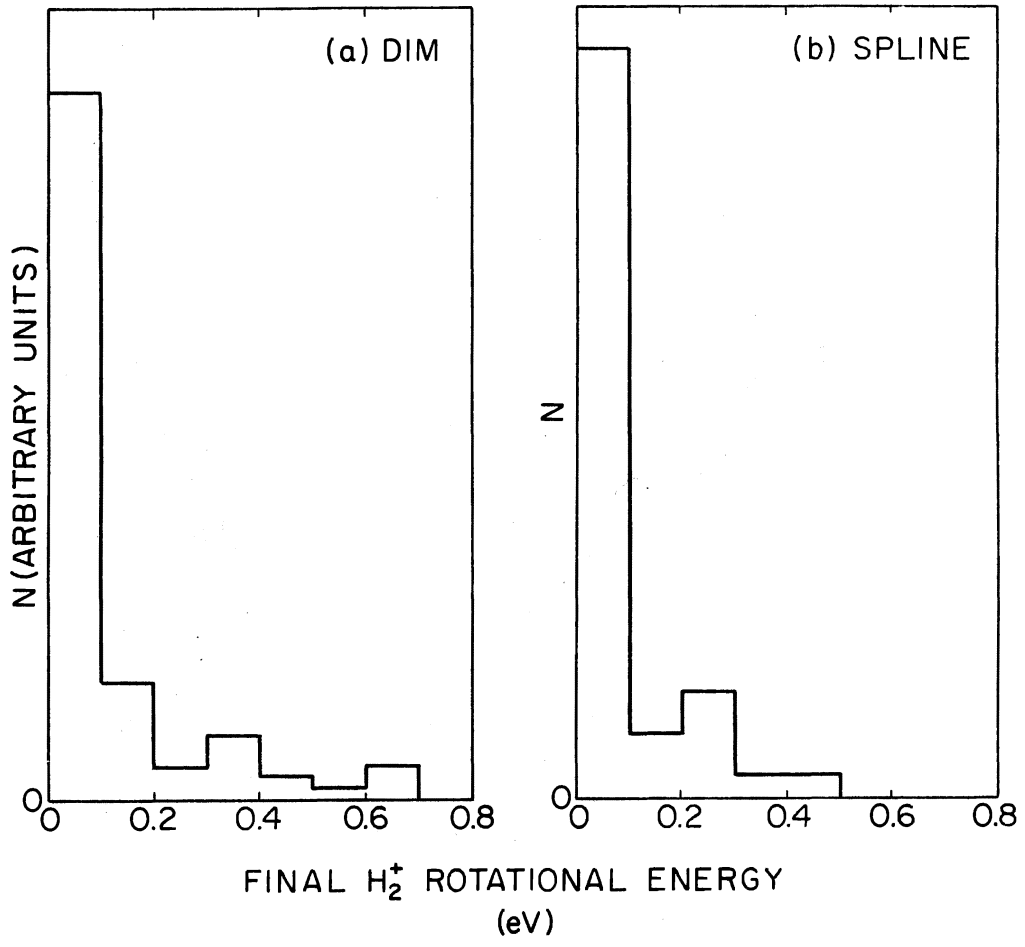

Figure 25. Distribution of Final H_2^+ Vibrational Energy for Inelastic He + H_2^+ Encounters. (a) DIM Surface. (b) Spline Fit

phase angle were carried out in the manner previously described (95).

TABLE XVII

COMPARISON OF AVERAGE RESULTS ON THE TWO SURFACES. $He + H_2^+$ SYSTEM

	Results	
	DIM Surface[a]	Spline Fitted Surface
Average scattering angle θ	30-40°	30-40°
Average scattering angle ϕ	90-100°	90-100°
Average final vibrational energy (eV)	0.21	0.20
Average final rotational energy (eV)	0.13	0.09

[a]Reference 91

Figures 26 and 27 compare the computed differential scattering cross sections for product DCl obtained from the two surfaces. The error bars shown on the distribution obtained from the analytic surface, Figure 26, represent one sigma limit. The statistical uncertainty for the spline surface is larger due to the lower number of total trajectories examined. The two distributions are very similar. Both indicate predominately backward scattering with a small forward component approximately one-third the intensity of the backward component, and both components have approximately the same half-widths.

Figure 28 shows the computed energy partitioning distribution for the exchange reaction where f_t represents the fraction of the total

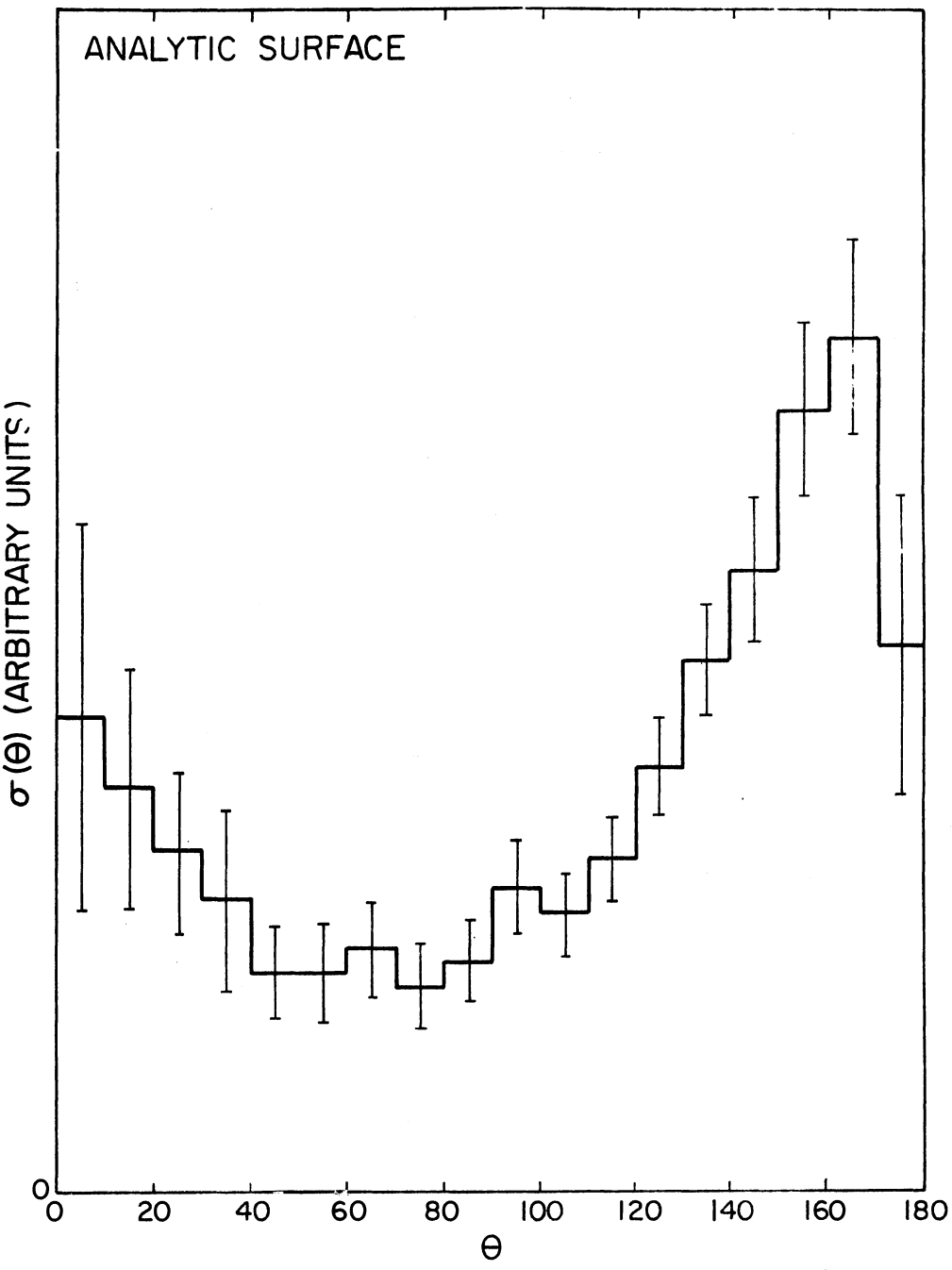

Figure 26. Differential Scattering Cross Section for DCl Scattering Obtained from the Analytic Surface. Error Bars Represent One Sigma Limit of Uncertainty

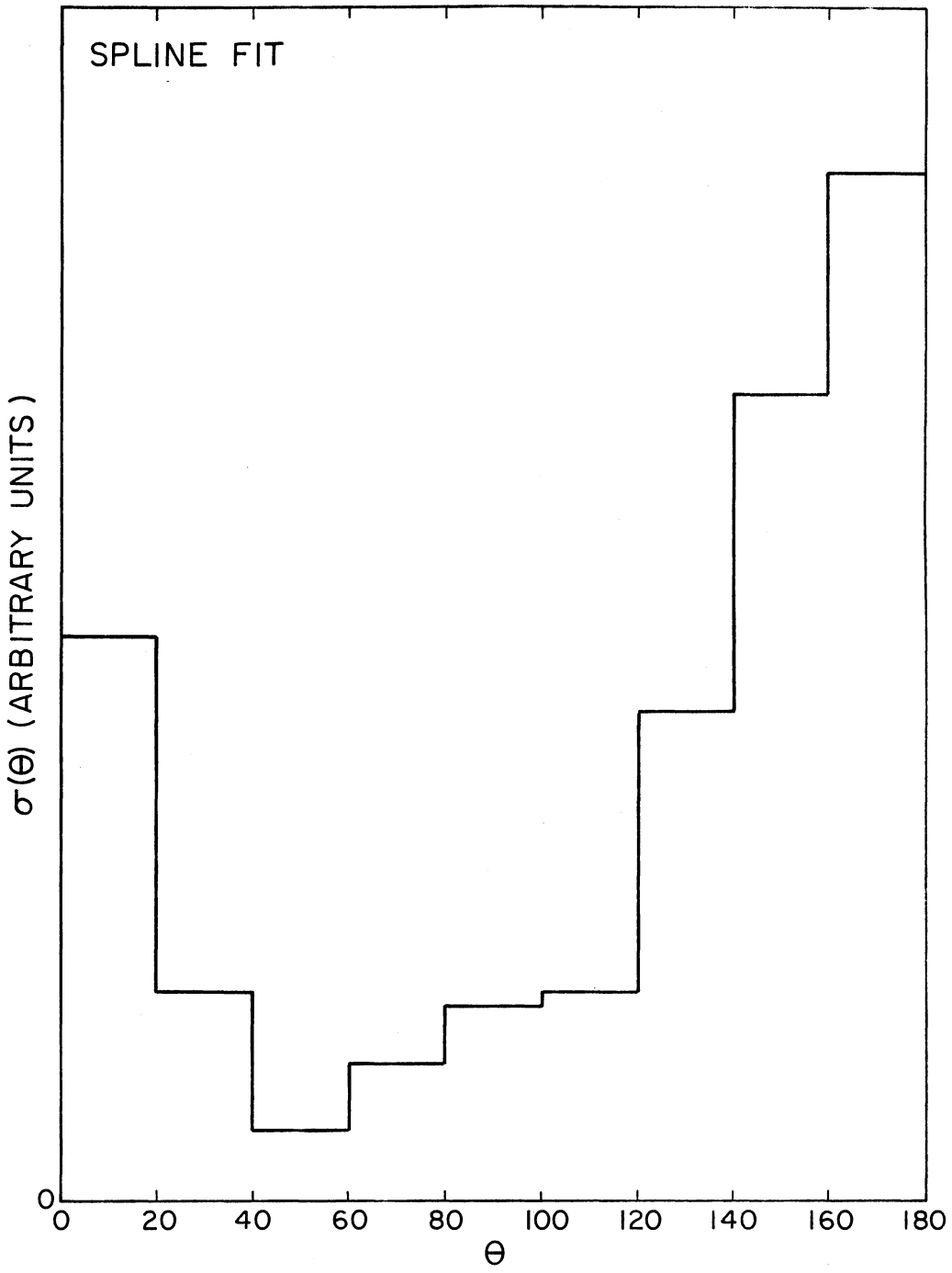

Figure 27. Differential Scattering Cross Section for DCl Scattering Obtained from a Spline Fit to the Analytic Surface

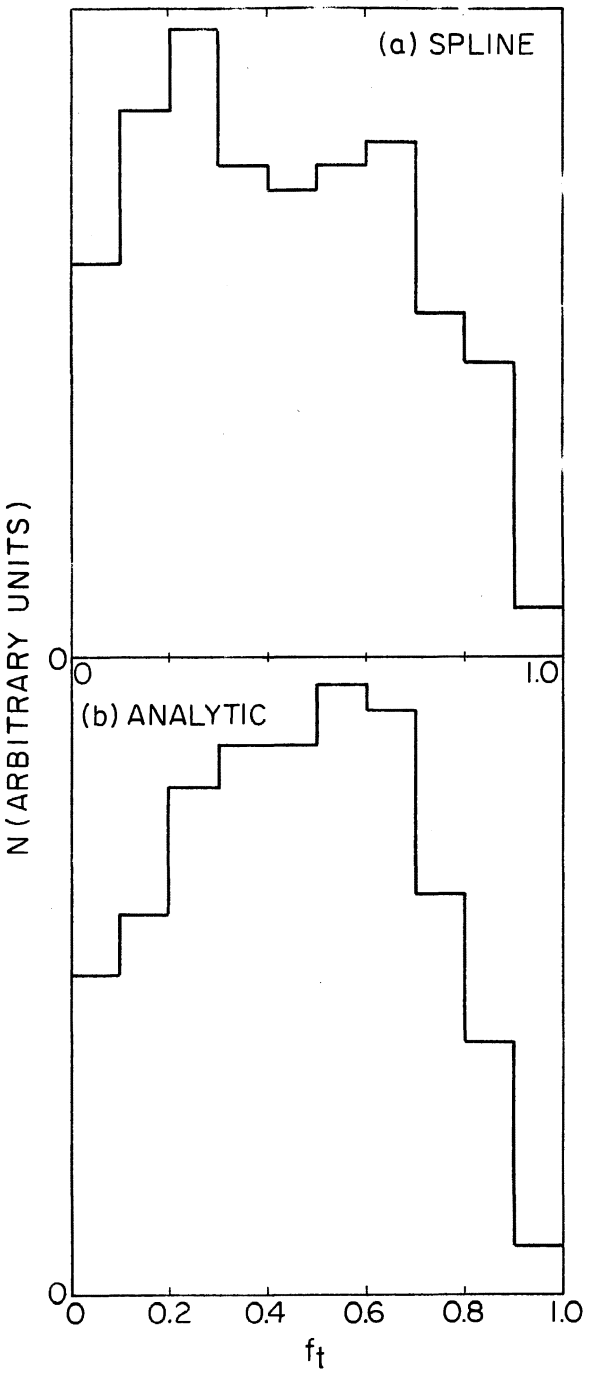

Figure 28. Energy Partitioning Distribution for the D + HCl Exchange Reaction. (a) Spline Fit. (b) Analytic Surface

available energy partitioned into relative translational motion. Again the spline distribution is very similar to that obtained from the full analytic surface. The spline distribution yields an average value of f_t of 0.43. This value is 0.46 on the analytic surface.

The computed total reaction cross sections for exchange are, within statistical error, identical. The spline fit gives a value of 3.25 ± 0.20 Å^2 compared to 3.38 ± 0.11 Å^2 from the analytic surface.

The above results suggest that the criterion of point-by-point trajectory matching may be unnecessarily demanding. If the $He + H_2^+$ and D + HCl systems can be taken to be typical, it would appear that a 3D cubic spline fit is capable of yielding reasonably accurate results for the quantities of interest.

It is of some interest to examine the CPU computation time requirements for use of spline surfaces. All present computations were carried out on an IBM 360/65 machine. For a (15 x 15 x 15) three-dimensional grid, 22 sec of CPU time were required to obtain the second, fourth, and sixth derivatives. These values may, of course, be stored on disk so that for a given spline fit this computation need not be repeated. For both the $He + H_2^+$ and D + HCl systems, the spline trajectories required a factor of 5.0-5.2 times the CPU time needed for integration on the analytic surfaces. These times could undoubtedly be reduced somewhat by optimized machine language coding as opposed to the Fortran codes used in the present work.

Summary and Conclusions

The accuracy of 1D spline fits to Morse and Lennard-Jones type potentials has been quantitatively examined, and the accuracy of 2D

spline fitting was investigated for the case of a collinear D-Cl-H potential-energy surface. A 3D spline algorithm developed by Jordan (85) was coded and tested against both a DIM surface (91) for He + H_2^+ and a DHCl surface (90). The adequacy of 3D spline surfaces in quasi-classical trajectory studies has been examined for both the He + H_2^+ and D + HCl systems. The results indicate the following:

(1) One-dimensional spline fitting is very accurate.

(2) An (a x a) 2D spline fit is substantially less accurate than a one-dimensional spline with a nodes.

(3) For the case examined an (a x a x a) 3D spline has less accuracy than an (a x a) 2D spline fit, but the decrease in accuracy is less than for the 1D-2D comparison.

(4) First derivatives obtained from the spline fit are generally less accurate than the corresponding function values.

(5) (15 x 15 x 15) cubic spline fits do not possess sufficient accuracy to give a point-by-point match of a quasiclassical trajectory to that obtained on the full analytic surface.

(6) Total reaction cross sections, energy partitioning distributions, and spatial scattering distributions computed by quasiclassical trajectories on spline surfaces were found to be in good accord with those obtained from the full analytic surface for the two cases examined. It therefore appears possible that the criterion of point-by-point matching of trajectories may be unnecessarily demanding.

(7) The computation time requirements for use of 3D-spline surfaces are considerably larger than for semiempirical analytic surfaces but are still within the range of present computer facilities.

CHAPTER IV

FIVE-BODY QUASICLASSICAL TRAJECTORY CALCULATIONS

The method of quasiclassical trajectory calculation for chemical systems, in general and CO_2-X system in particular has been described by Porter and Raff (96) and Suzukawa (58), respectively. The method adopted for CO_2-H_2 system closely follows that of Suzukawa and hence only the resulting equations are reported.

If atoms can be approximated as classical particles, their motions may be described by Hamilton's Equations:

$$\dot{q}_i = \partial H/\partial p_i$$

$$\dot{p}_i = -\partial H/\partial q_i \ , (i = 1,2,....3N) \ , \qquad \text{(IV-1)}$$

where the q_i's are the coordinates and the p_i's the conjugate momenta of an N-particle system. The dot on the variables represents the time derivative. H is the classical Hamiltonian of the system which for a conservative system is defined by

$$H = T + V = \text{constant}, \qquad \text{(IV-2)}$$

where T is the kinetic energy and V the potential-energy of the system.

It has been found that cartesian coordinates are the most suitable for systems with more than three atoms (99). The ones used in this study are:

(1) space-fixed XYZ.

(2) nonrotating, $X'Y'Z'$; parallel to XYZ but with its origin translating with the center of mass of carbon dioxide.

(3) rotating xyz; the molecule-fixed axis system for CO_2. The orientation of the x,y,z axes in the $X'Y'Z'$ coordinates are described by angles α, β, γ.

(4) $X'Y'Z'$, similar to $X'Y'Z'$, but with its origin translating with the center of mass of H_2.

(5) x'y'z', similar to xyz, but with orientation angles α_1', β_1', γ_1'. All these systems are represented in Figure 29. Using the cartesian coordinates described in Figure 30,

$$T = \tfrac{1}{2} \sum_{i=1}^{3} \left(\frac{1}{m_A} p_i^2 + \frac{1}{m_B} p_{i+3}^2 + \frac{1}{m_C} p_{i+6}^2 + \frac{1}{m_D} p_{i+9}^2 + \frac{1}{m_E} p_{i+12}^2\right)$$

$$V = V(q_1, q_2, \ldots . q_{15}) \ . \qquad \text{(IV-3)}$$

The potential has been described in Chapter II. The equations of motion are:

$$\dot{q}_i = p_i/m_i$$

$$\dot{p}_i = -\partial V/\partial q_i, \ i = 1,2,\ldots . .15 \qquad \text{(IV-4)}$$

where $m_i = m_A$ when i = 1,2,3, $m_i = m_B$ when i = 4,5,6, $m_i = m_C$ when i = 7,8,9, $m_i = m_D$ when i = 10,11,12 and $m_i = m_E$ when i = 13,14,15.

Description of vibrational motions of molecules is easier using normal coordinates. Q_1, Q_{2a}, Q_{2b} and Q_3 represent the normal coordinates of CO_2 and Q_H represents the normal coordinate of H_2. Assuming the molecular axes to be in the z and z' directions respectively for CO_2 and H_2, the normal coordinates are expanded in terms of molecule-fixed coordinates:

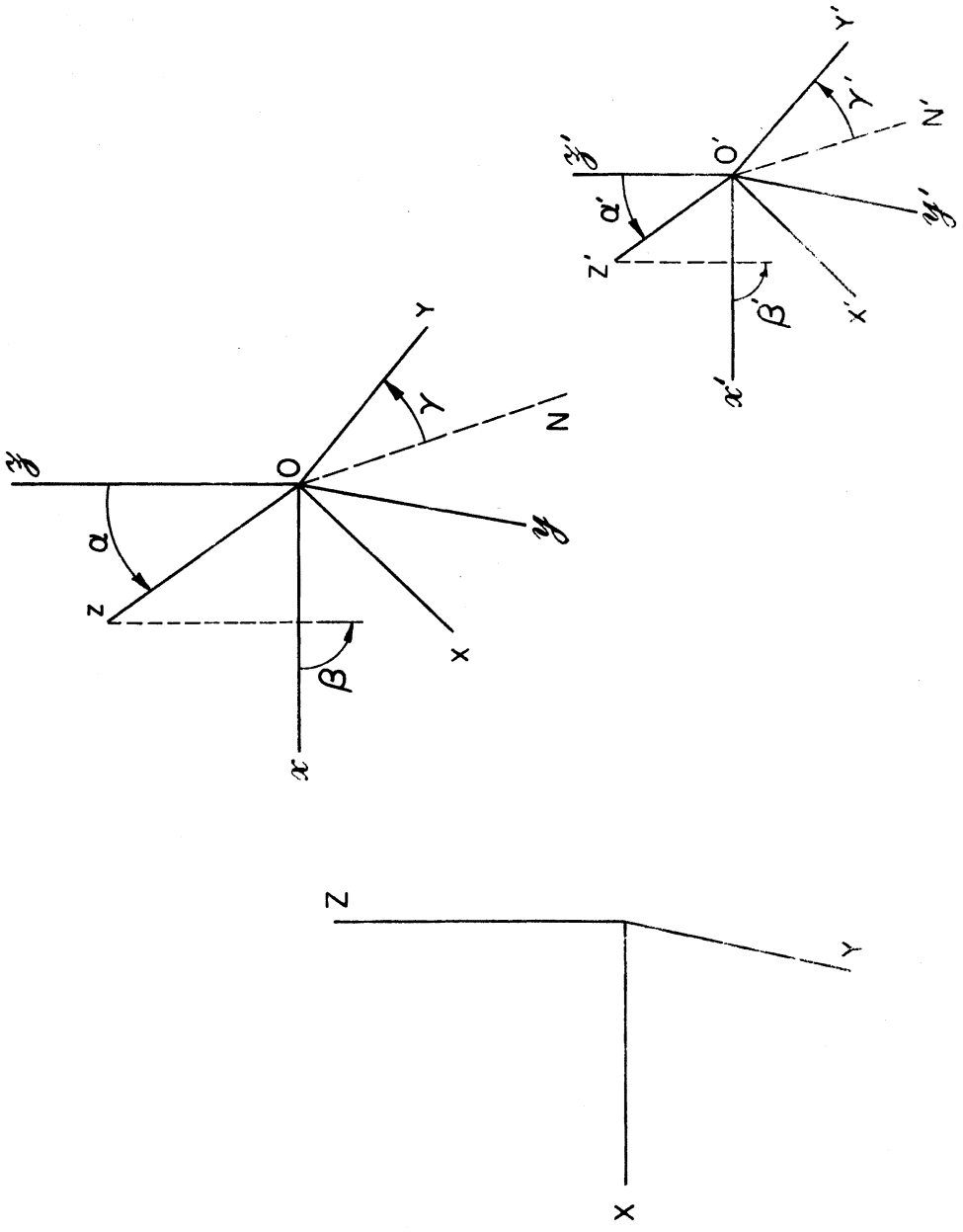

Figure 29. Coordinate Systems for the CO_2-H_2 System

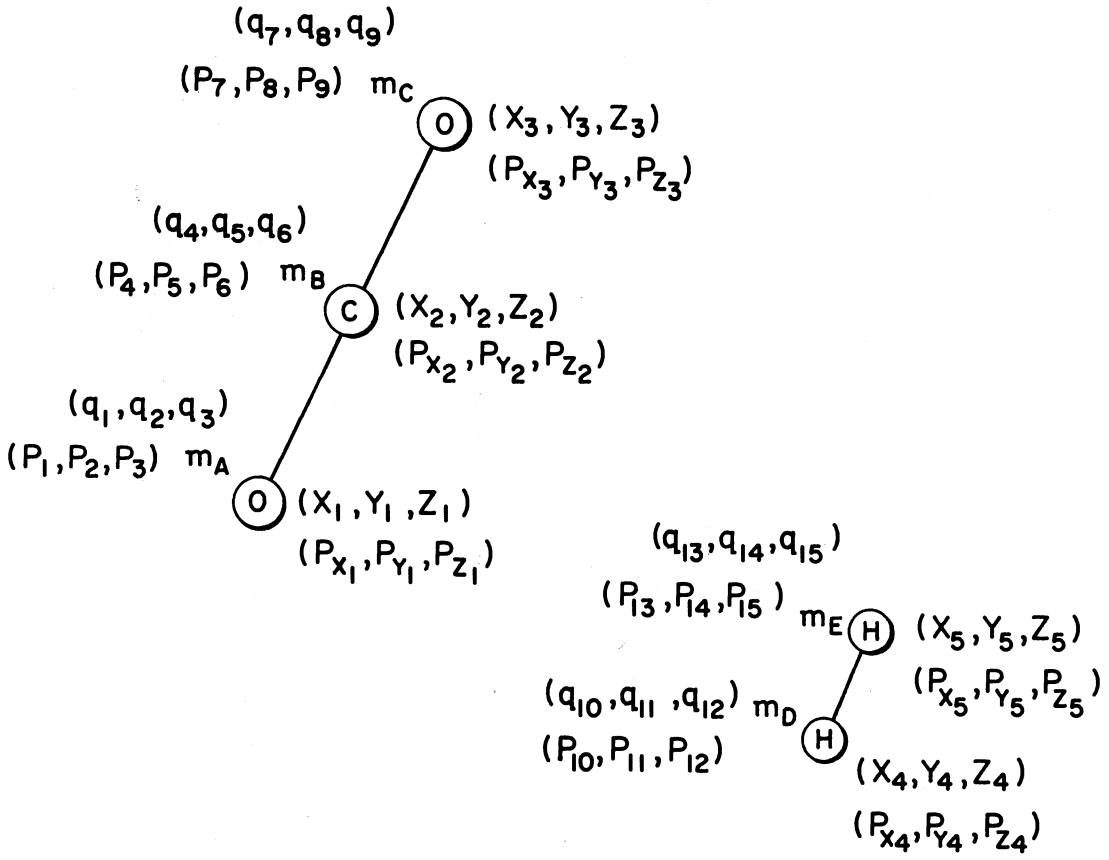

Figure 30. Cartesian Coordinates and Conjugate Momenta for the CO_2-H_2 System

$$Q_1 = \left[\frac{m_C}{2}\right]^{\frac{1}{2}} (\Delta z_3 - \Delta z_1)$$

$$Q_{2a} = \left[\frac{2m_C m_B}{m_T}\right]^{\frac{1}{2}} \left[\Delta x_2 - \tfrac{1}{2}(\Delta x_1 + \Delta x_3)\right]$$

$$Q_{2b} = \left[\frac{2m_C m_B}{m_T}\right]^{\frac{1}{2}} \left[\Delta y_2 - \tfrac{1}{2}(\Delta y_1 + \Delta y_3)\right]$$

$$Q_3 = \left[\frac{2m_C m_B}{m_T}\right]^{\frac{1}{2}} \left[\Delta z_2 - \tfrac{1}{2}(\Delta z_1 + \Delta z_3)\right]$$

$$Q_H = \left[\frac{m_H}{2}\right]^{\frac{1}{2}} (\Delta z_5 - \Delta z_4) \quad . \tag{IV-5}$$

The Δx, Δy, Δz's indicate displacements from the equilibrium x, y, z's.

$$\Delta x_1 = x_1 - x_1^{eq} \text{ etc., and} \tag{IV-6}$$

it is assumed that $m_A = m_C$, $m_D = m_E = m_H$ and $m_T = m_A + m_B + m_C$ = total mass of carbon dioxide.

Since energy transfer is the problem of interest to us, it is essential to separate translational, rotational and vibrational motions for each molecule. Translation is rigorously separable from the internal motions, but the vibrational and rotational motions are not. Certain approximations are therefore necessary. Let the origins of the molecule-fixed coordinate systems for CO_2 and H_2 be placed at $\underset{\sim}{R}_{cm}(CO_2)$ and $\underset{\sim}{R}_{cm}(H_2)$ respectively in the space-fixed system. Let the position of atom i in the CO_2-molecule-fixed system be $\underset{\sim}{r}_i (i = 1,2,3)$ and that of atom i in the H_2-molecule-fixed system be $\underset{\sim}{r}_i (i = 4,5)$. Let $\dot{\underset{\sim}{r}}_i = \underset{\sim}{v}_i$ be the corresponding velocities. Let the CO_2-molecule-fixed system and the H_2-molecule-fixed system rotate with angular velocities $\underset{\sim}{\omega}_{(CO_2)}$ and $\underset{\sim}{\omega}_{(H_2)}$, respectively. The total velocity of atom i, in the space-fixed frame is

$$(\underset{\sim}{v}_{total})_i = \dot{\underset{\sim}{R}}_{cm}(CO_2) + \underset{\sim}{\omega}_{(CO_2)} \times \underset{\sim}{r}_i + \dot{\underset{\sim}{r}}_i \quad , \quad i = 1,2,3 \tag{IV-7}$$

and

$$(\underset{\sim}{v}_{total})_i = \dot{\underset{\sim}{R}}_{cm}(H_2) + \underset{\sim}{\omega}_{(H_2)} \times \underset{\sim}{r}_i + \dot{\underset{\sim}{r}}_i, \quad i = 4,5 \; . \tag{IV-8}$$

The kinetic energy of the CO_2 molecule is,

$$\begin{aligned} T_{CO_2} &= \tfrac{1}{2} \sum_{i=1}^{3} m_i (v_{total})_i^2 \\ &= \tfrac{1}{2}[\dot{R}_{cm}^2(CO_2) \sum_{i=1}^{3} m_i + \sum_{i=1}^{3} m_i (\underset{\sim}{\omega}_{(CO_2)} \times \underset{\sim}{r}_i) \cdot (\underset{\sim}{\omega}_{(CO_2)} \times \underset{\sim}{r}_i) \\ &+ \sum_{i=1}^{3} m_i v_i^2 + 2 \dot{\underset{\sim}{R}}_{cm}(CO_2) \cdot \underset{\sim}{\omega}_{(CO_2)} \times \sum_{i=1}^{3} m_i \underset{\sim}{r}_i \\ &+ 2 \dot{\underset{\sim}{R}}_{cm}(CO_2) \cdot \sum_{i=1}^{3} m_i \underset{\sim}{v}_i + 2 \underset{\sim}{\omega}_{(CO_2)} \cdot \sum_{i=1}^{3} m_i \underset{\sim}{r}_i \times \underset{\sim}{v}_i] \end{aligned} \tag{IV-9}$$

and that of H_2 molecule is,

$$\begin{aligned} T_{H_2} &= \tfrac{1}{2}[\dot{R}_{cm}^2(H_2) \sum_{i=4}^{5} m_i + \sum_{i=4}^{5} m_i (\underset{\sim}{\omega}_{(H_2)} \times \underset{\sim}{r}_i) \cdot (\underset{\sim}{\omega}_{(H_2)} \times \underset{\sim}{r}_i) \\ &+ \sum_{i=4}^{5} m_i v_i^2 + 2 \dot{\underset{\sim}{R}}_{cm}(H_2) \cdot \underset{\sim}{\omega}_{(H_2)} \times \sum_{i=4}^{5} m_i \underset{\sim}{r}_i \\ &+ 2 \dot{\underset{\sim}{R}}_{cm}(H_2) \cdot \sum_{i=4}^{5} m_i \underset{\sim}{v}_i + 2 \underset{\sim}{\omega}_{(H_2)} \cdot \sum_{i=4}^{3} m_i \underset{\sim}{r}_i \times \underset{\sim}{v}_i] \; . \end{aligned} \tag{IV-10}$$

Imposing the condition that the origin of the molecule-fixed system is the molecular center of mass and the Eckart conditions, which come close to making the molecular angular momentum in the xyz frame equal to zero,

$$\begin{aligned} T_{CO_2} &= (\tfrac{1}{2})[\dot{R}_{cm}^2(CO_2) \sum_{i=1}^{3} m_i + \sum_{i=1}^{3} m_i (\underset{\sim}{\omega}_{(CO_2)} \times \underset{\sim}{r}_i) \cdot (\underset{\sim}{\omega}_{(CO_2)} \times \underset{\sim}{r}_i) \\ &+ \sum_{i=1}^{3} m_i v_i^2 + 2 \underset{\sim}{\omega}_{(CO_2)} \cdot \sum_{i=1}^{3} m_i (\Delta \underset{\sim}{r}_i \times \underset{\sim}{v}_i)] \; . \end{aligned} \tag{IV-11}$$

The first term of Equation (IV-11) is the translational energy of the molecular center of mass. This term need not be considered further

since the translational motion can be separated rigorously in the absence of external fields. The second and third terms are purely rotational and vibrational energies, respectively, while the fourth term arises from the rotational and vibrational motion. The existence of this fourth term, called the coriolis term, prevents the rigorous separation of the rotational and vibrational energies. Similarly,

$$T_{H_2} = (\tfrac{1}{2})[\dot{R}^2_{cm}(H_2) \sum_{i=4}^{5} m_i + \sum_{i=4}^{5} m_i(\underset{\sim}{\omega}(H_2) \times \underset{\sim}{r}_i) \cdot (\underset{\sim}{\omega}(H_2) \times \underset{\sim}{r}_i) + \sum_{i=4}^{5} m_i v_i^2] . \qquad \text{(IV-12)}$$

Note that coriolis term is zero for hydrogen molecule.

Cartesian coordinate displacements may be expressed as a linear combination of normal coordinates:

$$\Delta x_i = \sum_{k=1}^{4} \eta_{ik} Q_k$$

$$\Delta y_i = \sum_{k=1}^{4} \mu_{ik} Q_k$$

$$\Delta z_i = \sum_{k=1}^{4} \nu_{ik} Q_k, \quad i = 1,2,3 . \qquad \text{(IV-13)}$$

If the equilibrium position is defined to lie along the z axis,

$$\Delta x_1 = -\left(\frac{m_B}{2m_C m_T}\right)^{\frac{1}{2}} Q_{2a}$$

$$\Delta x_2 = \left(\frac{2m_C}{m_B m_T}\right)^{\frac{1}{2}} Q_{2a}$$

$$\Delta x_3 = -\left(\frac{m_B}{2m_C m_T}\right)^{\frac{1}{2}} Q_{2a}$$

$$\Delta y_1 = -\left(\frac{m_B}{2m_C m_T}\right)^{\frac{1}{2}} Q_{2b}$$

$$\Delta y_2 = \left(\frac{2m_C}{m_B m_T}\right)^{\frac{1}{2}} Q_{2b}$$

$$\Delta y_3 = -\left(\frac{m_B}{2m_C m_T}\right)^{\frac{1}{2}} Q_{2b}$$

$$\Delta z_1 = -\left(\frac{1}{2m_C}\right)^{\frac{1}{2}} Q_1 - \left(\frac{m_B}{2m_C m_T}\right)^{\frac{1}{2}} Q_3$$

$$\Delta z_2 = \left(\frac{2m_C}{m_B m_T}\right)^{\frac{1}{2}} Q_3$$

$$\Delta z_3 = \left(\frac{1}{2m_C}\right)^{\frac{1}{2}} Q_1 - \left(\frac{m_B}{2m_C m_T}\right)^{\frac{1}{2}} Q_3 \quad . \qquad \text{(IV-14)}$$

Similarly,

$$\Delta x_4 = \Delta x_5 = \Delta y_4 = \Delta y_5 = 0$$

$$\Delta z_4 = -\left(\frac{1}{2m_H}\right)^{\frac{1}{2}} Q_H$$

$$\Delta z_5 = \left(\frac{1}{2m_H}\right)^{\frac{1}{2}} Q_H \quad . \qquad \text{(IV-15)}$$

Substituting Equation (IV-14) in Equation (IV-11), the total kinetic energy in the molecular center of mass becomes

$$\begin{aligned} T_{CO_2} &= T_{vib}(CO_2) + T_{rot}(CO_2) \\ &= \tfrac{1}{2}\Big[I_{xx}\omega^2_{x(CO_2)} + I_{yy}\omega^2_{y(CO_2)} + I_{zz}\omega^2_{z(CO_2)} - 2I_{xy}\omega_{x(CO_2)}\omega_{y(CO_2)} \\ &\quad -2I_{xz}\omega_{x(CO_2)}\omega_{z(CO_2)} - 2I_{yz}\omega_{y(CO_2)}\omega_{z(CO_2)} + \sum_{i=1}^{4}\dot{Q}_k^2 \\ &\quad +2\omega_{x(CO_2)}(Q_{2b}\dot{Q}_3 - Q_3\dot{Q}_{2b}) + 2\omega_{y(CO_2)}(Q_3\dot{Q}_{2a} - Q_{2a}\dot{Q}_3) \\ &\quad +2\omega_{z(CO_2)}(Q_{2a}\dot{Q}_{2b} - Q_{2b}\dot{Q}_{2a})\Big] \qquad \text{(IV-16)} \end{aligned}$$

where I_{xx}, I_{yy}, I_{zz} are the instantaneous moments of inertia and I_{xy}, I_{yz} and I_{zx} are the instantaneous products of inertia for CO_2 defined as:

$$I_{xx} = \sum_i m_i (y_i^2 + z_i^2)$$

$$I_{yy} = \sum_i m_i (x_i^2 + z_i^2)$$

$$I_{zz} = \sum_i m_i (x_i^2 + y_i^2)$$

$$I_{xy} = \sum_i m_i x_i y_i$$

$$I_{yz} = \sum_i m_i y_i z_i$$

$$I_{zx} = \sum_i m_i z_i x_i \qquad \text{(IV-17)}$$

$$T_{H_2} = T_{vib}(H_2) + T_{rot}(H_2)$$

$$= \tfrac{1}{2}[I_H(\omega^2_{x(H_2)} + \omega^2_{y(H_2)}) + \dot{Q}^2_H] \qquad \text{(IV-18a)}$$

where I_H is the moment of inertia for H_2;

$$I_H = m_H z_4^2 + m_H z_5^2 \quad . \qquad \text{(IV-18b)}$$

From this expression for the kinetic energy, both the total angular momentum $\underset{\sim}{M}_{CO_2}$ and $\underset{\sim}{M}_{H_2}$ and the momenta conjugate to the normal coordinates P_k and P_H can be found:

$$M_{x(CO_2)} = \frac{\partial T_{CO_2}}{\partial \omega_{x(CO_2)}} = I_{xx}\omega_{x(CO_2)} - I_{xy}\omega_{y(CO_2)} - I_{xz}\omega_{z(CO_2)} + (Q_{2b}\dot{Q}_3 - Q_3\dot{Q}_{2b})$$

$$M_{y(CO_2)} = (\partial T_{CO_2}/\partial \omega_{y(CO_2)}) = I_{yy}\omega_{y(CO_2)} - I_{xy}\omega_{x(CO_2)} - I_{yz}\omega_{z(CO_2)}$$
$$+ (Q_3\dot{Q}_{2a} - Q_{2a}\dot{Q}_3)$$

$$M_{z(CO_2)} = \frac{\partial T_{CO_2}}{\partial \omega_{z(CO_2)}} = I_{zz}\omega_{z(CO_2)} - I_{xz}\omega_{x(CO_2)} - I_{yz}\omega_{y(CO_2)} + (Q_{2a}\dot{Q}_{2b} - Q_{2b}\dot{Q}_{2a})$$

$$M_{x(H_2)} = \frac{\partial T_{H_2}}{\partial \omega_{x(H_2)}} = I_H \omega_{x(H_2)}$$

$$M_{y(H_2)} = I_H \omega_{y(H_2)}$$

$$M_{z(H_2)} = 0 \qquad \text{(IV-19)}$$

and

$$P_1 = \frac{\partial T_{CO_2}}{\partial \dot{Q}_1} = \dot{Q}_1$$

$$P_{2a} = \frac{\partial T_{CO_2}}{\partial \dot{Q}_{2a}} = \dot{Q}_{2a} + \omega_{y(CO_2)} Q_3 - \omega_{z(CO_2)} Q_{2b}$$

$$P_{2b} = \frac{\partial T_{CO_2}}{\partial \dot{Q}_{2b}} = \dot{Q}_{2b} - \omega_{x(CO_2)} Q_3 + \omega_{z(CO_2)} Q_{2a}$$

$$P_3 = \frac{\partial T_{CO_2}}{\partial \dot{Q}_3} = \dot{Q}_3 + \omega_{x(CO_2)} Q_{2b} - \omega_{y(CO_2)} Q_{2a}$$

$$P_H = \frac{\partial T_{H_2}}{\partial \dot{Q}_H} = \dot{Q}_H \, . \qquad \text{(IV-20)}$$

The most convenient expression for the total vibrational kinetic energy for carbon dioxide is

$$T_{vib}(CO_2) = (\tfrac{1}{2}) \sum_k P_k^2 \, , \; (k = 1,2a,2b,3) \, . \qquad \text{(IV-21)}$$

However, there are terms in T_{vib} which also appear in the total angular momentum $\underset{\sim}{M}_{CO_2}$. Care must be taken to avoid counting these terms in both the vibrational and rotational energy. Therefore, the vibrational angular momentum is defined as:

$$\tilde{m}_x = -Q_3 P_{2b} + Q_{2b} P_3$$

$$\tilde{m}_y = Q_3 P_{2a} - Q_{2a} P_3$$

$$\tilde{m}_z = -Q_{2b} P_{2a} + Q_{2a} P_{2b} \quad . \tag{IV-22}$$

This vibrational angular momentum is subtracted from the total angular momentum, giving the total kinetic energy for CO_2 as

$$T_{CO_2} = \tfrac{1}{2}[(M_{x(CO_2)} - \tilde{m}_x)\omega_{x(CO_2)} + (M_{y(CO_2)} - \tilde{m}_y)\omega_{y(CO_2)} + (M_{z(CO_2)} - \tilde{m}_z)\omega_{z(CO_2)} + \sum_{k=1}^{4} P_k^2 \,] \quad . \tag{IV-23}$$

The rotational energy of CO_2 is therefore:

$$T_{rot}(CO_2) = E_{rot}(CO_2) = \tfrac{1}{2} \sum_{i=x}^{z} (M_{i(CO_2)} - \tilde{m}_i)\omega_{i(CO_2)} \quad . \tag{IV-24}$$

Summing up,

$$T_{vib}(CO_2) = \tfrac{1}{2} \sum_{k} P_k^2, \quad (k = 1, 2a, 2b, 3) \tag{IV-25a}$$

$$E_{rot}(CO_2) = \tfrac{1}{2} \sum_{i=x}^{z} (M_{i(CO_2)} - \tilde{m}_i)\omega_i(CO_2) \tag{IV-25b}$$

$$T_{vib}(H_2) = \tfrac{1}{2} P_H^2 \tag{IV-25c}$$

$$E_{rot}(H_2) = \tfrac{1}{2} I_H (\omega_{x(H_2)}^2 + \omega_{y(H_2)}^2) \quad . \tag{IV-25d}$$

The internal energy is now separated into a vibrational and a rotational component. The separation, however, depends upon the vibrational motion. The quantity labeled as rotational (or vibrational) energy will change with the evolution of time.

The vibrational energy of CO_2 can be subdivided further into the energies of the individual vibrational modes,

$$E_{vib}(CO_2) = T_{vib}(CO_2) + V_{CO_2} = \sum_k \varepsilon_k, \quad (k = 1, 2a, 2b, 3)$$

where

$$\varepsilon_k = \tfrac{1}{2}(P_k^2 + \lambda_k Q_k^2) \ . \tag{IV-26}$$

$$E_{vib}(H_2) = T_{vib}(H_2) + V_{H_2} = \varepsilon_H = \tfrac{1}{2}(P_H^2 + \lambda_H Q_H^2) \ . \tag{IV-27}$$

Since the potential energy used is not harmonic, normal coordinates and their energies can only approximate the real behavior of the molecule.

Selection of the Initial Conditions

The initial physical state of the quasiclassical carbon dioxide molecule - hydrogen molecule collision system is defined by the following parameters: for carbon dioxide the vibrational and rotational quantum numbers n_1, n_{2a}, n_{2b}, n_3 and J, the vibrational phase angles $\delta_1, \delta_{2a}, \delta_{2b}$ and δ_3, the orientation angles α, β and γ; for hydrogen, vibrational qauntum number n_H, rotational quantum number J_H, the vibrational phase angle δ_H, the orientation angles α_1, β_1, and γ_1; the impact parameter b; the initial relative velocity vector $\underset{\sim}{V}_R$; and the initial separation R_s between centers of masses of CO_2 and H_2.

The internal energy of CO_2 for a given quantum state is

$$\begin{aligned} E_{int}(CO_2) = {} & \omega_1(n_1 + \tfrac{1}{2}) + \omega_2(n_{2a} + n_{2b} + 1) + \omega_3(n_3 + \tfrac{1}{2}) \\ & + X_{11}(n_1 + \tfrac{1}{2})^2 + X_{22}(n_{2a} + n_{2b} + 1)^2 + X_{33}(n_3 + \tfrac{1}{2})^2 \\ & + X_{12}(n_1 + \tfrac{1}{2})(n_{2a} + n_{2b} + 1) + X_{13}(n_1 + \tfrac{1}{2})(n_3 + \tfrac{1}{2}) \\ & + X_{23}(n_{2a} + n_{2b} + 1)(n_3 + \tfrac{1}{2}) + B_J J(J+1) - D_J J^2 (J+1)^2 \\ & - [\alpha_1(n_1 + \tfrac{1}{2}) + \alpha_2(n_{2a} + n_{2b} + 1) + \alpha_3(n_3 + \tfrac{1}{2})] J(J+1) \end{aligned} \tag{IV-28}$$

where the constants are defined by Herzberg (97) and are given in Table XVIII. Division of cross terms in the Equation (IV-28) equally between the internal vibrations gives the normal energies:

$$\varepsilon_1 = \omega_1(n_1+\tfrac{1}{2}) + X_{11}(n_1+\tfrac{1}{2})^2 + \tfrac{1}{2}X_{13}(n_1+\tfrac{1}{2})(n_3+\tfrac{1}{2}) + \tfrac{1}{2}X_{12}(n_1+\tfrac{1}{2})(n_{2a}+n_{2b}+1)$$

$$\varepsilon_{2a} = \omega_2(n_{2a}+\tfrac{1}{2}) + X_{22}(n_{2a}+\tfrac{1}{2})^2 + \tfrac{1}{2}X_{12}(n_1+\tfrac{1}{2})(n_{2a}+\tfrac{1}{2}) + \tfrac{1}{2}X_{23}(n_{2a}+\tfrac{1}{2})(n_3+\tfrac{1}{2})$$

$$\varepsilon_{2b} = \omega_2(n_{2b}+\tfrac{1}{2}) + X_{22}(n_{2b}+\tfrac{1}{2})^2 + \tfrac{1}{2}X_{12}(n_1+\tfrac{1}{2})(n_{2b}+\tfrac{1}{2}) + \tfrac{1}{2}X_{23}(n_{2b}+\tfrac{1}{2})(n_3+\tfrac{1}{2})$$

$$\varepsilon_3 = \omega_3(n_3+\tfrac{1}{2}) + X_{33}(n_3+\tfrac{1}{2})^2 + \tfrac{1}{2}X_{13}(n_1+\tfrac{1}{2})(n_3+\tfrac{1}{2}) + \tfrac{1}{2}X_{23}(n_3+\tfrac{1}{2})(n_{2a}+n_{2b}+1)$$

$$E_{rot}(CO_2) = B_J J(J+1) - D_J J^2(J+1)^2 - [\alpha_1(n_1+\tfrac{1}{2}) + \alpha_2(n_{2a}+n_{2b}+1) + \alpha_3(n_3+\tfrac{1}{2})]J(J+1)\,. \qquad \text{(IV-29)}$$

The internal energy of H_2 for a given quantum state is

$$E_{int}(H_2) = \omega_H(n_H+\tfrac{1}{2}) + X_{HH}(n_H+\tfrac{1}{2})^2 + B_e J_H(J_H+1) - \alpha_e(n_H+\tfrac{1}{2})J_H(J_H+1) \qquad \text{(IV-30)}$$

where the constants are again defined by Herzberg (98) and are also given in Table XVIII. We assume that the vibrational energy is given by,

$$\varepsilon_H = \omega_H(n_H+\tfrac{1}{2}) + X_{HH}(n_H+\tfrac{1}{2})^2\,. \qquad \text{(IV-31a)}$$

The remaining internal energy is assigned to rotation:

$$E_{rot}(H_2) = B_e J_H(J_H+1) - \alpha_e(n_H+\tfrac{1}{2})J_H(J_H+1)\,. \qquad \text{(IV-31b)}$$

TABLE XVIII

SPECTROSCOPIC CONSTANTS OF CO_2 AND H_2

CO_2[a]

Harmonic Frequencies

$\omega_1 = 1351.2\ cm^{-1}$

$\omega_2 = 672.2\ cm^{-1}$

$\omega_3 = 2396.4\ cm^{-1}$

Anharmonic Constants

$X_{11} = -0.3\ cm^{-1}$, $X_{22} = -1.3\ cm^{-1}$

$X_{33} = -12.5\ cm^{-1}$, $X_{12} = 5.7\ cm^{-1}$

$X_{23} = -11.0\ cm^{-1}$, $X_{13} = -21.9\ cm^{-1}$

Rotational Constants

$B_J = 0.3906\ cm^{-1}$, $D_J = 0.00\ cm^{-1}$

$\alpha_1 = 0.00121\ cm^{-1}$

$\alpha_2 = -0.00072\ cm^{-1}$

$\alpha_3 = 0.00309\ cm^{-1}$

H_2[b]

$\omega_H = 4395.2\ cm^{-1}$

$X_{HH} = -117.90\ cm^{-1}$

$B_e = 60.809\ cm^{-1}$

$\alpha_e = 2.993\ cm^{-1}$

[a] Reference 97

[b] Reference 98

For a harmonic potential, the time dependence of the normal coordinate is

$$Q_k(t) = Q_k^o \cos(\lambda^{\frac{1}{2}} t + \delta_k), \quad k = 1,2a,2b,3,H \tag{IV-32}$$

where Q_k^o is the maximum displacement of $Q_k(t)$. The maximum displacement of a normal coordinate occurs at the point where all of the energy is in the potential-energy, thus

$$Q_k^o = \left[\frac{2\varepsilon_k}{\lambda_k}\right]^{\frac{1}{2}} \tag{IV-33}$$

with the values of Q_k^o and δ_k, $Q_k(t=0)$ is found. The $P_k(t=0)$ are obtained from the expression

$$P_k(t) = \pm \left[2\varepsilon_k - \lambda_k Q_k^2(t)\right]^{\frac{1}{2}} . \tag{IV-34}$$

The + sign is used when $0 \leq \delta_k \leq \pi$ and the negative sign when $\pi \leq \delta_k \leq 2\pi$.

The normal coordinates Q_k are transformed to the molecule-fixed cartesian coordinates:

$$x_1 = -\left(\frac{m_B}{2m_C m_T}\right)^{\frac{1}{2}} Q_{2a}$$

$$x_2 = \left(\frac{2m_C}{m_B m_T}\right)^{\frac{1}{2}} Q_{2a}$$

$$x_3 = -\left(\frac{m_B}{2m_C m_T}\right)^{\frac{1}{2}} Q_{2a} = x_1$$

$$y_1 = -\left(\frac{m_B}{2m_C m_T}\right)^{\frac{1}{2}} Q_{2b}$$

$$y_2 = \left(\frac{2m_C}{m_B m_T}\right)^{\frac{1}{2}} Q_{2b}$$

$$y_3 = -\left(\frac{m_B}{2m_C m_T}\right)^{\frac{1}{2}} Q_{2b} = y_1$$

$$z_1 = -\left(\frac{m_B}{2m_C m_T}\right)^{\frac{1}{2}} Q_3 - \left(\frac{1}{2m_C}\right)^{\frac{1}{2}} Q_1 - R_{eCO}$$

$$z_2 = \left(\frac{2m_C}{m_B m_T}\right)^{\frac{1}{2}} Q_3$$

$$z_3 = -\left(\frac{m_B}{2m_C m_T}\right)^{\frac{1}{2}} Q_3 + \left(\frac{1}{2m_C}\right)^{\frac{1}{2}} Q_1 + R_{eCO}$$

$$x_4 = y_4 = x_5 = y_5 = 0$$

$$z_4 = -\left(\frac{1}{2m_H}\right)^{\frac{1}{2}} Q_H - \tfrac{1}{2} R_{eHH}$$

$$z_5 = \left(\frac{1}{2m_H}\right)^{\frac{1}{2}} Q_H + \tfrac{1}{2} R_{eHH} \qquad \text{(IV-35)}$$

From these cartesian coordinates, the moments of inertia I_{xx}, I_{yy} and I_{zz} and the nonzero product of inertia I_{yz} for CO_2 and moment of inertia I_H for H_2 are calculated. The non-zero component of vibrational angular momentum $\tilde{m}_x$ for CO_2 is calculated from the Q_k and P_k using Equation (IV-22).

The angular momentum and angular velocity of CO_2 and H_2 are determined from their rotational energies. The CO_2 molecule is assumed to be linear, and the rotation of the molecule is assumed to be in a plane perpendicular to the xy plane and rotated away from the xz plane by the angle γ. Under these conditions, the components of the angular momentum are:

$$L_x(CO_2) = \left[2 I_{xx} E_{rot}(CO_2)\right] \cos\gamma$$

$$L_y(CO_2) = \left[2 I_{yy} E_{rot}(CO_2)\right]^{\frac{1}{2}} \sin\gamma$$

$$L_z(CO_2) = 0 \quad . \qquad \text{(IV-36)}$$

The components of the angular velocity are:

$$\omega_x(CO_2) = \frac{L_x(CO_2)}{I_{xx}}$$

$$\omega_\gamma(CO_2) = \frac{L_\gamma(CO_2)}{I_{yy}}$$

$$\omega_z(CO_2) = 0 \ . \qquad \text{(IV-37)}$$

Similarly,

$$L_x(H_2) = [2\, I_H E_{rot}(H_2)]^{\frac{1}{2}} \cos\gamma'$$

$$L_y(H_2) = [2\, I_H E_{rot}(H_2)]^{\frac{1}{2}} \sin\gamma'$$

$$L_z(H_2) = 0 \qquad \text{(IV-38)}$$

and

$$\omega_x(H_2) = \frac{L_x(H_2)}{I_H}$$

$$\omega_y(H_2) = \frac{L_y(H_2)}{I_H}$$

$$\omega_z(H_2) = 0 \ . \qquad \text{(IV-39)}$$

Given the Q_k's and P_k's and the angular velocity, the time derivatives of the normal coordinates are:

$$\dot{Q}_1 = P_1$$

$$\dot{Q}_{2a} = P_{2a} - \omega_y(CO_2)Q_3 + \omega_z(CO_2)Q_{2b}$$

$$\dot{Q}_{2b} = P_{2b} + \omega_x(CO_2)Q_3 - \omega_z(CO_2)Q_{2a}$$

$$\dot{Q}_3 = P_3 - \omega_x(CO_2)Q_{2b} + \omega_y(CO_2)Q_{2a}$$

$$\dot{Q}_H = P_H \ . \qquad \text{(IV-40)}$$

The conjugate momenta to the molecule-fixed coordinates are then:

$$P_{x_1} = -m_A\left(\frac{m_B}{2m_C m_T}\right)^{\frac{1}{2}} \dot{Q}_{2a} + m_A z_1 \omega_y(CO_2)$$

$$P_{x_2} = m_B\left(\frac{2m_C}{m_B m_T}\right)^{\frac{1}{2}} \dot{Q}_{2a} + m_B z_2 \omega_y(CO_2)$$

$$P_{x_3} = -m_C\left(\frac{m_B}{2m_C m_T}\right)^{\frac{1}{2}} \dot{Q}_{2a} + m_C z_3 \omega_y(CO_2)$$

$$P_{y_1} = -m_A\left(\frac{m_B}{2m_C m_T}\right)^{\frac{1}{2}} \dot{Q}_{2b} - m_A z_1 \omega_x(CO_2)$$

$$P_{y_2} = m_B\left(\frac{2m_C}{m_B m_T}\right)^{\frac{1}{2}} \dot{Q}_{2b} - m_B z_2 \omega_x(CO_2)$$

$$P_{y_3} = -m_C\left(\frac{m_B}{2m_C m_T}\right)^{\frac{1}{2}} \dot{Q}_{2b} - m_C z_3 \omega_x(CO_2)$$

$$P_{z_1} = -m_A\left[\left(\frac{m_B}{2m_C m_T}\right)^{\frac{1}{2}} \dot{Q}_3 + \left(\frac{1}{2m_C}\right)^{\frac{1}{2}} \dot{Q}_1\right] + m_A(y_1\omega_x(CO_2) - x_1\omega_y(CO_2))$$

$$P_{z_2} = m_B\left(\frac{2m_C}{m_B m_T}\right)^{\frac{1}{2}} \dot{Q}_3 + m_B(y_2\omega_x(CO_2) - x_2\omega_y(CO_2))$$

$$P_{z_3} = -m_C\left[\left(\frac{m_B}{2m_C m_T}\right)^{\frac{1}{2}} \dot{Q}_3 - \left(\frac{1}{2m_C}\right)^{\frac{1}{2}} \dot{Q}_1\right] + m_C(y_3\omega_x(CO_2) - x_3\omega_y(CO_2))$$

$$P_{x_4} = m_H z_4 \omega_y(H_2)$$

$$P_{x_5} = m_H z_5 \omega_y(H_2)$$

$$P_{y_4} = -m_H z_4 \omega_x(H_2)$$

$$P_{y_5} = -m_H z_5 \omega_x(H_2)$$

$$P_{z_4} = -m_H\left(\frac{1}{2m_H}\right)^{\frac{1}{2}} \dot{Q}_H$$

$$P_{z_5} = m_H\left(\frac{1}{2m_H}\right)^{\frac{1}{2}} \dot{Q}_H \,. \qquad \text{(IV-41)}$$

The molecule-fixed coordinates are now transformed to the space-fixed coordinate frame. The origin of the space-fixed frame is defined

as the center of mass of CO_2. The molecule-fixed coordinates of CO_2 are rotated by an angle α about the Y axis and an angle β about the Z axis using the rotation matrices given in Table XIX. The third Eulerian angle γ has already been used. The coordinates of H_2 are rotated by angle α_1 about the Y' axis and an angle β_1 about the Z' axis. The coordinate system $X'Y'Z'$ is at distance $\underset{\sim}{R}_s$ from the center of mass of CO_2 and hence the origin of the space-fixed frame. The coordinates of H_2 are therefore:

$$\begin{aligned} X_4 &= (R_s)_x + x_4 \\ Y_4 &= (R_s)_y + y_4 \\ Z_4 &= (R_s)_z + z_4 \\ X_5 &= (R_s)_x + x_5 \\ Y_5 &= (R_s)_y + y_5 \\ Z_5 &= (R_s)_z + z_5 \ . \end{aligned} \qquad \text{(IV-42)}$$

If the impact parameter is b and if the center of mass of H_2 is approaching from the -Z direction in the YZ plane,

$$(R_s)_x = 0, \ (R_s)_y = -b \text{ and } (R_s)_z = -(R_s^2 - b^2)^{\frac{1}{2}} \ . \qquad \text{(IV-43)}$$

There is no loss of generality if the relative velocity is defined to be along the Z axis and if it is defined such that the center of mass of the total system does not move with time. Thus, the center of mass of H_2 translates in the Z direction with velocity $\left(\frac{m_{CO_2}}{m_{CO_2} + m_{H_2}}\right)V_R$, and the center of mass of CO_2 translates in the -Z direction with the velocity $\left(\frac{m_{H_2}}{m_{CO_2} + m_{H_2}}\right)V_R$ where $m_{H_2} = 2m_H$ and $m_{CO_2} = m_A + m_B + m_C$.

The complete set of initial cartesian coordinates and momenta is now defined. The momenta in the space-fixed frame are:

TABLE XIX

THE ROTATION MATRICES. THE MATRIX $R_q(\psi)$ ROTATES COORDINATE AXES IN A COUNTERCLOCKWISE DIRECTION ABOUT AXIS q THROUGH AN ANGLE ψ

$$R_x(\psi) = \begin{bmatrix} 1 & 0 & 0 \\ 0 & \cos\psi & \sin\psi \\ 0 & -\sin\psi & \cos\psi \end{bmatrix}$$

$$R_y(\psi) = \begin{bmatrix} \cos\psi & 0 & -\sin\psi \\ 0 & 1 & 0 \\ \sin\psi & 0 & \cos\psi \end{bmatrix}$$

$$R_z(\psi) = \begin{bmatrix} \cos\psi & \sin\psi & 0 \\ -\sin\psi & \cos\psi & 0 \\ 0 & 0 & 1 \end{bmatrix}$$

$$P_{X_1} = P_{x_1}\ ,\ P_{Y_1} = P_{y_1}\ ,\ P_{Z_1} = P_{z_1} - m_A\left(\frac{m_{H_2}}{m_{CO_2} + m_{H_2}}\right)V_R$$

$$P_{X_2} = P_{x_2}\ ,\ P_{Y_2} = P_{y_2}\ ,\ P_{Z_2} = P_{z_2} - m_B\left(\frac{m_{H_2}}{m_{CO_2} + m_{H_2}}\right)V_R$$

$$P_{X_3} = P_{x_3}\ ,\ P_{Y_3} = P_{y_3}\ ,\ P_{Z_3} = P_{z_3} - m_C\left(\frac{m_{H_2}}{m_{CO_2} + m_{H_2}}\right)V_R$$

$$P_{X_4} = P_{x_4}\ ,\ P_{Y_4} = P_{y_4}\ ,\ P_{Z_4} = P_{z_4} + m_H\left(\frac{m_{CO_2}}{m_{CO_2} + m_{H_2}}\right)V_R$$

$$P_{X_5} = P_{x_5}\ ,\ P_{Y_5} = P_{y_5}\ ,\ P_{Z_5} = P_{z_5} + m_H\left(\frac{m_{CO_2}}{m_{CO_2} + m_{H_2}}\right)V_R\ . \quad \text{(IV-44)}$$

Numerical Integration of the Equations of Motion

Once the initial coordinates and momenta are defined, the thirty coupled first-order differential equations (Hamilton's Equations) may be solved numerically to study the evolution of the system.

In this study, an Adams-Moulton type fifth-order predictor-sixth-order corrector method of numerical integration with a fourth-order Runge-Kutta scheme as the initiator was employed (100).

The accuracy of the trajectory of integration was judged by three different criteria. The total energy and the total angular momentum were expected to be constant at the beginning and at the end of each trajectory. Results of back integration of a trajectory were expected to match the starting coordinates. Some of the trajectories were integrated twice; once with a step size h and next with half the original stepsize. Both of them were expected to yield the same final state of the molecules. The units employed in this study are listed in Table XX.

TABLE XX

UNITS USED IN THE COMPUTER CODE[a,c]

Quantity	Program Unit	CGS Unit[b]
energy	1 eV	1.6021×10^{-12} erg
mass	1 amu	$1.6604345 \times 10^{-24}$ gram
distance	1 Å	10^{-8} cm
time	1 time unit	$1.01804287 \times 10^{-14}$ sec.
velocity	1 velocity unit	0.9822769×10^{6} cm sec.$^{-1}$
momentum	1 momentum unit	1.631006×10^{-18} dyne sec.
angular momentum	1 angular momentum unit	1.631006×10^{-26} erg sec.
Planck's constant ($\hbar$)	0.0644531465	1.05450×10^{-27} erg sec.
Boltzmann constant (k)	8.6170651×10^{-5}	1.38054×10^{-16} erg $^{o}K^{-1}$

[a]These units are similar to the RMU units used by Raff et al., J. Chem. Phys. 56, 5998 (1972). The units differ only in the unit of distance.

[b]Units based on physical constants recommended by NAS-NRC and adopted by NBS (NBS Technical News Bulletin, Oct. 1963).

[c]Reference 58, p. 67.

Calculation of the Final State of the System

The final physical state of the collision system is determined from the positions and momenta at the end of the trajectory. The determination of the 'end' is rather easy for nonreactive collisions.

The centers of mass separation are required to be greater than or equal to R_s. In order to minimize errors in the calculation of change in energy in each mode, initial energies were calculated in the same way as described here for the calculation of final energies.

The total energy of the collision is defined by the classical Hamiltonian, Equation (IV-2) and (IV-3). The total angular momentum is

$$L^2 = L_x^2 + L_y^2 + L_z^2 \tag{IV-45}$$

where

$$\begin{aligned} L_x &= \sum_{i=1}^{5} Y_i P_{Z_i} - Z_i P_{Y_i} \\ L_y &= \sum_{i=1}^{5} Z_i P_{X_i} - X_i P_{Z_i} \\ L_z &= \sum_{i=1}^{5} X_i P_{Y_i} - Y_i P_{X_i} \end{aligned} \quad . \tag{IV-46}$$

The motion of the system center of mass has been set to zero. The final velocity of the H_2-center of mass is

$$\underset{\sim}{V}'_{H_2} = \left(\frac{\dot{X}_4 + \dot{X}_5}{2}, \frac{\dot{Y}_4 + \dot{Y}_5}{2}, \frac{\dot{Z}_4 + \dot{Z}_5}{2}\right) . \tag{IV-47}$$

The final relative velocity is

$$\underset{\sim}{V}'_R = \frac{m_{CO_2} + m_{H_2}}{m_{CO_2}} \underset{\sim}{V}'_{H_2} . \tag{IV-48}$$

The final relative translational energy is

$$\begin{aligned} E'_{trans} &= \tfrac{1}{2}\left(\frac{m_{CO_2} m_{H_2}}{m_{CO_2} + m_{H_2}}\right) V_R'^2 \\ &= \tfrac{1}{2} \frac{m_{H_2}}{m_{CO_2}} (m_{CO_2} + m_{H_2}) V_{H_2}'^2 \end{aligned} \quad . \tag{IV-49}$$

The center of mass scattering angle is also determined from $\underset{\sim}{V}'_R$. Since the initial direction of $\underset{\sim}{V}_R$ is along the Z axis, the scattering angle Ω_{CM} is given by

$$\Omega_{CM} = \arccos\left[\frac{(\underset{\sim}{V}'_R)_Z}{(\underset{\sim}{V}'_R \cdot \underset{\sim}{V}'_R)^{\frac{1}{2}}}\right] . \qquad \text{(IV-50)}$$

To compute the final internal energies, the space-fixed coordinates are transformed to the molecule-fixed coordinate frames. The motion of the molecular center of mass is subtracted from the molecular coordinates:

$$P_{x_i} = P_{X_i} + m_i\left(\frac{m_{H_2}}{m_{CO_2} + m_{H_2}}\right)(\underset{\sim}{V}'_R)_X$$

$$P_{y_i} = P_{Y_i} + m_i\left(\frac{m_{H_2}}{m_{CO_2} + m_{H_2}}\right)(\underset{\sim}{V}'_R)_Y$$

$$P_{z_i} = P_{Z_i} + m_i\left(\frac{m_{H_2}}{m_{CO_2} + m_{H_2}}\right)(\underset{\sim}{V}'_R)_Z , \quad (i = 1,2,3) .$$

$$P_{x_i} = P_{X_i} - m_i\left(\frac{m_{CO_2}}{m_{CO_2} + m_{H_2}}\right)(\underset{\sim}{V}'_R)_X$$

$$P_{y_i} = P_{Y_i} - m_i\left(\frac{m_{CO_2}}{m_{CO_2} + m_{H_2}}\right)(\underset{\sim}{V}'_R)_Y$$

$$P_{z_i} = P_{Z_i} - m_i\left(\frac{m_{CO_2}}{m_{CO_2} + m_{H_2}}\right)(\underset{\sim}{V}'_R)_Z , \quad (i = 4 \text{ and } 5). \qquad \text{(IV-51)}$$

The atomic coordinates relative to the respective molecular center of mass are:

$$x_i = X_i - \frac{1}{m_{CO_2}}(m_A X_1 + m_B X_2 + m_C X_3)$$

$$y_i = Y_i - \frac{1}{m_{CO_2}}(m_A Y_1 + m_B Y_2 + m_C Y_3)$$

$$z_i = Z_i - \frac{1}{m_{CO_2}}(m_A Z_1 + m_B Z_2 + m_C Z_3), \quad (i = 1, 2 \text{ and } 3).$$

$$x_i = X_i - \frac{1}{m_{H_2}}(m_H X_4 + m_H X_5)$$

$$y_i = Y_i - \frac{1}{m_{H_2}}(m_H Y_4 + m_H Y_5)$$

$$z_i = Z_i - \frac{1}{m_{H_2}}(m_H Z_4 + m_H Z_5), \quad (i = 4 \text{ and } 5) . \qquad \text{(IV-52)}$$

The normal coordinates Q_k ($k = 1, 2a, 2b, 3$ for CO_2 and $k = H$ for H_2) and their time derivatives $\dot{Q}_k$ are obtained from the transformation from molecule-fixed coordinates to normal coordinates, Equation (IV-5). Derivatives of the molecule-fixed coordinates are obtained from the conjugate momenta. The molecule-fixed coordinates are also used to calculate the moments of inertia and the products of inertia for CO_2 and H_2. The final angular momenta $\underset{\sim}{M}(CO_2)$ and $\underset{\sim}{M}(H_2)$ are obtained from:

$$M_x(CO_2) = \sum_{i=1}^{3} y_i P_{z_i} - z_i P_{y_i}$$

$$M_y(CO_2) = \sum_{i=1}^{3} z_i P_{xi} - x_i P_{z_i}$$

$$M_z(CO_2) = \sum_{i=1}^{3} x_i P_{y_i} - y_i P_{x_i}$$

$$M_x(H_2) = \sum_{i=4}^{5} y_i P_{z_i} - z_i P_{y_i}$$

$$M_y(H_2) = \sum_{i=4}^{5} z_i P_{x_i} - x_i P_{z_i}$$

$$M_z(H_2) = \sum_{i=4}^{5} x_i P_{y_i} - y_i P_{x_i} . \qquad \text{(IV-55)}$$

Angular velocities for CO_2 are obtained from Equation (IV-19) as follows:

$$\begin{bmatrix} \omega_x(CO_2) \\ \omega_y(CO_2) \\ \omega_z(CO_2) \end{bmatrix} = \begin{bmatrix} I_{xx} & -I_{xy} & -I_{xz} \\ -I_{xy} & I_{yy} & -I_{yz} \\ -I_{xz} & -I_{yz} & I_{zz} \end{bmatrix}^{-1} \begin{bmatrix} M_x(CO_2) - (Q_{2b}\dot{Q}_3 - Q_3\dot{Q}_{2b}) \\ M_y(CO_2) - (Q_3\dot{Q}_{2a} - Q_{2a}\dot{Q}_3) \\ M_z(CO_2) - (Q_{2a}\dot{Q}_{2b} - Q_{2b}\dot{Q}_{2a}) \end{bmatrix} . \qquad \text{(IV-56)}$$

If I is the moment of inertia matrix,

$$I^{-1} = \frac{1}{\det I} \tilde{I}^t \qquad \text{(IV-57)}$$

where $\tilde{I}^t$ is the transpose of the adjoint of I,

$$\tilde{I}^t = \begin{bmatrix} (I_{yy}I_{zz} - I_{yz}^2) & -(-I_{xy}I_{zz} - I_{xz}I_{yz}) & (I_{xy}I_{yz} + I_{xz}I_{yy}) \\ -(-I_{xy}I_{zz} - I_{yz}I_{xz}) & (I_{xx}I_{zz} - I_{xz}^2) & -(-I_{xx}I_{yz} - I_{xy}I_{xz}) \\ (I_{xy}I_{yz} + I_{yy}I_{xz}) & -(-I_{xx}I_{yz} - I_{xy}I_{xz}) & (I_{xx}I_{yy} - I_{xy}^2) \end{bmatrix} . \qquad \text{(IV-58)}$$

Angular velocities for H_2 are:

$$\begin{aligned} \omega_x(H_2) &= M_x(H_2)/I_H \\ \omega_y(H_2) &= M_y(H_2)/I_H \\ \omega_z(H_2) &= M_z(H_2)/I_H . \end{aligned} \qquad \text{(IV-59)}$$

The final normal momenta P_k are calculated using Equation (IV-20) and the vibrational angular momentum is found using Equation (IV-22).

The final rotational energies for CO_2 and H_2 are obtained from:

$$\begin{aligned} E'_{rot}(CO_2) &= \tfrac{1}{2} \sum_{i=x}^{z} (M_i(CO_2) - \tilde{m}_i)\omega_i(CO_2) \\ E'_{rot}(H_2) &= \tfrac{1}{2} I_H (\omega_x^2(H_2) + \omega_y^2(H_2) + \omega_z^2(H_2)) . \end{aligned} \qquad \text{(IV-60)}$$

The total internal energies of the molecules are:

$$E'_{int}(CO_2) = \tfrac{1}{2} \sum_{i=1}^{3} \frac{1}{m_i} (P_{x_i}^2 + P_{y_i}^2 + P_{z_i}^2) + V_{CO_2}$$

$$= E'_{vib}(CO_2) + E'_{rot}(CO_2)$$

and

$$E'_{int}(H_2) = \tfrac{1}{2} \sum_{i=4}^{5} \frac{1}{m_i} (P_{x_i}^2 + P_{y_i}^2 + P_{z_i}^2) + V_{H_2}$$

$$= E'_{vib}(H_2) + E'_{rot}(H_2) \quad . \qquad \text{(IV-61)}$$

The final vibrational energies are:

$$E'_{vib}(CO_2) = E'_{int}(CO_2) - E'_{rot}(CO_2)$$

$$E'_{vib}(H_2) = E'_{int}(H_2) - E'_{rot}(H_2) \quad . \qquad \text{(IV-62)}$$

Attempts are being made to calculate at least average normal energies for the carbon dioxide molecule.

The energy changes are the differences between the initial and final energies:

$$\Delta E_{trans} = E'_{trans} - E_{trans}$$

$$\Delta E_{rot}(CO_2) = E'_{rot}(CO_2) - E_{rot}(CO_2)$$

$$\Delta E_{rot}(H_2) = E'_{rot}(H_2) - E_{rot}(H_2)$$

$$\Delta E_{vib}(CO_2) = E'_{vib}(CO_2) - E_{vib}(CO_2)$$

$$\Delta E_{vib}(H_2) = E'_{vib}(H_2) - E_{vib}(H_2) \quad . \qquad \text{(IV-63)}$$

Ensemble Sampling and Averaging

In a chemical system, large numbers of collisions occur. Any theoretical study must therefore consider the various possible collisions in order to make the comparison with experimental results meaningful.

Each trajectory depends upon 19 physical parameters: the vibrational energies ($\varepsilon_1, \varepsilon_{2a}, \varepsilon_{2b}, \varepsilon_3$), their phases ($\delta_1, \delta_{2a}, \delta_3$), rotational

energy (E_{rot}), molecular orientation (α,β,γ) for CO_2 and similarly ε_H, δ_H, $E_{rot}(H_2)$, α_1, β_1 and γ_1 for H_2; the impact parameter b; and the initial relative velocity V_R. In this study, the initial $\varepsilon_1,\varepsilon_{2a}$, $\varepsilon_{2b},\varepsilon_3,\varepsilon_H$ and V_R are held constant, and the other variables are chosen at random from appropriate distribution functions (58) (96).

β, γ, and β_1 and γ_1 are determined by:

$$\begin{aligned} \beta &= 2\pi\,\xi_1 \\ \gamma &= 2\pi\,\xi_2 \\ \beta_1 &= 2\pi\,\xi_3 \\ \gamma_1 &= 2\pi\,\xi_4 \end{aligned} \qquad \text{(IV-64)}$$

where the ξ_i are random numbers uniformly distributed in the interval $0 \le \xi_i \le 1$.

α and α_1 are selected by requiring that

$$\begin{aligned} \cos\alpha &= 1-2\,\xi_5 \\ \cos\alpha_1 &= 1-2\,\xi_6 \end{aligned} \qquad \text{(IV-65)}$$

These choices weight the solid angle elements by $\sin\alpha$ and $\sin\alpha_1$, respectively, as required. The vibrational phase angles are determined by:

$$\begin{aligned} \delta_1 &= 2\pi\,\xi_7 \\ \delta_{2a} &= 2\pi\,\xi_8 \\ \delta_{2b} &= \delta_{2a} + \pi/2 \\ \delta_3 &= 2\pi\,\xi_9 \\ \delta_H &= 2\pi\,\xi_{10}\,. \end{aligned} \qquad \text{(IV-66)}$$

Assuming separability of rotational-vibrational motion and also assuming the molecules to be rigid rotors, for CO_2, it is the solution of

$$J = \tfrac{1}{2}\{-1 + [1 - 8IkT\ell n(1-\xi_{12})/\hbar^2]^{\frac{1}{2}}\} \qquad \text{(IV-67)}$$

and for H_2, it is the solution of

$$\xi_{13} = Q_r^{-1} \sum_{J'=0}^{J} (2J'+1) \exp[-J'(J'+1)\hbar^2/2IkT] \qquad \text{(IV-68)}$$

where

$$Q_r = \sum_{J=0}^{\infty} (2J+1) \exp[-J(J+1)\hbar^2/2IkT]. \qquad \text{(IV-69)}$$

The impact parameter is selected using a b^2 distribution between 0 and b_{max}:

$$b^2 = b_{max}^2 \xi_{11} \quad . \qquad \text{(IV-70)}$$

All the variables were chosen at random as above at a rotational temperature of 1000 K with CO_2 and H_2 in their ground vibrational states. The relative translational energy was kept at 1.0 eV. The results of preliminary studies of the dependence of translational energy transfer upon impact parameter are shown in Figure 31. As can be seen, at impact parameter above 3.5 A, little or no net energy transfer occurs. Thus, b_{max} in Equation (IV-70) was chosen to be 3.5 $\mathring{A}$.

Since the variables were chosen from appropriate distribution functions, Monte Carlo (96) averaging of energy transfer in different modes corresponds to a simple averaging of energy changes in individual trajectories over N trajectories computed for a particular set of initial v_1, v_{2a}, v_{2b}, v_3, v_H and V_R.

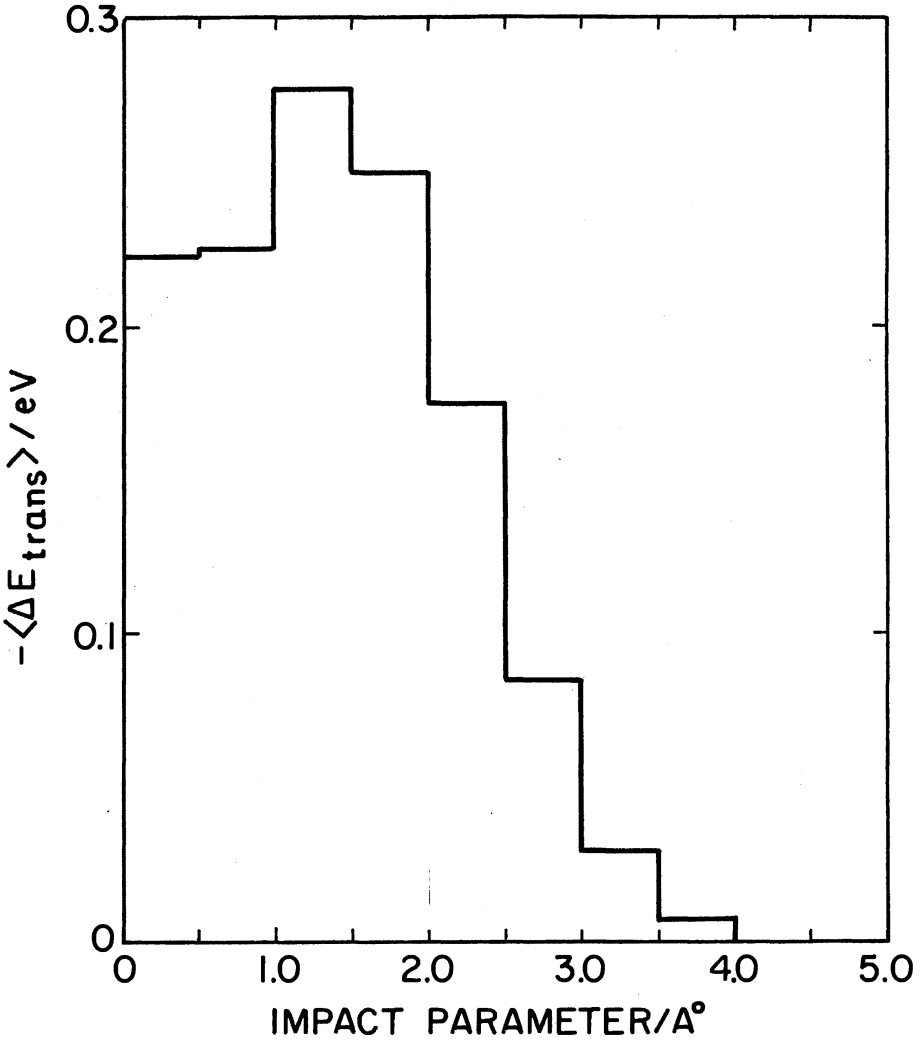

Figure 31. Translational Energy Transfer as a Function of Impact Parameter at E_{trans} = 1.0 eV

CHAPTER V

RESULTS AND DISCUSSION

Carbon dioxide - hydrogen molecule system is the first polyatomic molecule - molecule system to be investigated by detailed dynamical studies on an ab initio potential-energy surface. It poses several questions on energy transfer processes that have remained unanswered. There is a multitude of processes ($V\curvearrowright V$, $V\curvearrowright R$, $V\leftrightarrow V$, $V\leftrightarrow R$, $V\leftrightarrow T$ etc.) that can occur simultaneously and their mechanisms and relative importance may depend upon the conditions of molecular collisions. The calculation of relaxation times for each CO_2 normal mode and the investigation of the transfer mechanism requires a systematic analysis of the results obtained from numerous trajectories with varying initial conditions. Only preliminary results of such a study are reported here as the problem is being pursued further.

Energy transfer results from a quasiclassical trajectory study must be interpreted with care due to the nonquantized nature of the calculation. Quantum mechanical scattering calculations are difficult to carry out, but once completed, the results are easy to interpret. They simultaneously yield information about all channels considered in the process. Quasiclassical trajectory calculations, on the other hand, are relatively simple and straightforward. The main difficulty in interpreting their results lies in the "classical" nature of the system. Under the quasiclassical assumption, initially the system is

in a quantized energy state. However, once the trajectory is started, the system is completely classical in nature and the energy can flow from one mode into another in any amount. If, for example, the transition probability for a quantum of energy to be transferred is one in one hundred, it is necessary to assume that the same energy would be transferred in 100 classical collisions. Such assumptions may or may not be valid. Frequently one finds that the average classical energy transfer is too large.

In the preliminary investigations, an initial separation of the molecules of 5 $\mathring{A}$, b_{max} of 3.5 $\mathring{A}$ and a timestep of 0.02 molecular units were used. Initial vibrational states of the molecules and their relative translational energies were chosen to be specific values while rotational states were averaged over a thermal distribution at TK. All other variables were selected randomly from their appropriate distribution functions as was discussed in Chapter IV.

In the first set of calculations, the rotational temperature was set at 1000 K, and the relative translational energy was taken to be 1.0 eV. The impact parameter was restricted to be 0.0. The hydrogen molecule was placed in its v = 0 vibrational state and the average energy transfer was examined for CO_2 in either its (0000), (1000), (0100), (0010) or (0001) states. The numbers in parantheses represent vibrational quantum numbers for Q_1, Q_{2a}, Q_{2b}, and Q_3 modes, respectively. In each case 20 trajectories were run. The results are reported in Table XXI.

In the second set of calculations, the rotational temperature was changed to 300 K and the relative translational energy to 0.1 eV while the impact parameter was selected from a random b^2 distribution with

b_{max} = 3.5 Å. 150 trajectories for the (1000) state and 100 trajectories for the other (v_1, v_{2a}, v_{2b}, v_3) states were computed. The results are presented in Table XXII. For (0010), the calculations were repeated after suppressing the zero point energy from all modes.

When the relative translational energy is 1.0 eV, the main process would be expected to be the flow of energy from translational motion into internal modes of CO_2 and H_2. This is found to be the case: (T → V) seems to be the main process, about three fourths of the relative translational energy being converted into the vibrational energy of carbon dioxide. Except when the Q_3 mode is excited, the (T → V) process seems to be independent of the initial vibrational state of CO_2. The rest of the translational energy seems to be divided equally between rotational motions of CO_2 and H_2 internal energy. It is difficult to answer the question of which vibrational mode of CO_2 is excited during this (T → V) process. Extensive studies of Parr (101) show that normal mode energies are not separable; energy flows from one normal mode into another in its own potential field. However, it may be possible to obtain an average of the normal mode energies by allowing the CO_2 molecule to vibrate over a specified period of time after the collision and thus determine the normal mode that has been excited. This possibility is being investigated.

When the relative translational energy is low, the first excited normal modes of CO_2 have energies comparable to that of the translational motion. Hence energy could flow out of the internal modes of CO_2 and H_2. Indeed, $\langle E_v(CO_2)\rangle$ is found to be negative. It should be pointed out that it is negative even when the CO_2 molecule

TABLE XXI

RESULTS OF AVERAGE ENERGY TRANSFER[a] AT E_{trans} = 1.0 eV, b = 0.0, T_{rot} = 1000 K FOR DIFFERENT INITIAL VIBRATIONAL STATES OF CO_2

CO_2 Vibrational State	$\langle E_{trans} \rangle$	$\langle E_v(CO_2) \rangle$	$\langle E_r(CO_2) \rangle$	$\langle E_v(H_2) \rangle$	$\langle E_r(H_2) \rangle$
(0000)	-0.222	0.167(0.75)	0.023	0.015	0.02
(1000)	-0.189	0.139(0.74)	0.018	0.008	0.025
(0100)	-0.185	0.138(0.75)	0.016	0.014	0.019
(0010)	-0.199	0.152(0.76)	0.015	0.014	0.021
(0001)	-0.162	0.160(0.99)	0.014	0.013	0.021

[a]Units are in eV.

[b]Values in parentheses are fractions of the translational energy transferred into vibrational energy of CO_2.

TABLE XXII

RESULTS OF AVERAGE ENERGY TRANSFER[a] AT E_{trans} = 0.1 eV, b_{max} = 3.5 Å, T_{rot} = 300 K FOR DIFFERENT INITIAL VIBRATIONAL STATES OF CARBON DIOXIDE

CO_2 Vibrational State	$\langle E_{trans} \rangle$	$\langle E_v(CO_2) \rangle$	$\langle E_r(CO_2) \rangle$	$\langle E_v(H_2) \rangle$	$\langle E_r(H_2) \rangle$
(0000)	-0.00118	-0.00015	-0.00029	0.00027	0.00253
(1000)	-0.00021	-0.00208	0.00023	0.00246	0.00198
(0010)	-0.00091	-0.00055	-0.00018	-0.00144	0.00154
(0010)[b]	-0.00276	0.00131	0.00063	0.01136	0.00066

[a]Units are in eV.

[b]Initial state with zero point energy suppressed from all modes.

is in its ground vibrational state. This spurious result arises due to the "classical" nature of the system and may be avoided by suppressing the zero point energies of all the normal modes. Results of one such calculation are reported in Table XXII. It would be premature to draw any conclusion at this stage as this problem is currently under careful investigation.

CHAPTER VI

CONCLUSIONS

Our study on CO_2-H_2 system illustrates that it is now possible to employ LCAO-MO-SCF procedure using extended split valence shell gaussian basis set and compute intermolecular potential between two molecules, one of them having as many as 22 electrons. Utilizing the symmetry of the system and also the fact that certain regions of the potential-energy surface are not sampled during a trajectory, it was possible to compute intermolecular potentials at 1053 conformations. Three dimensional cubic spline interpolation procedure has been successfully applied to the problem of interpolating this table of 1053 numbers. By a combination of the splinefitted intermolecular potential with the available spectroscopic information on intramolecular potentials for individual molecules, it has been possible to construct potential-energy surface for CO_2-H_2 system and to evaluate the derivatives of the potential with respect to its coordinates which are required during a quasiclassical trajectory analysis. A computer code for performing five-body quasiclassical trajectory calculations is now available and has been tested for its accuracy as was explained in Chapter IV. Preliminary studies suggest the ($T \rightarrow V$) process to be the major mode of energy transfer at a relative translational energy of 1.0 eV and rotational temperature of 1000 K. It also seems to be independent of the initial vibrational state of CO_2 except when it is in its (0001) state.

At the present stage, for a specified set of initial conditions it is possible to compute a finite number of trajectories and calculate the amount of energy transferred from translational motion into vibrational and rotational motions of either one or both of the molecules or vice versa. Several questions remain to be answered: Of the four, which normal mode of CO_2 does gain or lose energy during such an energy transfer? Is it really meaningful to try to get an answer to this question when classical mechanics is used to study the molecular dynamics? Is it possible to suppress the zero point energy from all normal modes and then obtain a 'meaningful' measure of the energy transfer? These problems are currently being investigated.

A theoretical study is complete only if it is able to compute experimentally measurable quantities and compare them with previously measured results. In experiments on energy transfer processes, relaxation time is the most commonly measured quantity. We are yet to develop a formalism to calculate relaxation time from the amount of average energy transfer.

It would be worthwhile to study the detailed mechanism of energy transfer from each excited vibrational state of CO_2 and also of H_2. It would also be interesting to study the effect of mass on preferential mode of energy transfer by using D_2 instead of H_2. One good test for this whole study would be to calculate the relaxation time as a function of temperature and compare with the experimental result. This theoretical calculation would be highly valuable if it could predict the relaxation time for Q_1 mode as no experimental information is available on the energy transfer from this particular mode.

BIBLIOGRAPHY

(1) V. O. Knudsen and E. Fricke, J. Acoust. Soc. Am. 12, 255 (1940).

(2) T. G. Winter, J. Chem. Phys. 38, 2761 (1963).

(3) T. L. Cottrell and J. C. McCoubrey, "Molecular Energy Transfer in Gases", (Butterworths, London (1961).

(4) K. F. Herzfeld and T. A. Litovitz, "Absorption and Dispersion of Ultrasonic Waves", (Academic, New York, 1959).

(5) T. L. Cottrell and M. A. Day in "Molecular Relaxation Processes", publ. 20. The Chemical Society, London (Academic Press, Inc., 1966), p. 253.

(6) T. Rees and J. K. Bangu, J. Fluid. Mech. 39, 601 (1969).

(7) C. J. S. M. Simpson and T. R. D. Chandler, Proc. Roy. Soc. Lond. A. 317, 265 (1970).

(8) C. J. S. M. Simpson and J. M. Simmie, Proc. Roy. Soc. Lond. A. 325, 197 (1971).

(9) S. W. Behnen, H. L. Rothwell and R. C. Amme, Chem. Phys. Lett. 8, 318 (1971).

(10) R. C. Millikan and D. R. White, J. Chem. Phys. 39, 3209 (1963).

(11) R. C. Millikan in "Molecular Relaxation Processes", publ. 20. The Chemical Society, London (Academic Press Inc., 1966), pp. 221-226.

(12) For a review of data on several systems, see: R. L. Taylor and S. Bitterman, Rev. Mod. Phys. 41, 26 (1969).

(13) C. B. Moore, R. E. Wood, B. L. Hu and J. T. Yardley, J. Chem. Phys. 46, 4222 (1967).

(14) J. T. Yardley and C. B. Moore, J. Chem. Phys. 46, 4491 (1967).

(15) J. C. Stephenson, R. E. Wood and C. B. Moore, J. Chem. Phys. 54, 3097 (1971).

(16) J. C. Stephenson and C. B. Moore, J. Chem. Phys. 56, 1295 (1972).

(17) W. A. Rosser, Jr., and E. T. Gerry, J. Chem. Phys. 54, 4131 (1971).

(18) P. K. Cheo, Appl. Phys. Lett. 11, 38 (1967).

(19) W. A. Rosser, Jr., E. Hoag and E. T. Gerry, J. Chem. Phys. 57, 4153 (1972).

(20) L. O. Hocker, M. A. Kovacs, C. K. Rhodes, G. W. Flynn and A. Javan, Phys. Rev. Lett. 17, 233 (1966).

(21) R. L. Abrams and P. K. Cheo, Appl. Phys. Lett. 15, 177 (1969).

(22) J. C. Stephenson, R. E. Wood and C. B. Moore, J. Chem. Phys. 48, 4790 (1968).

(23) J. C. Stephenson and C. B. Moore, J. Chem. Phys. 52, 2333 (1970); 56, 1295 (1972).

(24) J. C. Stephenson, R. E. Wood and C. B. Moore, J. Chem. Phys. 56, 4813 (1972).

(25) J. C. Stephenson, J. Finzi and C. B. Moore, J. Chem. Phys. 49, 1432 (1968).

(26) C. B. Moore, "Fluorescence - Theory, Instrumentation and Practice", (Ed: G. G. Guilbault), (M. Dekker, Inc., New York, 1967), pp. 133-199.

(27) C. B. Moore, Accounts. Chem. Res. 2, 103 (1969).

(28) C. B. Moore, Adv. Chem. Phys. 23, 41 (1973).

(29) C. B. Moore, Laser and Unconventional Optics. Journal. 40, 7 (1972).

(30) For example, see: J. Ross, "Molecular Beams", (John Wiley & Sons, New York, 1966).

(31) L. Landau and E. Teller, Physik. Z. Sowjetunion 10, 34 (1936).

(32) C. Zener, Phys. Rev. 37, 556 (1931).

(33) a) R. N. Schwartz, Z. I. Slawsky and K. F. Herzfeld, J. Chem. Phys. 20, 1591 (1952); b) R. N. Schwartz and K. F. Herzfeld, J. Chem. Phys. 22, 767 (1954); c) K. F. Herzfeld, Disc. Faraday. Soc. 33, 22 (1962); d) K. F. Herzfeld, J. Chem. Phys. 47, 743 (1967).

(34) a) R. D. Sharma and C. A. Brau, Phys. Rev. Lett. 19, 1273 (1967); b) R. D. Sharma and C. A. Brau, J. Chem. Phys. 50, 924 (1969); c) R. D. Sharma, J. Chem. Phys. 50, 919 (1969).

(35) S. Sato, J. Chem. Phys. 23, 592 (1955).

(36) For example, see: a) H_2I_2: L. M. Raff, L. Stivers, R. N. Porter, D. L. Thompson and L. B. Sims, J. Chem. Phys. 52, 3449 (1970); b) H_2F: R. L. Jaffe and J. B. Anderson, J. Chem. Phys. 54, 2224 (1971); J. T. Muckermann, J. Chem. Phys. 56, 2997 (1972); R. L. Wilkins, J. Chem. Phys. 57, 912 (1972); c) HF_2: R. L. Wilkins, J. Chem. Phys., 59, 698 (1973); N. C. Blais, "Monte Carlo Trajectories: Dynamics of the Reaction H + F_2", LA-4687, Los Alamos Scientific Laboratory, 1971; d) H_2I: R. N. Porter, L. B. Sims, D. L. Thompson and L. M. Raff, J. Chem. Phys. 58, 2855 (1973).

(37) H_3: B. Liu, J. Chem. Phys. 58, 1925 (1973).

(38) FH_2: a) C. F. Bender, P. K. Pearson, S. V. O'Neil and H. F. Schaefer, III, J. Chem. Phys. 56, 4626 (1972); b) C. F. Bender, S. V. O'Neil, P. K. Pearson and H. F. Schaefer, III, Science 176, 1412 (1972).

(39) LiH_2^+: a) W. A. Lester, Jr., J. Chem. Phys. 53, 1511 (1970); 53, 1611 (1970); 54, 3171 (1971); b) W. Kutzelnigg, V. Staemmler and C. Hoheisel, Chem. Phys. 1, 27 (1973).

(40) For a review in this field up to 1969, refer to M. Krauss, Ann. Rev. Phys. Chem. 21, 39 (1970).

(41) HeH_2^+: P. J. Brown and E. F. Hayes, J. Chem. Phys. 55, 922 (1971).

(42) HeH_2: a) M. Krauss and F. H. Mies, J. Chem. Phys. 42, 2703 (1965); b) M. D. Gordon and D. Secrest, J. Chem. Phys. 52, 120 (1970); c) C. W. Wilson, R. Kapral and G. Burns, Chem. Phys. Lett. 24, 488 (1974).

(43) HF_2: S. V. O'Neil, P. K. Pearson, H. F. Schaefer, III and C. F. Bender, J. Chem. Phys. 58, 1126 (1973).

(44) HeH_3^+: M. J. Benson and D. R. Mclaughlin, J. Chem. Phys. 56, 1322 (1972).

(45) See: Indiana University, Quantum Chemistry Program Exchange, Catalog and Procedures, Vol X (1974).

(46) For example, D. R. Yarkoni, S. V. O'Neil, H. F. Schaefer, III, C. P. Baskin and C. F. Bender, J. Chem. Phys. 60, 855 (1974).

(47) D. R. Mclaughlin and D. L. Thompson, J. Chem. Phys. 59, 4393 (1973).

(48) Reference 45, Program #236.

(49) D. Secrest, Ann. Rev. Phys. Chem. 24, 379 (1973).

(50) T. F. George and J. Ross, Ann. Rev. Phys. Chem. 24, 263 (1973).

(51) G. E. Kellerhals, Ph.D. Thesis, Oklahoma State University, Stillwater, Oklahoma (1974).

(52) G. Wolken and M. Karplus, J. Chem. Phys. 60, 351 (1974).

(53) R. N. Porter, Ann. Rev. Phys. Chem. 25, 317 (1974).

(54) a) H. Eyring and M. Polanyi, Z. Phys. Chem. B 12, 279 (1931); b) F. T. Wall, L. A. Hiller and J. Mazur, J. Chem. Phys. 29, 255 (1958).

(55) M. Karplus, R. N. Porter and R. D. Sharma, J. Chem. Phys. 43, 3259 (1965).

(56) a) J. M. Bowman and A. Kuppermann, Chem. Phys. Lett. 12, 1 (1971); 19, 166 (1973); b) J. M. Bowman and A. Kuppermann, J. Chem. Phys. 59, 6524 (1973); c) G. C. Schatz, J. M. Bowman and A. Kuppermann, J. Chem. Phys. 58, 4023 (1973); d) J. M. Bowman, G. C. Schatz and A. Kuppermann, Chem. Phys. Lett. 24, 378 (1974).

(57) D. L. Thompson, J. Chem. Phys. 56, 3570 (1972); 57, 4164 (1972); 57, 4170 (1972).

(58) H. H. Suzukawa, Jr., Ph.D. Thesis, University of California, Irvine, California (1974).

(59) K. Kuchitsu and Y. Morino, Bull. Chem. Soc. Japan 38, 805 (1965).

(60) G. Herzberg, "Spectra of Diatomic Molecules", (van Nostrand, New York, 1950), p. 532.

(61) R. Ditchfield, W. J. Hehre and J. A. Pople, J. Chem. Phys. 54, 724 (1971).

(62) R. G. Gordon, "Proceedings of the Conference on Potential Energy Surfaces in Chemistry", (Ed: W. A. Lester, Jr.), (IBM Research Lab, California) RA18, January 14, 1971 (#14748) p. 19.

(63) D. W. Marquadt, J. Soc. Indust. Appl. Math. 11, 431 (1963).

(64) J. O. Hirschfelder, C. F. Curtiss and R. D. Bird, "Molecular Theory of Gases and Liquids", (Wiley, New York, 1954).

(65) a) $(HF)_2$: reference 46; b) H_2O-H_2: H. Lischka, Chem. Phys. 2, 191 (1973); c) HCN-HF: L. A. Curtiss and J. A. Pople, J. Mole. Spec. 48, 413 (1973); d) He_2, Ne_2, Ar_2: T. L. Gilbert and A. C. Wahl, J. Chem. Phys. 47, 3425 (1967).

(66) a) G. C. Maitland and E. B. Smith, Chem. Soc. Rev. 2, 181 (1973); b) H. F. Schaefer, "The Electronic Structure of Atoms and Molecules: A Survey of Rigorous Quantum

Mechanical Results", (Addison-Wesley, Reading, Massachusetts, 1972).

(67) M. Krauss and F. H. Mies, J. Chem. Phys. 42, 2703 (1965).

(68) M. D. Gordon and D. Secrest, J. Chem. Phys. 52, 120 (1970); 53, 4408 (1970).

(69) R. A. White and E. F. Hayes, J. Chem. Phys. 57, 2985 (1972).

(70) W. A. Lester, J. Chem. Phys. 54, 3171 (1971).

(71) I. G. Csizmadia, J. C. Polanyi, A. C. Roach, and W. H. Wong, Can. J. Chem. 47, 4097 (1969).

(72) F. T. Wall and R. N. Porter, J. Chem. Phys. 36, 3256 (1962).

(73) I. G. Csizmadia, R. E. Kari, J. C. Polanyi, A. C. Roach and M. A. Robb, J. Chem. Phys. 52, 6205 (1970).

(74) J. C. Polanyi and J. L. Schreiber, "Distribution of Reaction Products (Theory). X. Investigation of an Ab Initio Energy-Surface for $F + H_2 \rightarrow HF + H$", Chem. Phys. Lett. (to be published).

(75) C. F. Bender, S. V. O'Neil, P. K. Pearson and H. F. Schaefer, III, Science 176, 1412 (1972).

(76) L. Pederson and R. N. Porter, J. Chem. Phys. 47, 4751 (1967); L. M. Raff, L. Stivers, R. N. Porter, D. L. Thompson and L. B. Sims, ibid 52, 3449 (1970).

(77) M. H. Alexander and E. V. Berard, J. Chem. Phys. 60, 3950 (1974).

(78) D. Secrest, J. Chem. Phys. 61, 3867 (1974).

(79) M. H. Alexander, J. Chem. Phys. 61, 3868 (1974).

(80) D. L. Bunker and C. A. Parr, J. Chem. Phys. 52, 5700 (1970).

(81) D. R. Yarkoni, S. V. O'Neil, H. F. Schaefer, III, C. P. Baskin and C. F. Bender, J. Chem. Phys. 60, 855 (1974).

(82) D. R. McLaughlin and D. L. Thompson, J. Chem. Phys. 59, 4393 (1973).

(83) M. J. Benson and D. R. McLaughlin, J. Chem. Phys. 56, 1322 (1972).

(84) a) J. L. Walsh, J. H. Ahlberg and E. N. Nilson, J. Math. Mech., 11, 225 (1962); b) J. H. Ahlberg, E. N. Nilson and J. L. Walsh, "The Theory of Splines and their Application",

(Academic, New York, 1967); c) I. J. Schoenberg, "Approximations with Special Emphasis on Spline Functions", (Academic, New York, 1969); d) T. N. E. Greville, "Theory and Application of Spline Functions", (Academic, New York, 1969).

(85) T. L. Jordan, "Smoothing and Multivariable Interpolation with Splines", Los Alamos Scientific Laboratory - Report LA-3137 (1965).

(86) C. DeBoor, J. Math. Phys. 41, 212 (1962).

(87) G. C. Maitland and E. B. Smith, Chem. Soc. Rev. 2, 181 (1973).

(88) B. Liu and A. D. Mclean, J. Chem. Phys. 59, 4557 (1973).

(89) B. Schneider, J. Chem. Phys. 58, 4447 (1973).

(90) R. N. Porter, L. B. Sims, D. L. Thompson and L. M. Raff, J. Chem. Phys. 58, 2855 (1973).

(91) P. J. Kuntz, Chem. Phys. Lett. 16, 581 (1972).

(92) L. M. Raff, D. L. Thompson, L. B. Sims, and R. N. Porter, J. Chem. Phys. 56, 5998 (1972).

(93) M. Karplus, R. N. Porter and R. D. Sharma, J. Chem. Phys. 43, 3259 (1965).

(94) L. M. Raff, H. H. Suzukawa, Jr., and D. L. Thompson, J. Chem. Phys. 62, 3743 (1975).

(95) R. N. Porter, D. L. Thompson, L. M. Raff and J. M. White, J. Chem. Phys. 62, 2429 (1975).

(96) R. N. Porter and L. M. Raff in "Modern Theoretical Chemistry", Vol. 8, "Dynamics of Molecular Collisions", (Ed: W. H. Miller), (Plenum, New York, 1975).

(97) G. Herzberg, "Molecular Spectra and Molecular Structure", Vol. II. "Infrared and Raman Spectra of Polyatomic Molecules", (van Nostrand, New York, 1949), p. 153.

(98) Reference 60, p. 532 and p. 107.

(99) L. M. Raff, J. Chem. Phys. 60, 2220 (1974).

(100) T. M. Latta, University of Illinois, Graduate College, Digital Computer Laboratory, 7090/7094 Library Routine D2-UOI-ADM-3-36-SR (unpublished).

(101) C. A. Parr, Ph.D. Thesis, California Institute of Technology, Pasadena, California, 1969.

(102) J. C. Polanyi, Accounts. Chem. Research 5, 161 (1972).

(103) D. S. Perry, J. C. Polanyi and C. W. Wilson, Jr., Chem. Phys. 3, 317 (1974).

(104) J. B. Anderson, J. Chem. Phys. 52, 3849 (1970).

(105) D. J. Douglas, J. C. Polanyi and J. J. Sloan, J. Chem. Phys. 59, 6679 (1973).

(106) J. M. White and D. L. Thompson, J. Chem. Phys. 61, 719 (1974).

(107) J. Dubrin and M. J. Heuchman in MTP International Review of Science, Physical Chemistry Series One. Vol. 9, "Chemical Kinetics", (Ed: J. C. Polanyi, University Park Press, Baltimore, 1972), p. 213.

(108) For example, a) W. A. Chupka, J. Berkowitz and M. E. Russell, "VII International Conference on the Physics of Electronic and Atomic Collisions", (M.I.T., Cambridge, Massachusetts, 1969), p. 71; b) W. A. Chupka, M. E. Russell and K. Refaey, J. Chem. Phys. 48, 1518 (1968); c) L. P. Theard and W. T. Huntress, Jr., J. Chem. Phys. 60, 2840 (1974); R. Johnsen and M. A. Biondi, J. Chem. Phys. 61, 2112 (1974).

(109) C. Edmiston, J. Doolittle, K. Murphy, K. C. Tang and W. Wilson, J. Chem. Phys. 52, 3419 (1970).

(110) P. J. Kuntz, Chem. Phys. Lett. 16, 581 (1972).

(111) D. J. Kouri and M. Baer, Chem. Phys. Lett. 24, 37 (1974).

(112) J. T. Adams, "Collinear Quantum Mechanical Calculations for the Reaction: $He + H_2^+ \rightarrow H$", (to be published).

(113) For example, Br + HCl: reference 105; H + HBr, Br + HBr: reference 106; $H_2 + I$: R. N. Porter, L. B. Sims, D. L. Thompson and L. M. Raff, J. Chem. Phys. 58, 2855 (1973); $H_2 + I_2$: L. M. Raff, D. L. Thompson, L. B. Sims and R. N. Porter, J. Chem. Phys. 56, 5998 (1972).

(114) J. W. Duff and D. G. Truhlar, J. Chem. Phys. 62, 2477 (1975).

(115) M. Baer (private communication).

(116) W. S. Dorn and D. D. McCracken, "Numerical Methods with Fortran Case Studies", (John Wiley & Sons, Inc., 1972), pp. 267-284.

APPENDIX A

ROLE OF VIBRATIONAL ENERGY IN REACTIVE COLLISIONS: $He + H_2^+ \rightarrow HeH^+ + H$

The role of vibrational energy in reactive collisions has become of particular interest in recent years because of its importance in infrared chemical lasers (102-106) and the possibility of using vibrational excitation followed by competitive reaction as a means of effective isotopic separation. It is experimentally easier to select the vibrational state of reactants in the case of ion-molecules than in neutral species (107). A great wealth of information is available for ion-molecule reactions (108). On the other hand, very little has been done towards a detailed understanding of the problem, from a theoretical viewpoint. This is due, in part, to the nonadiabatic nature of many ion-molecule reactions.

We chose to investigate the effect of vibrational energy of reactants on the probability of the reaction

$$He + H_2^+ \rightarrow HeH^+ + H$$

for the following reasons:

(1) Chupka and coworkers (108a) have reported reaction cross sections for several (0 - 5) initial vibrational states of H_2^+ at a wide range of total energies (1.0 - 4.0 eV). These results indicate a large vibrational enhancement of the reaction rate.

(2) This is an endoergic reaction (ΔH = 0.8 eV), and Polanyi et al. (103) have recently investigated the problem for a general A + BC reaction. This would enable us to compare the theoretical results for neutral reactions with those of ion-molecule reactions.

(3) Ab initio LCAO-MO-SCF potential-energy surface (109) (41) is available for this system; a semiquantitative analytic fit (110) to that surface is also available, thus making reaction dynamics studies computationally less expensive.

(4) Two independent quantum mechanical studies (111) (112) have been made on this system and neither of them is in agreement with experimental results. In addition, they indicate that the common belief (103-106) that vibrational energy is more effective than translational energy in endoergic reactive collisions may not be a general effect. This system provides a unique opportunity to compare quasiclassical trajectory results with the experimental and quantum mechanical values.

The molecules collisions were restricted to be collinear, and were studied by quasiclassical trajectory methods on the ab initio potential-energy surface of Brown and Hayes (41), fitted to an analytic function by Kuntz (110). Figure 32 shows the potential-energy contours for the collinear $[He\text{-}H\text{-}H]^+$ system obtained from the analytic function.

The initial vibrational state of H_2^+ was varied systematically from 0 to 3. The relative translational energy was chosen such that the total translational plus vibrational) energy is 0.94, 1.0, 1.1, 1.2 and 1.4 eV's. For each translational energy and vibrational state chosen, 200 trajectories were run and the reaction probabilities were computed. The mathematical procedures employed in these calculations have been described elsewhere (55).

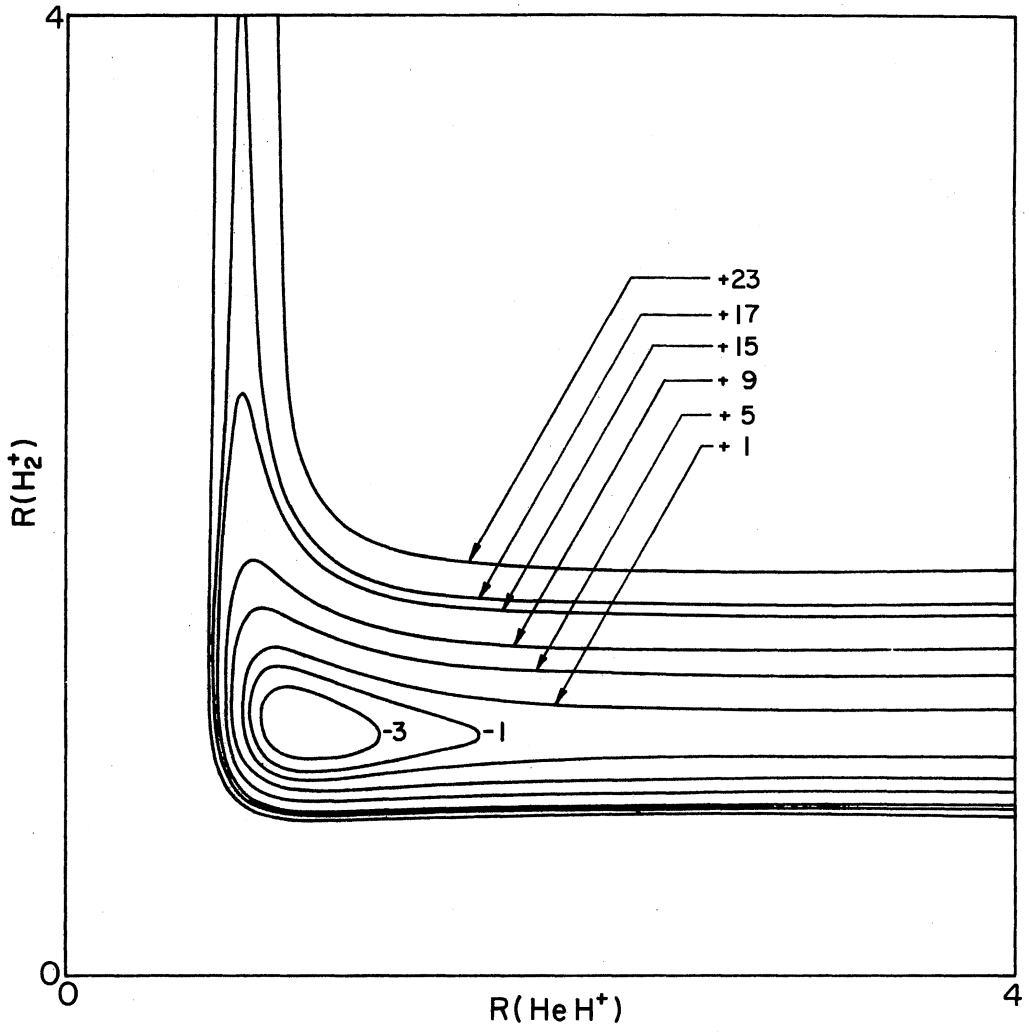

Figure 32. Collinear Potential-Energy Surface (111) for HeH_2^+. Energies are in kcal/mole, Distances in Å

The results of the trajectory analysis are plotted in Figure 33. The reaction probabilities are strikingly higher for lower vibrational states in contrast to the experimental (108a) reaction cross sections reported in Figure 34. The quantum mechanical results of Kouri and Baer (112) are plotted in Figure 35. Figures 36 through 39 compare results from quantal and classical calculations for individual vibrational states of the H_2^+ molecule. The classical results are in qualitative agreement with the quantal results in spite of the fact that the potential-energy barrier is asymmetric. This result is interesting since recent results obtained by Kellerhals (51) and by Schatz, Bowman and Kuppermann (56c) have shown large differences between quantum mechanical and classical results for systems having asymmetric potential-energy barriers.

The results of this theoretical study are hard to understand in light of the pioneering works of Polanyi and coworkers (102) (103) on the role of vibrational energy in reactive collisions. For several endoergic systems (113), vibrational energy has proven to be more effective than translational energy in enhancing reaction rate. The unusual behavior of the He + H_2^+ system may be due to the unique behavior of ion-molecule reactions yet to be explored by detailed theoretical dynamical studies. Alternately, the results may be due to the location of the position of maximum curvature (114) along the reaction coordinate relative to the position of energy release. This may have its origin in the lack of understanding of potential-energy surfaces of ion-molecule systems.

In this system nonlinear collisions may be very important and collinear trajectories may be unrealistic as was pointed out by Kouri

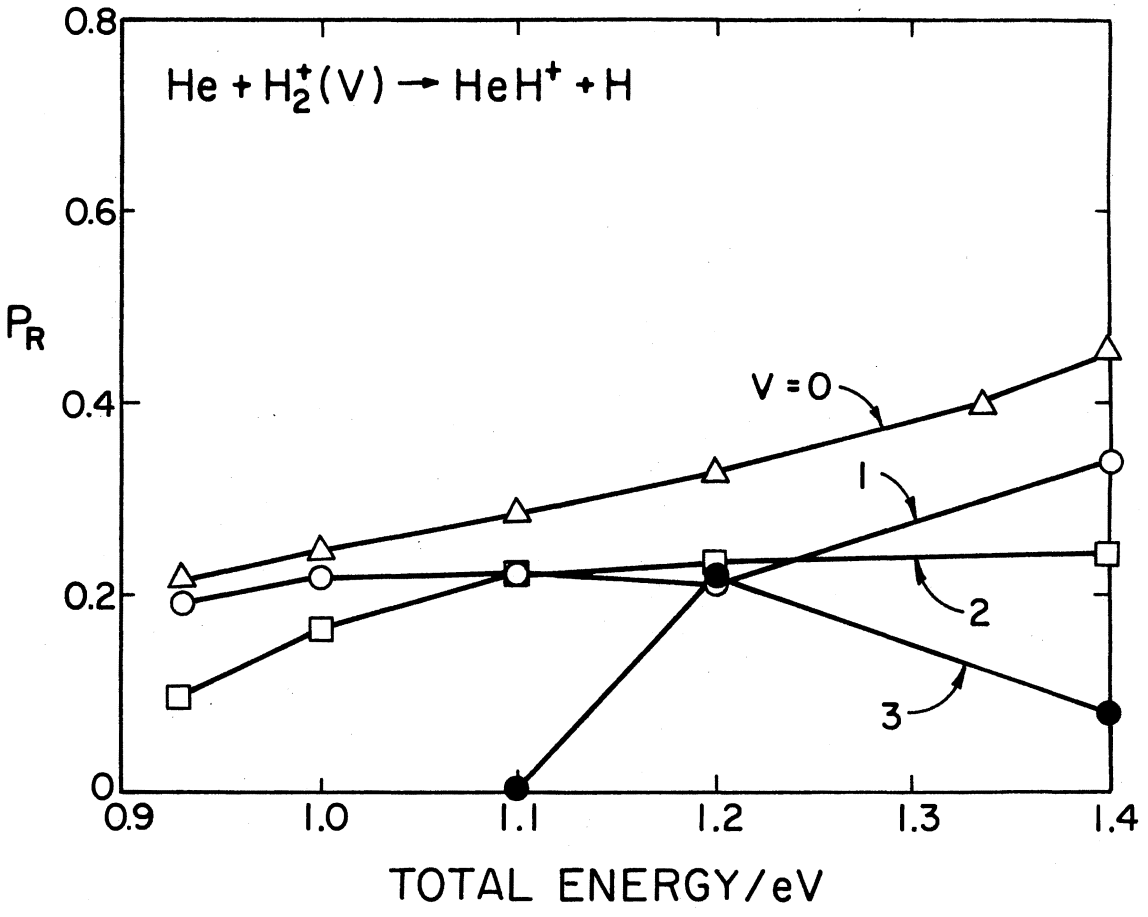

Figure 33. Quasiclassical Reaction Probability as a Function of Total Energy of the System for Different Vibrational States

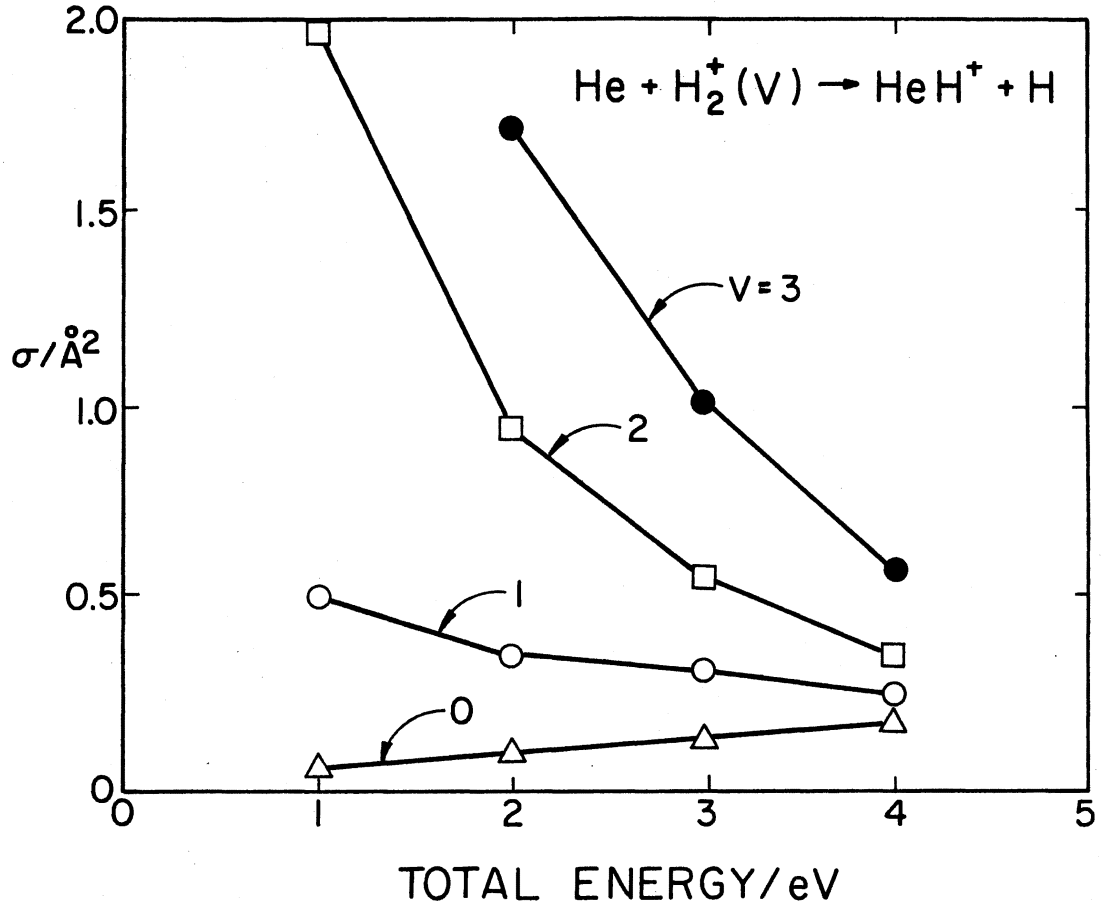

Figure 34. Experimental Reaction Cross Section as a Function of Total Energy of the System for Different Vibrational States

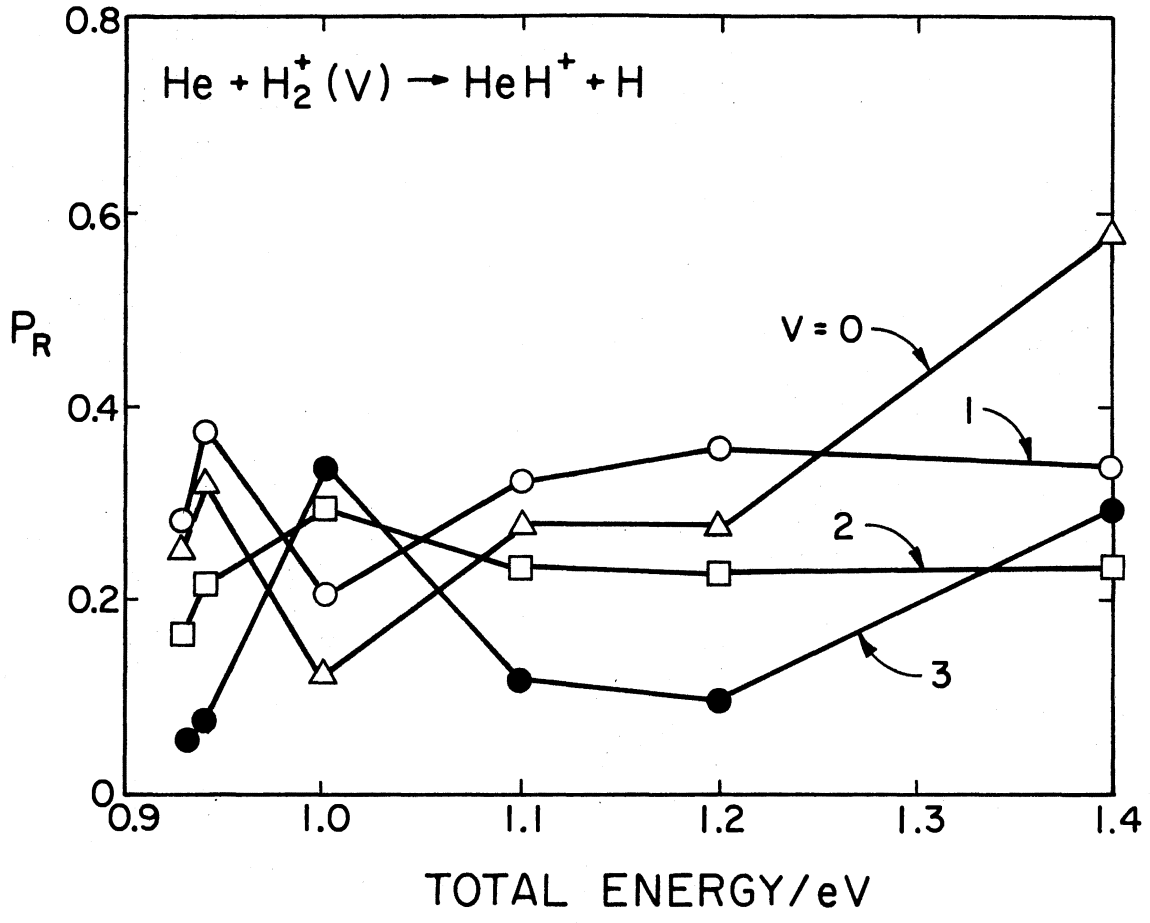

Figure 35. Quantum Mechanical Reaction Probabilities (115) as a Function of Total Energy of the System for Different Vibrational States

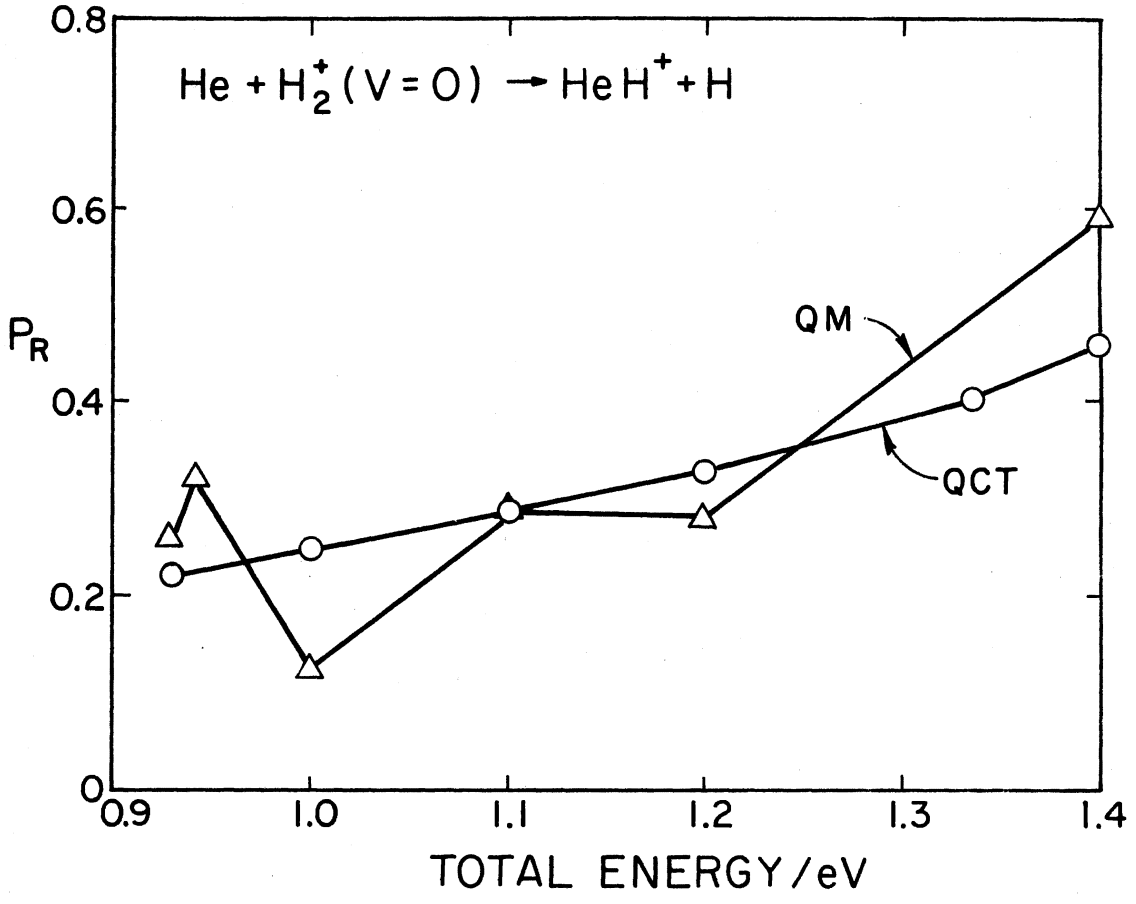

Figure 36. Comparison of Quasiclassical and Quantum Mechanical (115) Reaction Probabilities for v = 0 State of H_2^+

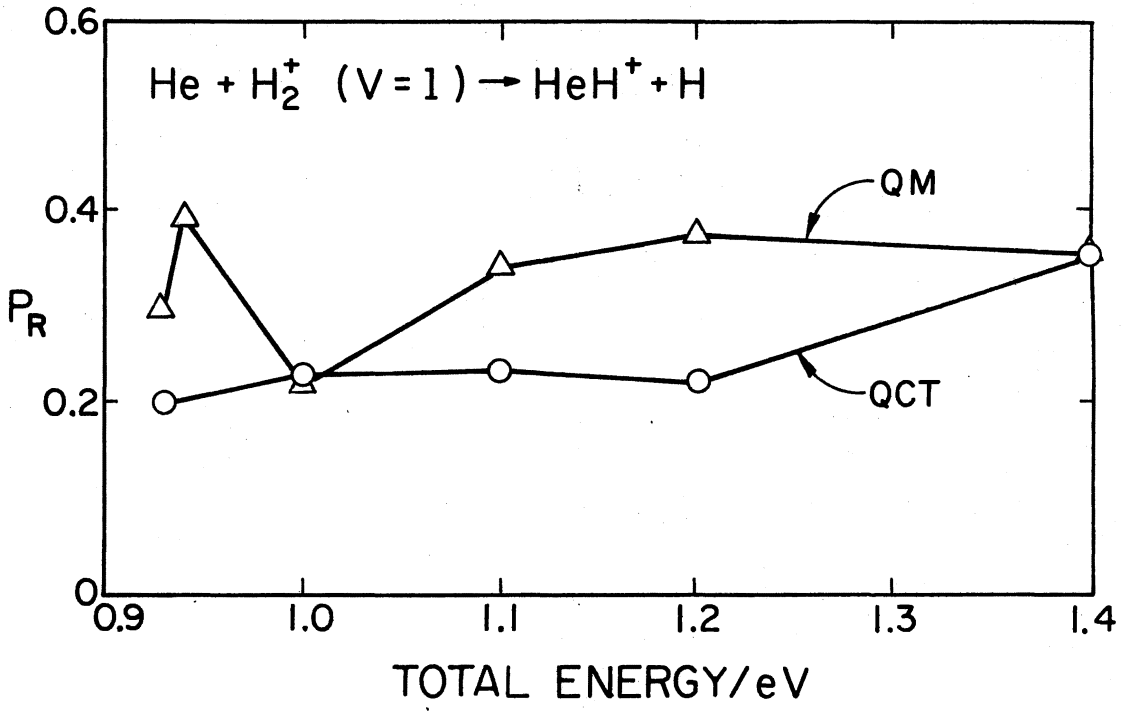

Figure 37. Comparison of Quasiclassical and Quantum Mechanical (115) Reaction Probabilities for v = 1 State of H_2^+

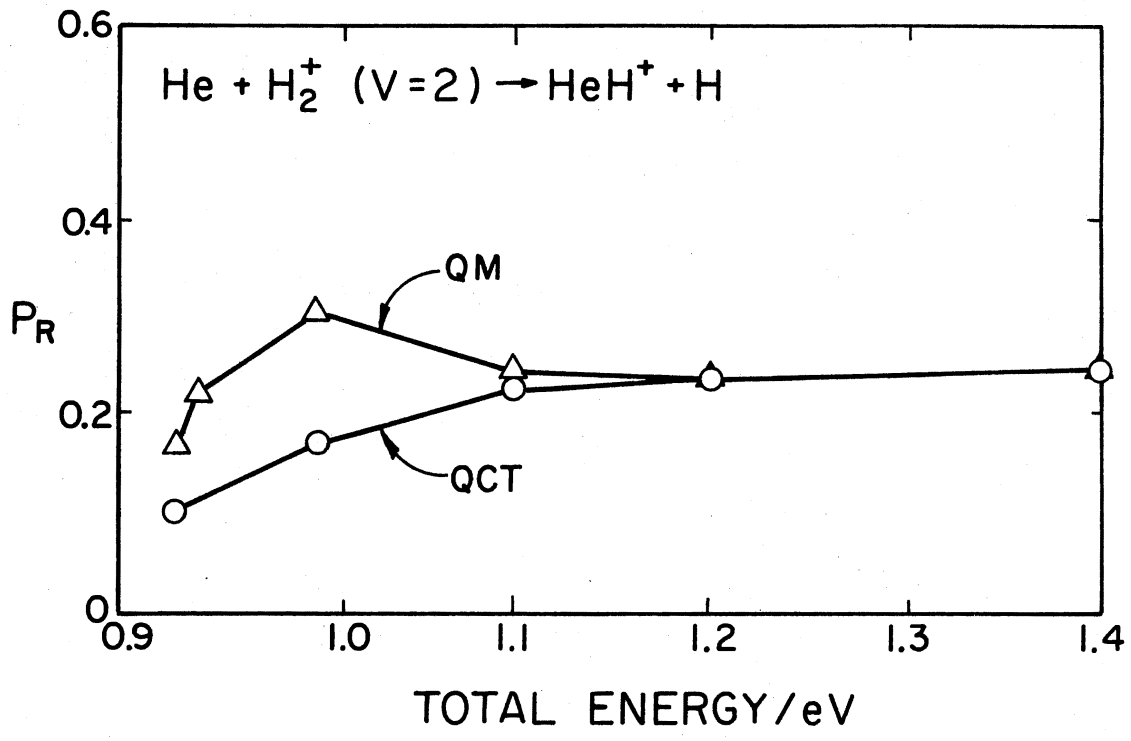

Figure 38. Comparison of Quasiclassical and Quantum Mechanical (115) Reaction Probabilities for v = 2 State of H_2^+

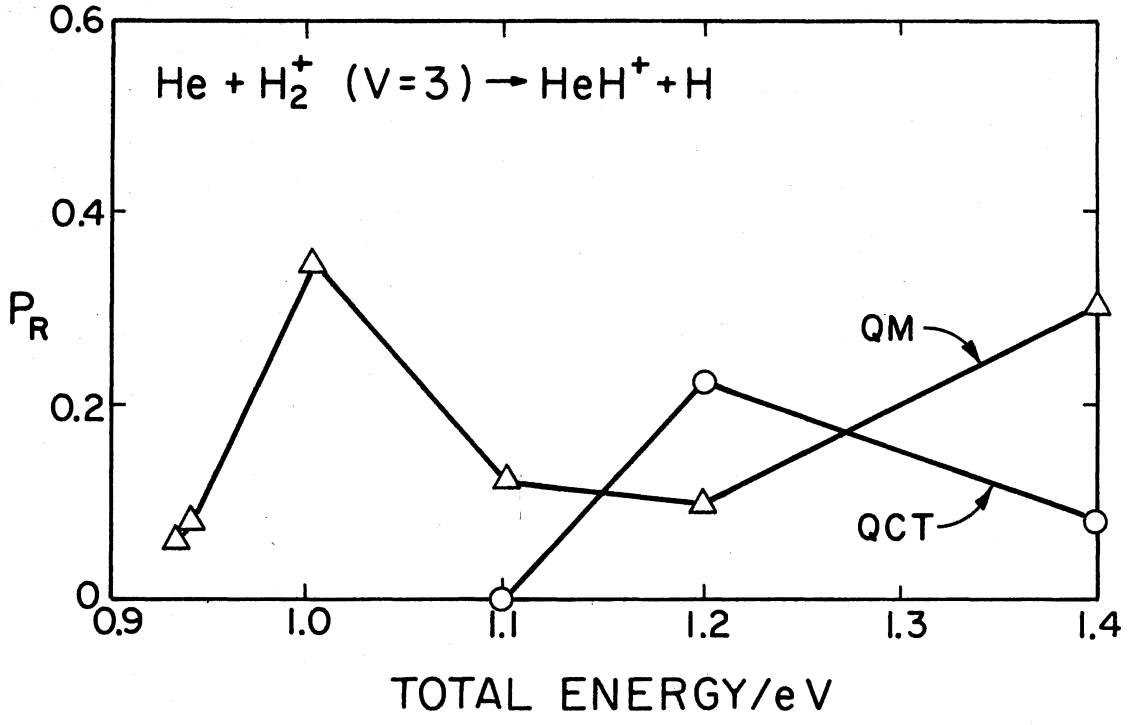

Figure 39. Comparison of Quasiclassical and Quantum Mechanical (115) Reaction Probabilities for v = 3 State of H_2^+

and Baer (111). It is known (77) that slight changes in potential-energy surfaces may have significant bearing on the outcomes of the collisions. The analytic functional fit to the potential-energy surface employed in this and the two quantum mechanical calculations may not be appropriate for dynamical studies and a numerical spline interpolation procedure may be able to better reproduce the features of the LCAO-MO-SCF surface. This problem along with an investigation of the reaction path curvature is currently under study. If these studies should indicate that no significant errors exist in the calculations, a reinvestigation of the experimental details would appear to be in order.

APPENDIX B

DESCRIPTION OF THE BASIS SET USED IN THE LCAO-MO-SCF PROCEDURE FOR CO_2-H_2 SYSTEM

An extended (split valence) Gaussian basis (4-31G) set is used. That is, the inner shell of each atom is represented by a single basis function taken as a sum of four Gaussians and each valence orbital is split into inner and outer parts described by three and one Gaussian function, respectively. For carbon and oxygen, we may represent the functions as

$$\phi_{1s}(\vec{r}) = \sum_{k=1}^{4} d_{1s,k} g_s(\alpha_{1k}, \vec{r})$$

$$\phi'_{2s}(\vec{r}) = \sum_{k=1}^{3} d_{2s,k'} g_s(\alpha'_{2k}, \vec{r})$$

$$\phi'_{2p_x}(\vec{r}) = \sum_{k=1}^{3} d_{2p,k'} g_{p_x}(\alpha'_{2k}, \vec{r})$$

$$\phi''_{2s}(\vec{r}) = d_{2s} g_s(\alpha''_{2k}, \vec{r})$$

$$\phi''_{2p_x}(\vec{r}) = d_{2p} g_{p_x}(\alpha''_{2k}, \vec{r}) \qquad \text{(B-1)}$$

and similarly for p_y and p_z orbitals. g's are Gaussian functions defined as

$$g_s(\alpha, \vec{r}) = (2\alpha/\pi)^{3/4} \exp(-\alpha r^2)$$

$$g_{p_x}(\alpha, \vec{r}) = (128\alpha^5/\pi^3)^{1/4} \times \exp(-\alpha r^2). \qquad \text{(B-2)}$$

For hydrogen, there is no inner shell and we may take two functions

$$\phi'_{1s}(\vec{r}) = \sum_{k=1}^{3} d'_k g_s(\alpha'_k, \vec{r})$$

$$\phi''_{1s}(\vec{r}) = d_s g_s(\alpha''_k, \vec{r}) \qquad \text{(B-3)}$$

representing the valence shell. The values of d's and α's are given in Table XXIII and are due to Pople and coworkers (48).

TABLE XXIII

BASIS SET COMPONENTS

Atom	Orbital Type	Gaussian Functions		
		Exponent (α)	s coef (d_s)	p coef (d_p)
Carbon	1s			
		0.486967E 3	0.177258E-1	0.0
		0.733711E 2	0.123478E 0	0.0
		0.164135E 2	0.433875E 0	0.0
		0.434498E 1	0.561504E 0	0.0
	2sp			
		0.867352E 1	-0.121384E 0	0.635453E-1
		0.209662E 1	-0.227338E 0	0.298268E 0
		0.604651E 0	0.118517E 1	0.762103E 0
	2sp			
		0.183558E 0	0.100000E 1	0.100000E 1
Oxygen				
	1s			
		0.883273E 3	0.175506E-1	0.0
		0.133129E 3	0.122829E 0	0.0
		0.299064E 2	0.434884E 0	0.0
		0.797868E 1	0.560011E 0	0.0
	2sp			
		0.161944E 2	-0.113401E 0	0.685452E-1
		0.378008E 1	-0.177286E 0	0.331225E 0
		0.107098E 1	0.115041E 1	0.734608E 0
	2sp			
		0.283880E 0	0.100000E 1	0.100000E 1
Hydrogen	1s			
		0.187311E 2	0.334946E-1	0.0
		0.282539E 1	0.234727E 0	0.0
		0.640121E 0	0.813757E 0	0.0
	1s			
		0.161278E 0	0.100000E 1	0.0

APPENDIX C

THE TRIAL FUNCTION

The following is a fifty parameters function that was used in our initial attempts to fit the CO_2-H_2 intermolecular potential to an analytic function. It is a combination of Buckingham-6,8,10-exp function (64) and several trigonometric functions.

$$
\begin{aligned}
V(R,\theta,\phi,\tau) = &\{(B(1)+B2*C+B(3)*TC)+(B(4)+B(5)*C+B(6)*TC)A \\
&+(B(7)+B(8)*C+B(9)*TC)TB\}* \\
&\exp-[\{(B(10)+B(11)*C+B(12)*TC)+(B(13)+B14*C+ \\
&B15*TC)*A+(B(16)+B(17)*C+B(18)*TC)*TB\}R] \\
&-\{(B(19)+B(20)*C+B21*TC)+(B(22)+B(23)*C+ \\
&B(24)*TC)\ A+(B(25)+B26*C+B27*TC)TB\}/R^6 \\
&-\{(B(28)+B(29)*C+B(30)*TC)+(B(31)+B(32)*C+ \\
&B(33)*TC)A+(B(34)+B(35)*C+B(36)*TC)TB\}/R^8 \qquad \text{(C-1)}
\end{aligned}
$$

where

$$
\begin{aligned}
TB &= \sin^2\theta \\
TC &= \sin^2\phi \\
S &= \sin^2\tau \\
A &= \sin\theta \\
C &= \sin\phi \\
D &= \sin\tau \\
B2 &= B(2)+B(37)*D+B(38)*S \\
B3 &= B(3)+B(39)*D+B(40)*S \\
B14 &= B(14)+B(43)*D+B(44)*S \\
B15 &= B(15)+B(45)*D+B(46)*S
\end{aligned}
$$

$$B21 = B(21) + B(47) * D + B(48) * S$$

$$B26 = B(26) + B(41) * D + B(42) * S$$

and

$$B27 = B(27) + B(49) * D + B(50) * S \qquad \text{(C-2)}$$

The fifty parameters B(1) through B(50) are given in Table XXIV.

TABLE XXIV

PARAMETER VALUES FOR ANALYTIC FITTING OF $V(R,\theta,\phi,\tau)$

B(1)	0.71035096D 06	B(26)	-0.25954166D 05
B(2)	-0.12740077D 05	B(27)	0.27012564D 05
B(3)	-0.11727264D 06	B(28)	0.12570335D 06
B(4)	-0.12277416D 07	B(29)	0.11194548D 06
B(5)	-0.10838327D 07	B(30)	-0.10913717D 06
B(6)	0.13680391D 07	B(31)	-0.18074127D 06
B(7)	0.53013337D 06	B(32)	-0.63544123D 06
B(8)	0.11096923D 07	B(33)	0.61934263D 06
B(9)	-0.12437767D 07	B(34)	0.55334830D 05
B(10)	0.32882276D 01	B(35)	0.52692803D 06
B(11)	-0.90996557D-01	B(36)	-0.51257380D 06
B(12)	0.78209131D-01	B(37)	0.24255182D 05
B(13)	-0.27517143D 00	B(38)	-0.18281349D 05
B(14)	-0.49846722D 01	B(39)	-0.21947453D 05
B(15)	0.41263227D 01	B(40)	0.64945996D 04
B(16)	0.69771398D-01	B(41)	0.12452563D 04
B(17)	0.59850064D 01	B(42)	-0.10562951D 04
B(18)	-0.45218171D 01	B(43)	0.15478484D 00
B(19)	-0.25686016D 04	B(44)	-0.22004310D 00
B(20)	-0.509465250 04	B(45)	-0.15303357D 00
B(21)	0.23422928D 04	B(46)	0.18600425D 00
B(22)	0.87107345D 04	B(47)	0.32501662D 03
B(23)	0.291885120 05	B(48)	-0.86975072D 03
B(24)	-0.27496241D 05	B(49)	-0.14460331D 04
B(25)	-0.60212051D 04	B(50)	0.14197774D 04

APPENDIX D

THE DERIVATIVES OF THE POTENTIAL

The expressions for derivatives of the potential with respect to cartesian coordinates are given below:

$$\frac{\partial V}{\partial x_1} = \frac{\partial V}{\partial R_1}\frac{\partial R_1}{\partial x_1} + \frac{\partial V}{\partial R_3}\frac{\partial R_3}{\partial x_1} + \frac{\partial V}{\partial \theta}\frac{\partial \theta}{\partial x_1}$$

$$\frac{\partial V}{\partial y_1} = \frac{\partial V}{\partial R_1}\frac{\partial R_1}{\partial y_1} + \frac{\partial V}{\partial R_3}\frac{\partial R_3}{\partial y_1} + \frac{\partial V}{\partial \theta}\frac{\partial \theta}{\partial y_1}$$

$$\frac{\partial V}{\partial z_1} = \frac{\partial V}{\partial R_1}\frac{\partial R_1}{\partial z_1} + \frac{\partial V}{\partial R_3}\frac{\partial R_3}{\partial z_1} + \frac{\partial V}{\partial \theta}\frac{\partial \theta}{\partial z_1}$$

$$\frac{\partial V}{\partial x_2} = \frac{\partial V}{\partial R_1}\frac{\partial R_1}{\partial x_2} + \frac{\partial V}{\partial R_2}\frac{\partial R_2}{\partial x_2} + \frac{\partial V}{\partial R}\frac{\partial R}{\partial x_2} + \frac{\partial V}{\partial \theta}\frac{\partial \theta}{\partial x_2} + \frac{\partial V}{\partial \phi}\frac{\partial \phi}{\partial x_2}$$

$$\frac{\partial V}{\partial y_2} = \frac{\partial V}{\partial R_1}\frac{\partial R_1}{\partial y_2} + \frac{\partial V}{\partial R_2}\frac{\partial R_2}{\partial y_2} + \frac{\partial V}{\partial R}\frac{\partial R}{\partial y_2} + \frac{\partial V}{\partial \theta}\frac{\partial \theta}{\partial y_2} + \frac{\partial V}{\partial \phi}\frac{\partial \phi}{\partial y_2}$$

$$\frac{\partial V}{\partial z_2} = \frac{\partial V}{\partial R_1}\frac{\partial R_1}{\partial z_2} + \frac{\partial V}{\partial R_2}\frac{\partial R_2}{\partial z_2} + \frac{\partial V}{\partial R}\frac{\partial R}{\partial z_2} + \frac{\partial V}{\partial \theta}\frac{\partial \theta}{\partial z_2} + \frac{\partial V}{\partial \phi}\frac{\partial \phi}{\partial z_2}$$

$$\frac{\partial V}{\partial x_3} = \frac{\partial V}{\partial R_2}\frac{\partial R_2}{\partial x_3} + \frac{\partial V}{\partial R_3}\frac{\partial R_3}{\partial x_3}$$

$$\frac{\partial V}{\partial y_3} = \frac{\partial V}{\partial R_2}\frac{\partial R_2}{\partial y_3} + \frac{\partial V}{\partial R_3}\frac{\partial R_3}{\partial y_3}$$

$$\frac{\partial V}{\partial z_3} = \frac{\partial V}{\partial R_2}\frac{\partial R_2}{\partial z_3} + \frac{\partial V}{\partial R_3}\frac{\partial R_3}{\partial z_3}$$

$$\frac{\partial V}{\partial x_4} = \frac{\partial V}{\partial R_4}\frac{\partial R_4}{\partial x_4} + \frac{\partial V}{\partial R}\frac{\partial R}{\partial x_4} + \frac{\partial V}{\partial \theta}\frac{\partial \theta}{\partial x_4} + \frac{\partial V}{\partial \phi}\frac{\partial \phi}{\partial x_4}$$

$$\frac{\partial V}{\partial y_4} = \frac{\partial V}{\partial R_4}\frac{\partial R_4}{\partial y_4} + \frac{\partial V}{\partial R}\frac{\partial R}{\partial y_4} + \frac{\partial V}{\partial \theta}\frac{\partial \theta}{\partial y_4} + \frac{\partial V}{\partial \phi}\frac{\partial \phi}{\partial y_4}$$

$$\frac{\partial V}{\partial z_4} = \frac{\partial V}{\partial R_4}\frac{\partial R_4}{\partial z_4} + \frac{\partial V}{\partial R}\frac{\partial R}{\partial z_4} + \frac{\partial V}{\partial \theta}\frac{\partial \theta}{\partial z_4} + \frac{\partial V}{\partial \phi}\frac{\partial \phi}{\partial z_4}$$

$$\frac{\partial V}{\partial x_5} = \frac{\partial V}{\partial R_4}\frac{\partial R_4}{\partial x_5} + \frac{\partial V}{\partial R}\frac{\partial R}{\partial x_5} + \frac{\partial V}{\partial \theta}\frac{\partial \theta}{\partial x_5} + \frac{\partial V}{\partial \phi}\frac{\partial \phi}{\partial x_5}$$

$$\frac{\partial V}{\partial y_5} = \frac{\partial V}{\partial R_4}\frac{\partial R_4}{\partial y_5} + \frac{\partial V}{\partial R}\frac{R}{y_5} + \frac{\partial V}{\partial \theta}\frac{\partial \theta}{\partial y_5} + \frac{\partial V}{\partial \phi}\frac{\partial \phi}{\partial y_5}$$

$$\frac{\partial V}{\partial z_5} = \frac{\partial V}{\partial R_4}\frac{\partial R_4}{\partial z_5} + \frac{\partial V}{\partial R}\frac{\partial R}{\partial z_5} + \frac{\partial V}{\partial \theta}\frac{\partial \theta}{\partial z_5} + \frac{\partial V}{\partial \phi}\frac{\partial \phi}{\partial z_5} \quad . \qquad \text{(D-1)}$$

APPENDIX E

FOUR-POINT LAGRANGIAN INTERPOLATION (116)

FORMULA AND 1D SPLINE

Let us consider $x_1 < x_2 < x_3 < x_4$ and $x_1 < x < x_4$. Let $y_1 = f(x_1)$, $y_2 = f(x_2)$, $y_3 = f(x_3)$ and $y_4 = f(x_4)$:

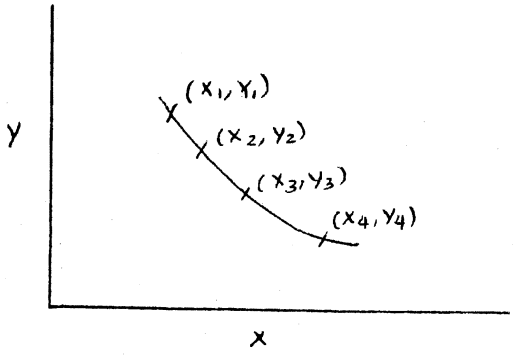

Let us consider

$$f(x) = a_0 + a_1 x + a_2 x^2 + a_3 x^3 \qquad \text{(E-1)}$$

passing through those four points. Let

$$\begin{aligned} \pi_1(x) &= (x - x_2)(x - x_3)(x - x_4) \\ \pi_2(x) &= (x - x_1)(x - x_3)(x - x_4) \\ \pi_3(x) &= (x - x_1)(x - x_2)(x - x_4) \\ \pi_4(x) &= (x - x_1)(x - x_2)(x - x_3) \ . \end{aligned} \qquad \text{(E-2)}$$

$$\pi_1(x_1) \neq 0, \quad \pi_2(x_2) \neq 0, \quad \pi_3(x_3) \neq 0, \quad \pi_4(x_4) \neq 0 \ . \qquad \text{(E-3)}$$

$$\pi_1(x_2) = \pi_1(x_3) = \pi_1(x_4) = \pi_2(x_1) = \pi_2(x_3) = \pi_2(x_4)$$
$$= \pi_3(x_1) = \pi_3(x_2) = \pi_3(x_4) = \pi_4(x_1) = \pi_4(x_2) = \pi_4(x_3) = 0. \quad \text{(E-4)}$$

Expand $f(x)$ in terms of $\pi_1(x)$, $\pi_2(x)$, $\pi_3(x)$ and $\pi_4(x)$

$$f(x) = b_1\pi_1(x) + b_2\pi_2(x) + b_3\pi_3(x) + b_4\pi_4(x) \quad \text{(E-5)}$$

$$\begin{aligned} y_1 &= f(x_1) = b_1\pi_1(x_1) \\ y_2 &= f(x_2) = b_2\pi_2(x_2) \\ y_3 &= f(x_3) = b_3\pi_3(x_3) \\ y_4 &= f(x_4) = b_4\pi_4(x_4) \end{aligned} \quad \text{(E-6)}$$

$$b_1 = \frac{y_1}{\pi_1(x_1)}\ ,\ b_2 = \frac{y_2}{\pi_2(x_2)}\ ,\ b_3 = \frac{y_3}{\pi_3(x_3)} \text{ and } b_4 = \frac{y_4}{\pi_4(x_4)}\ . \quad \text{(E-7)}$$

Therefore,

$$\begin{aligned} f(x) &= y_1\frac{\pi_1(x)}{\pi_1(x_1)} + y_2\frac{\pi_2(x)}{\pi_2(x_2)} + y_3\frac{\pi_3(x)}{\pi_3(x_3)} + y_4\frac{\pi_4(x)}{\pi_4(x_4)} \\ &= y_1\left(\frac{x-x_2}{x_1-x_2}\right)\left(\frac{x-x_3}{x_1-x_3}\right)\left(\frac{x-x_4}{x_1-x_4}\right) + y_2\left(\frac{x-x_1}{x_2-x_1}\right)\left(\frac{x-x_3}{x_2-x_3}\right)\left(\frac{x-x_4}{x_2-x_4}\right) \\ &+ y_3\left(\frac{x-x_1}{x_3-x_1}\right)\left(\frac{x-x_2}{x_3-x_2}\right)\left(\frac{x-x_4}{x_3-x_4}\right) + y_4\left(\frac{x-x_1}{x_4-x_1}\right)\left(\frac{x-x_2}{x_4-x_2}\right)\left(\frac{x-x_3}{x_4-x_3}\right) \end{aligned} \quad \text{(E-8)}$$

$$\begin{aligned} f'(x) = &\frac{y_1}{(x_1-x_2)(x_1-x_3)(x_1-x_4)}\left\{(x-x_3)(x-x_4) + (x-x_2)(x-x_4) + (x-x_2)(x-x_3)\right\} \\ &+ \frac{y_2}{(x_2-x_1)(x_2-x_3)(x_2-x_4)}\left\{(x-x_3)(x-x_4) + (x-x_1)(x-x_4) + (x-x_1)(x-x_3)\right\} \\ &+ \frac{y_3}{(x_3-x_1)(x_3-x_2)(x_3-x_4)}\left\{(x-x_2)(x-x_4) + (x-x_1)(x-x_4) + (x-x_1)(x-x_2)\right\} \\ &+ \frac{y_4}{(x_4-x_1)(x_4-x_2)(x_4-x_3)}\left\{(x-x_2)(x-x_3) + (x-x_1)(x-x_3) + (x-x_1)(x-x_2)\right\} \end{aligned} \quad \text{(E-9)}$$

$$f'(x_1) = \frac{y_1}{(x_1-x_2)} + \frac{y_1}{(x_1-x_3)} + \frac{y_1}{(x_1-x_4)}$$
$$+ \frac{y_2(x_1-x_3)(x_1-x_4)}{(x_2-x_1)(x_2-x_3)(x_2-x_4)} + \frac{y_3(x_1-x_2)(x_1-x_4)}{(x_3-x_1)(x_3-x_2)(x_3-x_4)}$$
$$+ \frac{y_4(x_1-x_2)(x_1-x_3)}{(x_4-x_1)(x_4-x_2)(x_4-x_3)} \quad . \tag{E-10}$$

Considering a set of points $x_{N-3} < x_{N-2} < x_{N-1} < x_N$ and $x_{N-3} < x < x_N$,

$$f'(x_N) = \frac{y_{N-3}(x_N - x_{N-2})(x_N - x_{N-1})}{(x_{N-3} - x_{N-2})(x_{N-3} - x_{N-1})(x_{N-3} - x_N)}$$
$$+ \frac{y_{N-2}(x_N - x_{N-3})(x_N - x_{N-1})}{(x_{N-2} - x_{N-3})(x_{N-2} - x_{N-1})(x_{N-2} - x_N)}$$
$$+ \frac{y_{N-1}(x_N - x_{N-3})(x_N - x_{N-2})}{(x_{N-1} - x_{N-3})(x_{N-1} - x_{N-2})(x_{N-1} - x_N)}$$
$$+ \frac{y_N}{(x_N - x_{N-3})} + \frac{y_N}{(x_N - x_{N-2})} + \frac{y_N}{(x_N - x_{N-1})} \quad . \tag{E-11}$$

Considering the problem of splinefit procedure discussed in Chapter III, first derivatives at x_1 and x_N can thus be known from a four-point Lagrangian interpolation of (F_1, F_2, F_3, F_4) and (F_{N-3}, F_{N-2}, F_{N-1}, F_N). Recall Equation (III-5):

$$S_i'(x) = -F_i'' \frac{(x_{i+1}-x)^2}{2\Delta_i} + F_{i+1}'' \frac{(x-x_i)^2}{2\Delta_i} + \frac{F_{i+1} - F_i}{\Delta_i} - (F_{i+1}'' - F_i'') \frac{\Delta_i}{6} \quad . \tag{E-12}$$

By substituting $i = 1$, and $x = x_1$,

$$\frac{\Delta_1}{3} F_1'' = \frac{\Delta_1}{6} F_2'' = \frac{F_2 - F_1}{\Delta_1} - S_1'(x_1) \quad . \tag{E-13}$$

Similarly,

$$\frac{\Delta_N}{6} F''_{N-1} + \frac{\Delta_N}{3} F''_N = S'_N(x_N) - \frac{F_N - F_{N-1}}{\Delta_N} \quad . \qquad \text{(E-14)}$$

Equations (E-13) and (E-14) provide the two additional equations required in solving N-2 equations and N unknowns.

VITA

Narayanasami Sathyamurthy

Candidate for the Degree of

Doctor of Philosophy

Thesis: AB INITIO DYNAMICAL STUDY OF CO_2-H_2 VIBRATIONAL ENERGY TRANSFER

Major Field: Chemistry

Biographical:

Personal Data: Born in India, July 10, 1951

Education: Graduate from Government High School, Panruti, India in April, 1966; received the Bachelor of Science degree from Annamalai University, India in May, 1970; received the Master of Science degree from Annamalai University, India in May, 1972; completed requirements for the Doctor of Philosophy degree at Oklahoma State University, July, 1975.

Professional Experience: National Science Talent Scholar (India), Annamalai University, India, 1967-1972; CONOCO Fellow, Oklahoma State University, summer 1973; Oklahoma State University College of Arts and Sciences Summer Research Awardee, summer 1974; National Science Foundation Research Assistant, Oklahoma State University, 1974-1975; Graduate Teaching Assistant, Oklahoma State University, 1972-1975.

Membership in Honorary and Professional Societies: Member of Phi Lambda Upsilon, Honorary Chemical Society.